

University of Groningen

Imaging proliferation with [18F]FLT-PET

Been, Lukas Berend

IMPORTANT NOTE: You are advised to consult the publisher's version (publisher's PDF) if you wish to cite from it. Please check the document version below.

Document Version

Publisher's PDF, also known as Version of record

Publication date:

2008

[Link to publication in University of Groningen/UMCG research database](#)

Citation for published version (APA):

Been, L. B. (2008). *Imaging proliferation with [18F]FLT-PET: therapy evaluation studies*. [s.n.].

Copyright

Other than for strictly personal use, it is not permitted to download or to forward/distribute the text or part of it without the consent of the author(s) and/or copyright holder(s), unless the work is under an open content license (like Creative Commons).

The publication may also be distributed here under the terms of Article 25fa of the Dutch Copyright Act, indicated by the "Taverne" license. More information can be found on the University of Groningen website: <https://www.rug.nl/library/open-access/self-archiving-pure/taverne-amendment>.

Take-down policy


If you believe that this document breaches copyright please contact us providing details, and we will remove access to the work immediately and investigate your claim.

Downloaded from the University of Groningen/UMCG research database (Pure): <http://www.rug.nl/research/portal>. For technical reasons the number of authors shown on this cover page is limited to 10 maximum.



**Imaging
proliferation
with
[¹⁸F]FLT-PET:
therapy
evaluation
studies**

L.B. Been



**Imaging
proliferation
with
[¹⁸F]FLT-PET:
therapy
evaluation
studies**

L.B. Been

Stellingen

behorende bij het proefschrift:

“Imaging proliferation with [^{18}F]FLT-PET: therapy evaluation studies”

1. Ondanks het feit dat 10 jaar geleden de eerste publicatie over [^{18}F]FLT verschenen is, kennen we nog steeds de werkelijke waarde niet van deze PET tracer in de oncologie.
2. [^{18}F]FLT-PET zal meer waarde hebben in de evaluatie van therapie dan in de detectie en stadiëring van tumoren.
3. Fusie van [^{18}F]FLT-PET met morfologische beeldvormende technieken als CT en/of MRI is zeer behulpzaam bij de differentiatie tussen fysiologische en pathologische tracer opname.
4. Positron emissie tomografie heeft geen waarde in het opsporen van okselkliermetastasen bij patiënten met mammacarcinoom.
5. De in verhouding hogere opname van [^{18}F]FDG in tumoren ten opzichte van [^{18}F]FLT is deels te verklaren door het feit dat [^{18}F]FDG opname vertoont in ontstekingsweefsel rondom maligne cellen en [^{18}F]FLT niet.
6. Een verhoogde proliferatieactiviteit is niet alleen aanwezig in maligne cellen, maar (soms) ook in ontstekingen.
7. Door de veranderde werktijden van specialisten en assistenten in opleiding wordt opleiden en opgeleid worden volgens de leermeester-gezel verhoudingen steeds moeilijker.
8. ‘De geneeskunde heeft zo’n enorme ontwikkeling doorgemaakt dat er nagenoeg geen gezond mens meer is’ (Aldoux Huxley).
9. Met de invoering van de ‘Beter af Polis’ hebben zorgverzekeraars het solidariteitsprincipe verlaten.
10. Het begrip ‘vriend’ heeft na de komst van Hyves een andere waarde gekregen.
11. De letter c in de naam ‘Lukas’ is erg hardnekkig gebleken.
12. ‘Vroeg grijs’ zijn is niet geassocieerd met ‘vroeg oud’ worden. (Med Hypotheses 1991;36:404-411)



Lukas Been
Imaging proliferation with [¹⁸F]FLT-PET: therapy evaluation studies
Thesis University of Groningen
ISBN 978-90-367-3391-5

Paranimfen

Ir. T. Been
A. Riemslag

This research was supported by a grant from

KWF Kankerbestrijding

Financial support for this thesis was kindly given by

KWF Kankerbestrijding
Ortho Biotech
Universitair Medisch Centrum Groningen, afdeling Chirurgie
GUIDE
Stichting TRACE

Layout and cover design

Fleur Bominaar, FYN Werk, www.fynwerk.nl

Printed by

Gildeprint Drukkerijen, www.gildeprint.nl

Cover image

'De Wiekeneer' by Frans Carlier, Maastricht

©2008, Lukas Been; Groningen, the Netherlands

All rights reserved. No part of this publication may be reproduced, stored in a retrieval system, or transmitted, in any form or by any means, electronically, mechanically, by photocopying, recording, or otherwise, without the prior written consent of the author.

RIJKSUNIVERSITEIT GRONINGEN

Imaging proliferation with [^{18}F]FLT-PET: therapy evaluation studies

Proefschrift

ter verkrijging van het doctoraat in de
Medische Wetenschappen
aan de Rijksuniversiteit Groningen
op gezag van de
Rector Magnificus, dr. F. Zwarts,
in het openbaar te verdedigen op
woensdag 28 mei 2008
om 14.45 uur

door

Lukas Berend Been

geboren op 19 april 1976
te Vlagtwedde

| | |
|--------------------|----------|
| Centrale | U |
| Medische | M |
| Bibliotheek | C |
| Groningen | G |

Promotores Prof. dr. H.J. Hoekstra
Prof. dr. P.H. Elsinga

Copromotor Dr. A.J.H. Suurmeijer

Beoordelingscommissie Prof. dr. J.Th.M. Plukker
Prof. dr. R.A. Dierckx
Prof. dr. O.S. Hoekstra



Contents

| | | | | |
|-----------|---|---|-----|--------------------------|
| 1 | Introduction and outline of the thesis | ■ | 7 | |
| 2 | [¹⁸ F]FLT-PET in oncology; current status and opportunities <i>Eur J Nucl Med and Mol Imaging 2004;12:1659-1672</i> | ■ | 17 | |
| 3 | Positron emission tomography in patients with breast cancer using [¹⁸ F]-3'-deoxy-3'-fluoro-L-thymidine ([¹⁸ F]-FLT) <i>Eur J Surg Oncol 2005;32:39-43</i> | ■ | 45 | |
| 4 | Early response of sigma receptor ligands and metabolic PET tracers to three forms of chemotherapy: an in vitro study in glioma cells <i>J Nucl Med 2006;47:1538-1545</i> | ■ | 55 | |
| 5 | [¹⁸ F]Fluorodeoxythymidine PET for evaluating hyperthermic isolated limb perfusion for locally advanced soft-tissue sarcomas <i>J Nucl Med 2007;48:367-382</i> | ■ | 75 | <input type="checkbox"/> |
| 6 | [¹⁸ F]FLT-PET in patients with metastatic nonseminomatous testicular germ cell tumors <i>Submitted for publication</i> | ■ | 91 | <input type="checkbox"/> |
| 7 | [¹⁸ F]FLT-PET and [¹⁸ F]FDG-PET in the evaluation of radiotherapy for laryngeal cancer <i>Submitted for publication</i> | ■ | 103 | <input type="checkbox"/> |
| 8 | Summary and future perspectives | ■ | 115 | <input type="checkbox"/> |
| | Samenvatting | ■ | 125 | |
| 9 | Dankwoord | ■ | 135 | <input type="checkbox"/> |
| 10 | Curriculum vitae | ■ | 139 | <input type="checkbox"/> |







**Introduction
and
outline of
the thesis**



Imaging in oncology

The incidence of various types of cancer is rising in the developed world. Detection, staging the disease and evaluating the response to therapy largely depends on conventional imaging modalities such as simple X-rays (chest X-ray, mammography), computerized tomography (CT), magnetic resonance imaging (MRI) and ultrasonography (US). With these imaging modalities, excellent anatomical information can be obtained. However, for many indications, anatomical information is not enough and functional information would provide better answers to the clinical questions of physicians. Examples of functional imaging techniques in oncology are bone scintigraphy, sentinel lymph node scintigraphy, single photon emission tomography (SPECT) and positron emission tomography (PET). These imaging modalities offer only limited anatomical information, whereas they can visualize different metabolic pathways in vivo non-invasively. Recent developments in imaging in oncology are the combination of both anatomical and functional imaging modalities, resulting in PET/CT, PET/MR and SPECT/CT scanners.

Positron emission tomography

History

The basis of positron emission tomography was established in 1934 when Irene Curie and Frédéric Joliot discovered they could produce radioactivity, for which they both received the Nobel Prize. In 1951, William Sweet at the Massachusetts General Hospital was the first to detect positron emission in a patient ¹. In the 1970s only ten research groups were investigating positron emission, among which the group from Groningen. It took until 1973 before the first PET camera was developed (Washington University, MO) and since then, subsequent developments have included refinements in algorithms, improved crystal detector materials and enormous improvements in computer power. However, the basic principles of the PET camera, developed in the early 1970s, is still the same today. In the last decades, PET has evolved into an increasingly popular imaging modality in oncological practice.

Technique

PET uses positron-emitting radionuclides that are incorporated into radiopharmaceuticals (tracers) to visualize metabolic pathways. Radionuclides are produced in a cyclotron by bombarding a target with accelerated particles (protons or deuterons). The most frequently applied radionuclides for PET imaging are [¹⁵O], [¹¹C], [¹³N], and [¹⁸F], with half-lives ranging from 2 to 110 minutes.



Introduction and outline of the thesis

Positron emitting radionuclides are unstable because of a surplus of positively charged particles. To reach stability, they either capture an electron or emit a positron. When a positron is emitted, it travels for a small distance (range) until it collides with an electron. The two particles annihilate, resulting in the emission of two photons at an angle of 180° with 511 keV of energy (Fig. 1).

A PET camera is composed of a ring of detectors. It makes use of the fact that two photons are emitted in opposite directions, since it only gives a signal when opposite detectors capture photons within 12 nanoseconds (line of response, LOR). Using complicated mathematical techniques, all LORs are reconstructed into an image of the distribution of radioactivity in the patient. The spatial resolution that can be obtained by modern PET cameras is approximately 4-5 mm. However, the intrinsic spatial resolution of the PET technique is limited because of the distance between emitting the positron and collision with an electron (range), which ranges from a few millimeters to less than 1 mm for [^{18}F].

To obtain quantitative PET images, several corrections must be applied. Dead-time and randoms corrections are usually performed by the PET system itself. Scatter correction is performed during reconstruction and is preferably performed using a scatter model based on the activity distribution and tissue densities. Tissue density can be obtained from the attenuation scan, which must also be performed to correct for the absorption of radiation in the body. Approximately 10% of 511 keV photons are lost for each centimeter of tissue traversed. Attenuation causes an underestimation of the true number of counts by 80-95%, depending on the body region. Attenuation

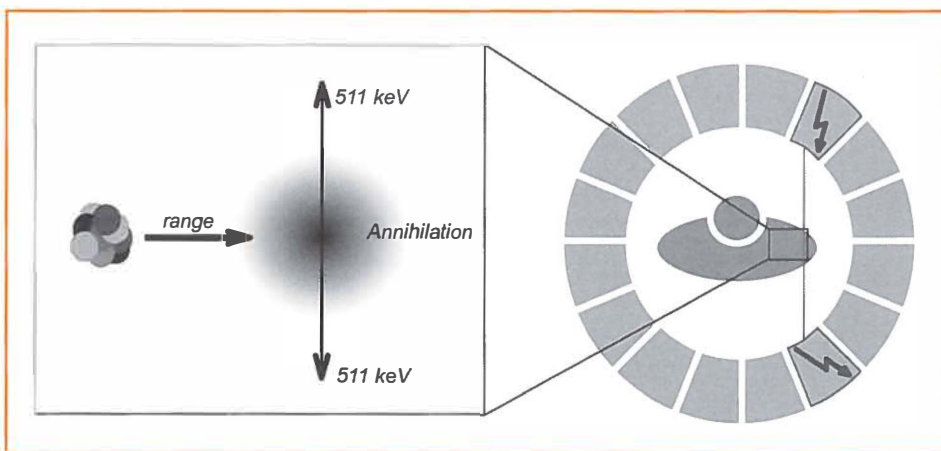


Figure 1

Basic principle of positron emission and positron emission tomography

correction is accomplished by applying a correction factor for the number of measured events for each LOR. For example, if 10 events were recorded in one LOR and it is known that only 10% of all photon pairs survive, then the attenuation correction is $10 \times 10 = 100$ events. There are three methods with which the correction factors can be obtained:

- By calculation, presuming the outer contour of the body is known and assuming a uniform tissue attenuation. This method is used primarily in brain imaging.
- By an orbiting radionuclide source. In conventional PET systems a ^{68}Ge source is commonly used.
- By using CT data. This method is used in modern PET/CT systems.

Finally, PET systems must be calibrated so that images can be expressed in Bq/cc or mmol/cc.

Two methods are used for quantification of metabolic processes with PET. The gold standard is the use of kinetic modeling. This method allows an absolute quantification (for example in mmol/ml/min). However, this technique requires dynamic scanning (usually combined with arterial sampling) which is an additional burden for the patient. Alternatively, the standardized uptake value (SUV) can be calculated as a surrogate measure. The SUV is the ratio between the measured radioactivity in tissue and the radioactivity in tissue in case it was distributed homogeneously in the body. This method is less time-consuming and more patient-friendly. Therefore, this method has become very popular, but one has to be cautious since the SUV is influenced by the patient's conditions (e.g. perfusion, metabolism) as well as by the acquisition protocol and the reconstruction parameters. This also requires special caution if SUV values are to be compared between different PET facilities.

PET scans are displayed on computer screens, after which visual and (semi)quantitative analysis can take place. A region of interest (ROI) can be placed in a plane over areas of abnormal tracer uptake. Three-dimensional volumes of interest (VOI) can also be used for SUV calculation. In this ROI or VOI, maximum and mean SUV can be calculated.

Radiopharmaceuticals (tracers)

A wide variety of PET tracers has been developed and is still used in oncological imaging, each using different metabolic pathways for visualizing tumors.

^{18}F FDG is the most widely used PET tracer, using the glucose metabolism for PET imaging. It is the only approved PET tracer for routine clinical use in oncology. ^{18}F FDG is a glucose analogue that enters the cell by active transport, after which it is phosphorylated by hexokinase. After phosphorylation, ^{18}F FDG is trapped in the cell. In tumor cells, hexokinase activity is increased, leading to increased ^{18}F FDG uptake.

Other metabolic properties of malignant tissue have been subject for PET imaging. For example, tissue blood flow can be visualized and measured using ^{15}O - H_2O . Hypoxia is visualized using ^{18}F fluoromisonidazole (^{18}F FMISO) and more recently



[¹⁸F]fluoroazomycin arabinoside ([¹⁸F]FAZA) ³. Protein synthesis has been studied with [¹¹C]methionine, [¹¹C]tyrosine and [¹⁸F]fluoroethyltyrosine ^{4,5}. [¹¹C]choline is currently used for imaging prostate cancer ⁶. Recently, [¹⁸F]DOPA and [¹¹C]-5-HTP have been introduced for detection of neuroendocrine tumors, and first reports show promising results ^{7,8}.

Tumor cell proliferation was firstly visualized in PET imaging using [¹¹C]thymidine ⁹. Since then, several proliferation tracers have been investigated for use in oncology (for example [¹⁸F]FMAU and [¹⁸F]FLT). Each of these tracers has advantages and disadvantages. [¹¹C]thymidine has the advantage of being the native compound. However, its rapid degradation into metabolites makes routing clinical use difficult, since one has to take all metabolites into account in kinetic models. Furthermore, [¹¹C]-labeling hampers widespread use of this tracer because of the short half-life. Both [¹⁸F]FMAU and [¹⁸F]FLT can be used to image proliferation *in vivo*. These tracers can be distributed commercially to other PET facilities owing to the longer half-life of [¹⁸F].

[¹⁸F]FLT as a proliferation tracer proliferation

Unlabeled FLT was introduced in the late 1980s as an antiviral agent for the treatment of HIV and AIDS ¹⁰. However, after the report of serious toxicity and two deaths in a phase II clinical trial, further investigations were abandoned. In 1997, Grierson and Shields ¹¹ described the radiolabelling of no-carrier added [¹⁸F]FLT and in 1998, [¹⁸F]FLT was firstly applied for PET imaging ¹².

Visualizing and measuring the proliferation rate of tumor cells is an attractive target for PET imaging, since it offers the potential to differentiate between malignant and benign lesions, measure the tumor aggressiveness *in vivo* and measure the response to therapy.

Proliferating cells synthesize DNA in the S phase of the cell cycle. There are two DNA synthetic pathways: the endogenous or 'de novo' pathway and the exogenous or 'salvage' pathway (Fig. 2).

[¹⁸F]FLT is a thymidine analogue, which uses the 'salvage' pathway for PET imaging. After [¹⁸F]FLT is taken up by the cell by diffusion and facilitated transport, it is phosphorylated by thymidine kinase 1 (TK₁) into [¹⁸F]FLT-monophosphate ([¹⁸F]FLT-MP), causing intracellular entrapment (Fig. 3).

In quiescent cells, TK₁ activity is virtually absent, whereas it increases sharply in the late G₁ and S phase of proliferating cells. It has been reported that in some malignant cells, TK₁ activity is 3 to 4 times higher than in normal cells. Furthermore, TK₁ activity is not limited to G₁ and S phase, but it is also active in other phases of the cell cycle. Therefore, TK₁ activity and [¹⁸F]FLT uptake can be seen as a marker of the proliferation rate of tumors.

Outline of the thesis

This thesis is part of a larger research project that was supported by a grant of *the Dutch Cancer Society* (grant 2000-2299).

As a part of this grant, Cobben et al. previously investigated the value of [¹⁸F]FLT in detection and staging of different tumor types ¹³⁻¹⁶. Furthermore, Van Waarde et al. used an inflammation model to compare [¹⁸F]FLT and [¹⁸F]FDG in differentiating between infection and tumor tissue ¹⁷.

The emphasis of the studies in this thesis lies on the evaluation of therapy with [¹⁸F]FLT.

- In **Chapter 2**, the currently available literature regarding [¹⁸F]FLT-PET is reviewed.
- **Chapter 3** describes the feasibility of [¹⁸F]FLT to visualize breast cancer and axillary lymph node metastases.
- The response of different PET tracer to three forms of chemotherapy in glioma cells is described in **Chapter 4**.
- In **Chapter 5**, the response to hyperthermic isolated limb perfusion in patients with locally advanced soft tissue sarcomas is evaluated with [¹⁸F]FLT-PET.
- The uptake of [¹⁸F]FLT in retroperitoneal lymph-node metastases in patients with nonseminomatous testicular germ cell tumors before and after chemotherapy is investigated in **Chapter 6**.
- [¹⁸F]FDG-PET and [¹⁸F]FLT-PET are compared in patients with primary laryngeal cancer undergoing curative radiotherapy in **Chapter 7**.

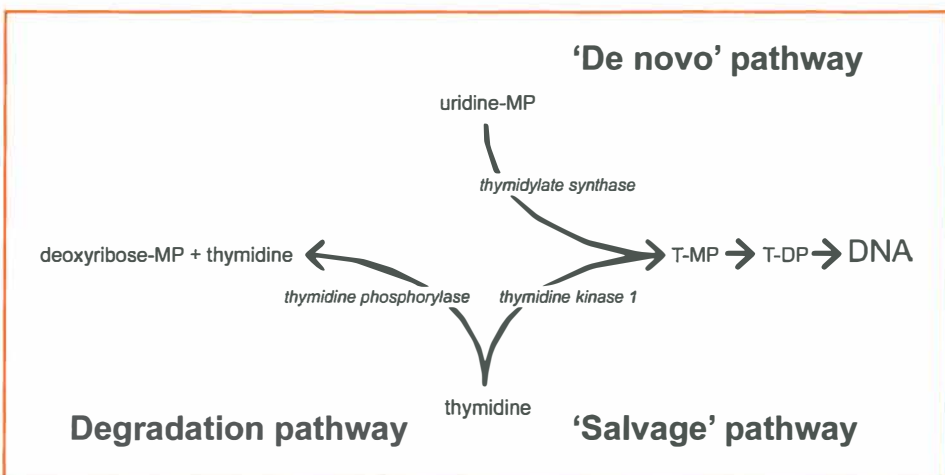


Figure 2
Two different DNA synthetic pathways

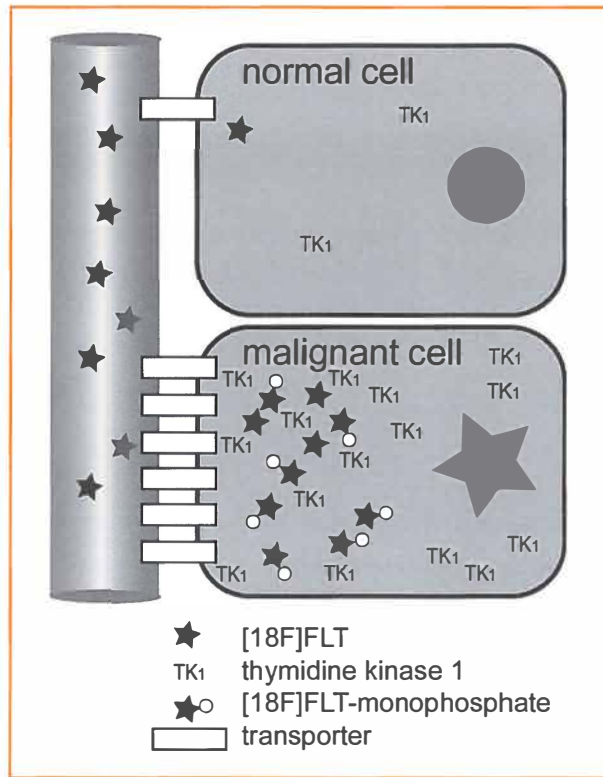


Figure 3

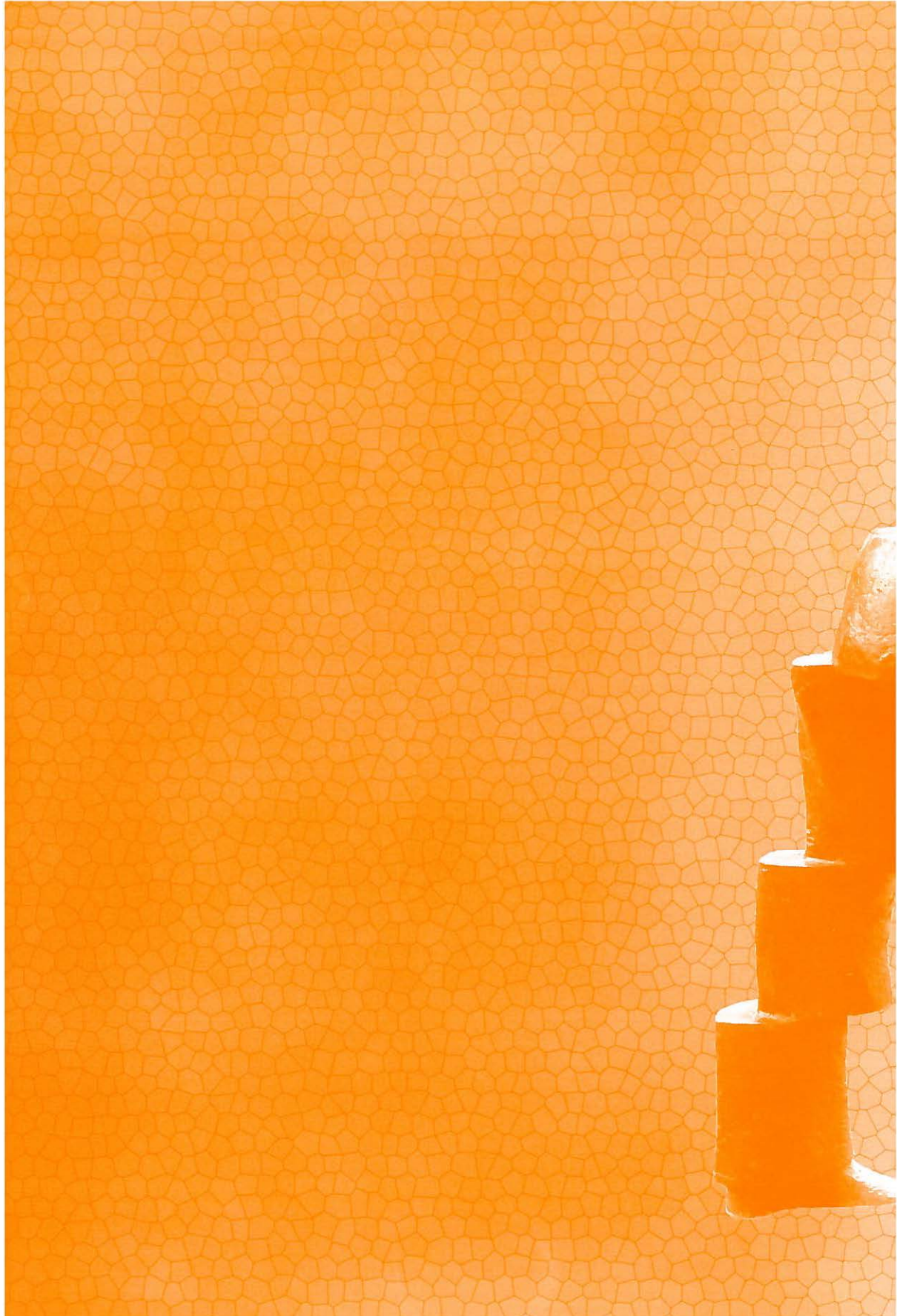
Uptake mechanism and phosphorylation of [¹⁸F]FLT

References

1. SWEET WH. The uses of nuclear disintegration in the diagnosis and treatment of brain tumor. *N Engl J Med* 1951;245:875-878.
2. Lewis JS and Welch MJ. PET imaging of hypoxia. *Q J Nucl Med* 2001;45:183-188.
3. Pieter M, Machulla HJ, Picchio M, Reischl G, Ziegler S, Kumar P et al. Hypoxia-specific tumor imaging with ¹⁸F-fluoroazomycin arabinoside. *J Nucl Med* 2005;46:106-113.
4. Weber WA, Wester HJ, Grosu AL, Herz M, Dzewas B, Feldmann HJ et al. O-(2-[¹⁸F]fluoroethyl)-L-tyrosine and L-[methyl-¹⁴C]methionine uptake in brain tumours: initial results of a comparative study. *Eur J Nucl Med* 2000;27:542-549.
5. Jager PL, Vaalburg W, Pruim J, de Vries EG, Langen KJ, and Piers DA. Radiolabeled amino acids: basic aspects and clinical applications in oncology. *J Nucl Med* 2001;42:432-445.
6. Jong de IJ, I, Pruim J, Elsinga PH, Vaalburg W, and Mensink HJ. Visualization of prostate cancer with ¹¹C-choline positron emission tomography. *Eur Urol* 2002;42:18-23.
7. Hoegerle S, Althoefer C, Ghanem N, Koehler G, Waller CF, Scheruebl H et al. Whole-body ¹⁸F dopa PET for detection of gastrointestinal carcinoid tumors. *Radiology* 2001;220:373-380.
8. Koopmans KP, de Vries EG, Kema IP, Elsinga PH, Neels OC, Sluiter WJ et al. Staging of carcinoid tumours with ¹⁸F-DOPA PET: a prospective, diagnostic accuracy study. *Lancet Oncol* 2006;7:728-734.

9. Christman D, Crawford EJ, Friedkin M, and Wolf AP. Detection of DNA synthesis in intact organisms with positron-emitting (methyl-¹¹C)thymidine. *Proc Natl Acad Sci U S A* 1972;69:988-992.
10. Hartmann H, Vogt MW, Durno AG, Hirsch MS, Hunsmann G, and Eckstein F. Enhanced in vitro inhibition of HIV-1 replication by 3'-fluoro-3'-deoxythymidine compared to several other nucleoside analogs. *AIDS Res Hum Retroviruses* 1988;4:457-466.
11. Grierson JR and Shields AF. Radiosynthesis of 3'-deoxy-3'-[¹⁸F]fluorothymidine: [¹⁸F]FLT for imaging of cellular proliferation in vivo. *Nucl Med Biol* 2000;27:143-156.
12. Shields AF, Grierson JR, Dohmen BM, Machulla HJ, Stayanoff JC, Lawhorn-Crews JM et al. Imaging proliferation in vivo with [F-¹⁸]FLT and positron emission tomography. *Nat Med* 1998;4:1334-1336.
13. Cobben DC, Jager PL, Elsinga PH, Maas B, Suurmeijer AJ, and Hoekstra HJ. 3'-[¹⁸F]-Fluoro-3'-Deoxy-L-Thymidine: A New Tracer for Staging Metastatic Melanoma? *J Nucl Med* 2003;44:1927-1932.
14. Cobben DC, Elsinga PH, Suurmeijer AJ, Vaalburg W, Maas B, Jager PL et al. Detection and grading of soft tissue sarcomas of the extremities with [¹⁸F]-3'-fluoro-3'-deoxy-L-thymidine. *Clin Cancer Res* 2004;10:1685-1690.
15. Cobben DC, van der Laan BF, Maas B, Vaalburg W, Suurmeijer AJ, Hoekstra HJ et al. ¹⁸F-FLT PET for Visualization of Laryngeal Cancer: Comparison with [¹⁸F]-FDG PET. *J Nucl Med* 2004;45:226-231.
16. Cobben DC, Elsinga PH, Hoekstra HJ, Suurmeijer AJ, Vaalburg W, Maas B et al. Is ¹⁸F-3'-fluoro-3'-deoxy-L-thymidine useful for the staging and restaging of non-small cell lung cancer? *J Nucl Med* 2004;45:1677-1682.
17. Van Waarde A, Cobben DCP, Suurmeijer AJH, Maas B, Vaalburg W, De Vries EFJ et al. Selectivity of 3'-deoxy-3'-[¹⁸F]fluorothymidine (FLT) and 2-[¹⁸F]fluoro-2-deoxy-D-glucose (FDG) for tumor versus inflammation in a rodent model. *J Nucl Med* 2004;45:695-700.







[¹⁸F]FLT-PET in oncology; current status and opportunities

review article

*Lukas B. Been^{1,2}, Albert J.H. Suurmeijer³, David C.P. Cobben^{1,2},
Pieter L. Jager³, Harald J. Hoekstra¹, Philip H. Elsinga²*

*¹Department of Surgical Oncology; ²Department of Nuclear
Medicine and Molecular Imaging; ³Department of Pathology
and Laboratory Medicine; University Medical Center
Groningen, University of Groningen*

Eur J Nucl Med and Mol Imaging 2004;12:1659-1672

2

Abstract

In recent years, [¹⁸F]-fluoro-3'-deoxy-3'-L-fluorothymidine ([¹⁸F]FLT) has been developed as a proliferation tracer. Imaging and measuring proliferation with PET could provide us with a non-invasive staging tool and a tool to monitor the response to anticancer treatment.

In this review, the basis of [¹⁸F]FLT as a proliferation tracer is discussed. Furthermore, an overview of the current status of [¹⁸F]FLT-PET research is given. The results of this research show that although [¹⁸F]FLT is a tracer that visualizes cellular proliferation, it also has certain limitations. In comparison with the most widely used PET tracer, [¹⁸F]FDG, [¹⁸F]FLT uptake is lower in most cases. Furthermore, [¹⁸F]FLT uptake does not always reflect the proliferation rate of tumor cell, for example during of shortly after certain chemotherapy regimens.

The opportunities provided by, and the limitations of [¹⁸F]FLT as a proliferation tracer are addressed in this review and directions are given for further research, taking into account the strong and weak points of the new tracer.

Introduction

During the past few years, [^{18}F]-fluoro-3'-deoxy-3'-L-fluorothymidine ([^{18}F]FLT) has attracted a lot of attention by many research groups as a proliferation tracer for positron emission tomography (PET). In this review, the basis of [^{18}F]FLT as a proliferation tracer is discussed. Furthermore, an overview is given of the current status of preclinical and clinical [^{18}F]FLT research. Finally, the limitations of [^{18}F]FLT as a proliferation tracer, and the opportunities that it affords, are addressed.

The basis of [^{18}F]FLT as a proliferation tracer

In contrast to quiescent cells, proliferating cells synthesize DNA in the S phase of the cell cycle. Imaging and measuring proliferation in vivo with PET is a very attractive target for both preclinical research and oncological practice, because it could offer the possibility of differentiating between benign and malignant tissues, measuring tumor aggressiveness and evaluating early response to therapy.

The pyrimidine analogue thymidine is incorporated in DNA but not in RNA. Therefore, the use of [^{18}F]FLT for PET imaging seems logical. [^{18}F]FLT is taken up by the cell via both passive diffusion and facilitated transport by Na^+ -dependent carriers. Subsequently, [^{18}F]FLT is phosphorylated by thymidine kinase 1 (TK_1) into [^{18}F]FLT-monophosphate, after which it is trapped in the cell (Fig. 1). TK_1 is a principal enzyme in the salvage pathway of DNA synthesis. The enzymatic activity of TK_1 is virtually absent in quiescent cells, but in proliferating cells it reaches a maximum in the late G_1 and S phase of the cell cycle ¹. Therefore, the phosphorylation by TK_1 forms the basis of [^{18}F]FLT as a proliferation tracer.

It has been reported that TK_1 activity is three to four times higher in malignant cells (U1-Mel, HTB-152 and Hep-2 cells) than in benign cells (GM 2906A, GM2936B, GM2305 cells) ². Moreover tumor cells can carry mutations in the carboxyl terminus of TK_1 . This can cause impaired degradation of TK_1 after the M phase and can result in deregulation of TK_1 activity ³. These changes in TK_1 activity in cancer cells will lead to increased phosphorylation and intracellular trapping of [^{18}F]FLT in malignant cells throughout the cell cycle.

Does this make [^{18}F]FLT a reliable proliferation marker? Clearly, some issues need to be addressed. As mentioned above, [^{18}F]FLT uses the salvage pathway of DNA synthesis, but it is not incorporated into DNA. In vitro research comparing [^3H]FLT uptake with [^3H]thymidine uptake showed that after 60 min of incubation, more than 90% of [^3H]thymidine but only 0.2% of [^3H]FLT was incorporated into the DNA of A549 lung cancer cells. [^3H]FLT is not incorporated into DNA because it acts as a chain terminator



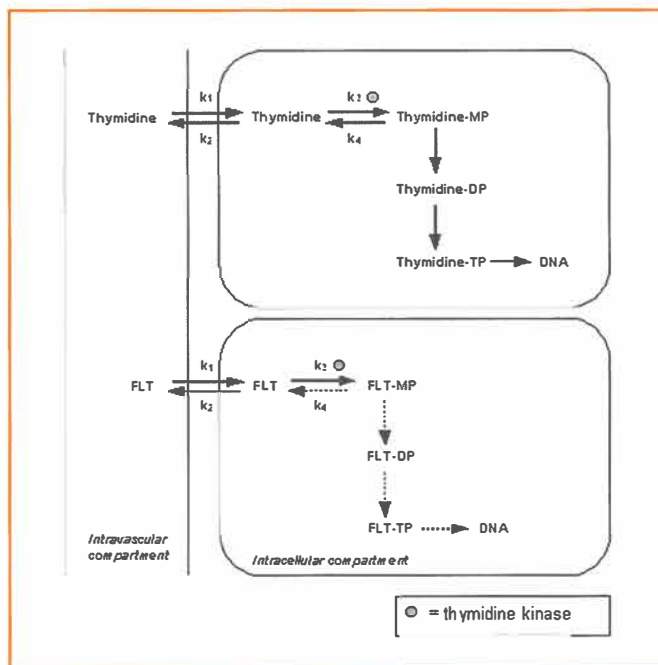


Figure 1
 Uptake mechanism of thymidine and [¹⁸F]FLT. After uptake, [¹⁸F]FLT is phosphorylated by TK₁ and trapped intracellularly. Incorporation in DNA is limited

owing to the absence of 3'-hydroxyl. [³H]FLT uptake therefore only visualizes the first step of the salvage pathway of DNA synthesis. However, [³H]thymidine uptake and [³H]FLT uptake showed a strong correlation ($r=0.88$; $P<0.0001$), suggesting that [³H]FLT uptake represents the totality of the salvage pathway ⁴.

Another question that needs to be answered is: Do [¹⁸F]FLT uptake and TK₁ activity always reflect cellular proliferation? It is a well known fact that different tumors vary in respect of the relative contributions of the salvage pathway and the de novo pathway of DNA synthesis ^{5,6}. For instance, Schwartz et al. ⁷ showed that proliferation in two out of six tumor cell lines was less dependent on TK₁ activity and, subsequently, no significant correlation was found between TK₁ activity and the S phase fraction of cells (SPF). Furthermore, it has to be kept in mind that when tumor cells are treated with chemotherapeutic agents as 5-fluorouracil and methotrexate, TK₁ activity remains high, whereas tumor cell proliferation is impaired ⁸. 5-fluorouracil and methotrexate cause cells to arrest in S phase, leading to increased TK₁ activity ^{9,10}. Another mechanism is that some chemotherapeutic agents activate the salvage pathway of DNA synthesis, causing increased TK₁ activity. Thus, in these situations, [¹⁸F]FLT uptake does not reflect cellular proliferation.

There are several methods to determine cellular proliferation in tumor tissue. Immunostaining of Ki-67 with MIB-1 (Ki-67 index) is widely used in oncological research and also in [¹⁸F]FLT-PET studies (see Table 1). The protein Ki-67 is expressed mainly in the S, G₂ and M phases of the cell cycle¹¹. As mentioned above, the enzymatic activity of TK₁ is also mainly present in the S phase. Another way to determine cellular proliferation is by estimating the percentage of cells in S phase by flow cytometry. However, by excluding proliferating cells in G₁ and G₂ phases, the true percentage of proliferating cells is possibly underestimated. To our knowledge, only one study has compared these proliferation markers¹². In this study, in which 185 breast cancer tumor samples were evaluated, a linear relation was found between Ki-67 index and SPF. However, TK₁ and Ki-67 index showed a non-linear relation. This supports the notion that in malignant cells, the regulation of TK₁ enzymatic activity is not always as cell cycle dependent as it is in normal proliferating cells. Therefore, it would be useful if SPF, Ki-67 index and TK₁ activity (or TK₁ immunoassay) were determined in tumor samples in future [¹⁸F]FLT-PET studies, since this would allow clarification of the relations between these markers and [¹⁸F]FLT uptake.

Table 1
[¹⁸F]FLT as a proliferation tracer

| Tumor type (N=) | Proliferation marker | Correlation | Reference |
|-----------------------------|----------------------|------------------------------|-------------------------------------|
| SPN (N=30) | Ki-67 | r = 0.87 ^a | Buck et al. ⁴⁴ |
| SPN (N=11) | Ki-67 | r = 0.84 ^a | Veselle et al. ⁴⁵ |
| Malignant lymphoma (N=9) | Ki-67 | r = 0.95 ^a | Wagner et al. ⁶⁸ |
| SPN (N=26) | Ki-67 | r = 0.92 ^a | Buck et al. ⁴⁹ |
| Colorectal carcinoma (N=13) | Ki-67 | r = 0.8 ^a | Francis et al. ⁶⁶ |
| Lymphoma (N=26) | Ki-67 | r = 0.9 ^a | Buck et al. ⁶⁹ |
| Mice; lymphoma | BRDU | r = 0.63 ^a | Wagner et al. ⁶⁸ |
| Soft tissue sarcoma (N=17) | Mitotic count; Ki-67 | r = 0.55 – 0.75 ^a | Cobben et al. ⁷¹ |
| Breast cancer (N=12) | Ki-67 | R ² = 0.01 | Smyczek-Gargya et al. ⁵³ |

^a p-level at least <0.05



Toxicity data of [¹⁸F]FLT

In the late 1980s, unlabeled FLT (alovudine) was investigated as an antiviral agent in the treatment of HIV and AIDS ¹³. For this reason, the toxicity of FLT was investigated in a phase II clinical trial by Flexner et al. ¹⁴ In this study, serious (grade 3) haematological side effects were seen at a mean cumulative drug exposure of 417 ng h/mL. In some patients a mild peripheral neuropathy occurred at 50 ng h/mL. However, this randomized concentration controlled trial was terminated early after the unexpected death of two patients. Both patients had developed hepatic failure after several weeks of FLT treatment. One patient received 200 ng h/mL and the other patient a fixed dose of 10 mg/24 h. It can be concluded that administration of therapeutic dosages of FLT for several weeks could be responsible for haematological side-effects, impaired liver function and peripheral neuropathy. For most [¹⁸F]FLT-PET studies however, 200-400 MBq [¹⁸F]FLT is used with a specific activity of at least 10 TBq/mmol [¹⁸F]FLT. In general, a bolus of maximum 10 µg of [¹⁸F]FLT is injected. Therefore, no major side-effects are expected in patients undergoing an [¹⁸F]FLT-PET scan. However, for safety reasons, exclusion criteria are recommended: the patient's haematological parameters and liver and kidney function test results should be within the normal range before an [¹⁸F]FLT-PET scan is performed, and there should be no history of peripheral neuropathy. A few weeks after the scan, these blood tests should be repeated to monitor any changes.

Synthesis of [¹⁸F]FLT

The preparation of [¹⁸F]FLT is still in the process of optimization. The different research groups use different labeling procedures. Two labeling strategies can be distinguished based on structural differences of the precursor: (1) 5'-O- and N-protected nosylate derivatives of thymidine and (2) 2,3'-anhydrothymidine derivatives (Fig. 2).

The first method, using the nosylate strategy, was published by Grierson and Shields ¹⁵. The precursor, protected on the 5'-O and the N-position with 4,4'-dimethoxytrityl and dimethoxybenzyl, respectively, was prepared in seven reaction steps from L-thymidine. After the nucleophilic fluorination step (100 °C, 10 min) the protecting groups were removed by oxidation with cerium ammonium nitrate (CAN). Decay corrected radiochemical yields of 13% with a synthesis time of 100 min were reported. A great disadvantage of this first method was the appearance of precipitates after the CAN oxidation, leading to automation problems and losses of radioactivity in the filtration step. Other groups replaced the N-dimethoxybenzyl protective group for an N-Boc group ¹⁶⁻¹⁹, enabling easy deprotection with hydrochloric acid. As a result, no precipitation occurred. Variation of the leaving group showed that the nosylate compound

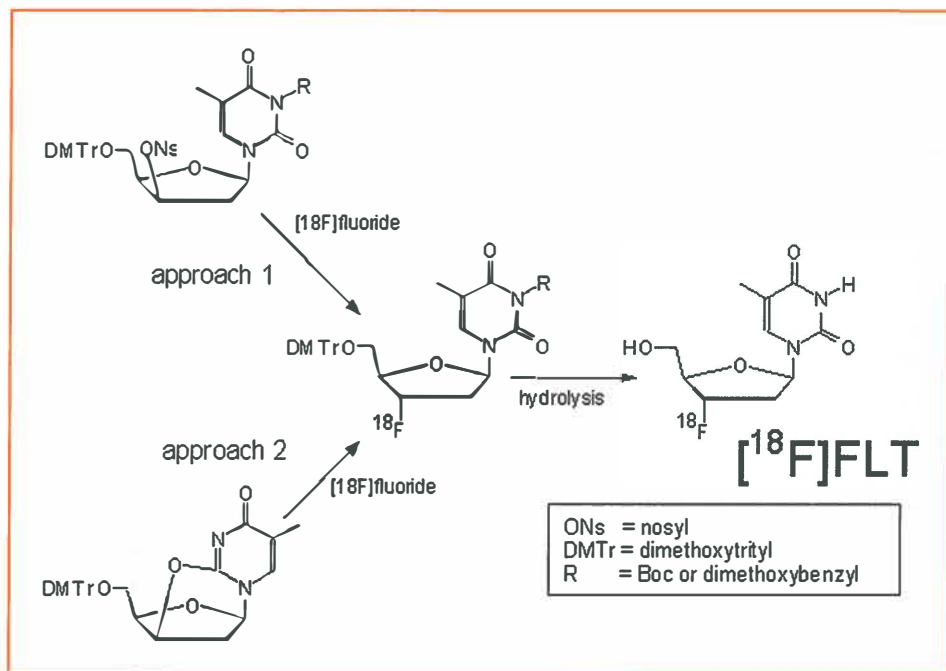


Figure 2

Two different approaches for the synthesis of [^{18}F]FLT

gave higher radiochemical yields than the tosylate or mesylate ¹⁶. This latter procedure could easily be automated with a commercially available synthesis module ¹⁷. Radiochemical yields were 11.5% (EOB) using 10 mg precursor and 33% with 40 mg precursor. The synthesis time was 40 min.

Further attempts to optimize the procedure showed that protection of the 5'-O position was not essential ¹⁸. Variation of temperature, precursor concentration and reaction time and comparison of 5'-O-unprotected and -protected precursor gave the highest radiochemical yields of about 40% (EOB) using 30 mg of precursor. Fluorinations lasting longer than 5 min resulted in lower radiochemical yields. Unprotected precursor required a higher reaction temperature than the protected (130 °C vs. 110 °C). The total synthesis time was 60 min.

The optimized procedures thus far required high amounts of precursor, which can cause problems at the stage of preparative high performance liquid chromatography (HPLC) purification. The use of an ionic liquid to catalyze the nucleophilic fluorination made it possible to decrease the amount of precursor to 5 mg ¹⁹. The obtained radiochemical yields were 30% with fluorination conditions of 120°C for 15 min. Synthesis time was 60 min.

Regarding the second strategy to prepare [¹⁸F]FLT, Machulla et al.²⁰ published a simplified one pot synthesis a few months after the first publication of Grierson and Shields¹⁵. To circumvent a lengthy seven-step procedure to prepare precursor material, 2,3'-anhydrothymidine could be prepared in one step from thymidine and the DMTr-protected anhydrothymidine in two steps. Furthermore, no protection at the pyrimidine N atom was required. Using anhydrothymidine as precursor and fluorination conditions of 130°C for 30 min, a radiochemical yield of 5.3% was reported. For DMTr-protected anhydrothymidine the radiochemical yield was 14.3% using 160°C for 10 min, followed by deprotection with 1N HCl. Although the reported radiochemical yields are relatively low as compared to the nosylate approach, many research groups still use this method. An explanation for the low radiochemical yield was found in the fact that the anhydro compound undergoes an elimination reaction upon heating. For this reason reaction times of >10 min seem to be useless. Cleij et al.²¹ reported that the yield could be improved by first dissolving the dried [¹⁸F]fluoride in dimethyl sulfoxide (DMSO) and then adding the precursor in DMSO.

For both synthetic strategies, precursors are commercially available and are relatively stable. Based on the results as published in the literature until now, both methods have become relatively straightforward and are suitable for automation. The radiochemical yields are higher for the first method. A great improvement in the procedure would ensue if the final preparative HPLC-purification could be replaced by a sequence of sample preparation cartridges, as is being used in the preparation of 2-[¹⁸F]-fluoro-2-deoxy-D-glucose ([¹⁸F]FDG).

A question that needs then to be solved is whether 'cold' thymidine, originating from hydrolyzed, unreacted precursor, may be safely administered to humans. Alternatively, a cartridge-based separation method for thymidine and [¹⁸F]FLT should be developed. Radiochemical yields should be increased further to allow offsite production of [¹⁸F]FLT and distribution of the tracer to PET facilities without a cyclotron, as is being done with [¹⁸F]FDG.

Preclinical studies

Preclinical [¹⁸F]FLT studies comprise tumor cell line studies and animal studies. Some of these studies have investigated the claim that [¹⁸F]FLT, as a proliferation tracer, is a more cancer-specific tracer than [¹⁸F]FDG. Moreover, in some studies, the value of [¹⁸F]FLT for evaluating the response to different types of therapy has been evaluated.

Specificity of [¹⁸F]FLT

Several research groups have postulated that [¹⁸F]FLT will prove to be a more cancer specific tracer than [¹⁸F]FDG. In SW-979 and BxPc-3 pancreatic cancer cells, Seitz et

al.²² showed that [¹⁸F]FLT uptake was 18.4% and 5.2% of the administered radioactivity, respectively, while [¹⁸F]FDG uptake was only 0.6% and 0.3% of the administered radioactivity. In normal pancreatic lobules, no increased [¹⁸F]FLT uptake was seen, whereas [¹⁸F]FDG did show a time-dependent increased uptake, suggesting that [¹⁸F]FLT is more tumor specific for pancreatic cancer. However, there are no in vivo studies in which [¹⁸F]FLT-PET and [¹⁸F]FDG-PET have been compared in patients with pancreatic cancer. When [¹⁸F]FLT was introduced as a proliferation tracer, it was claimed that [¹⁸F]FLT, in contrast to [¹⁸F]FDG, would not show uptake in inflammatory tissues. Carter et al.²³ studied rats with either infection or tumor with [¹⁸F]FDG and [¹⁸F]FLT. Infection was established by injecting *Escherichia coli* in the thigh and the tumor consisted of a sarcoma in the thigh. The tumor to non-tumor ratio (T/NT) was greater for [¹⁸F]FDG than for [¹⁸F]FLT in tumor-bearing rats (7.39 vs. 2.76). [¹⁸F]FDG accumulation in infectious tissue was lower than in the tumors, but still elevated (ratio 3.29). In contrast, [¹⁸F]FLT accumulation in infectious tissue was only slightly elevated as compared with the normal tissue (ratio 1.14). Other preliminary results of Lee et al.²⁴ support the finding that [¹⁸F]FDG uptake in tumors is higher than [¹⁸F]FLT uptake, but again, selectivity for neoplasms is greater for [¹⁸F]FLT than for [¹⁸F]FDG. A recent study by Van Waarde et al.²⁵ compared [¹⁸F]FLT and [¹⁸F]FDG uptake in rats with tumor and inflammation. Rats were injected with C6 glioma cells in the right shoulder. Inflammation was established by injecting turpentine in the left calf of the rats. The [¹⁸F]FDG tumor-to-muscle ratio was higher than the [¹⁸F]FLT tumor-to-muscle ratio (13 vs. 8) [¹⁸F]FDG showed increased uptake at the site of inflammation whereas [¹⁸F]FLT did not.

These data are the only available data deriving from studies in which [¹⁸F]FLT uptake and [¹⁸F]FDG uptake have been compared in inflammatory tissues. They confirm that [¹⁸F]FLT is a more cancer-specific tracer and they suggest that fewer false-positive [¹⁸F]FLT-PET scans are expected in cancer patients. However, this property of [¹⁸F]FLT was investigated only in acute inflammation models. It is unknown whether [¹⁸F]FLT also does not show uptake in chronic inflammatory tissues. Furthermore, the differentiation between tumor and (acute or chronic) inflammation has not yet been evaluated in humans.

Treatment evaluation with [¹⁸F]FLT-PET

Measuring tumor proliferative activity by [¹⁸F]FLT-PET offers great potential for assessing the viability of tumor cells during or early after treatment. In cancer cell lines, this potential has been investigated by several research groups (Table 2). In OSC-1 esophageal squamous cell carcinoma cells, [¹⁸F]FLT uptake was measured after incubation with four different cytostatic drugs. An early seven- to tenfold increase of [¹⁸F]FLT uptake was reported after incubation with 5-fluorouracil and methotrexate, rather than a decrease. Treatment with gemcitabine also resulted in a fivefold increase in uptake, but cell cultures incubated with cisplatin showed a moderately decreased [¹⁸F]FLT up-

Table 2
[¹⁸F]FLT and treatment evaluation

| Tumor type | Treatment | Decreased or increased uptake | Reference |
|--------------------------------------|---|---|--------------------------------|
| Breast cancer | Chemotherapy | 23.9% decreased uptake | Silverman et al. ³² |
| Esophageal cancer cells | CDDP or 5-FU or MTX or GEM ^a | 7-10 fold increase after 5-FU and MTX, 5-fold increase after GEM, decrease after CDDP | Dittmann et al. ⁹ |
| Mice; radiation induced fibrosarcoma | 5-FU | Decrease from 5.7 to 1.8%ID/g in 48h | Barthel et al. ²⁸ |
| Lung cancer cells and glioma cells | Adriamycin | 21-42% and 80% decrease resp. | Yeo et al. ²⁷ |
| Colorectal cancer cells | 5-FU | 8-15-fold increase | Francis et al. ²⁶ |
| Mice; prostate cancer | 25 Gy radiation | Initial decreased, later on back to baseline | Huang et al. ²⁹ |
| Mice; ovarian tumor | CDK2 inhibitor | Decrease in T/NT from 6.7 to 4.3 in 180 h | Bonab et al. ³¹ |
| Mice; prostate cancer | DES or castration | Decreased uptake during and after therapy | Oyama et al. ³⁰ |
| Mice; A431 tumor | PKI-166 | Decrease in T/NT from 9.5 to 1.9 in 7d | Waldherr et al. ³² |

^a CDDP: cisplatin; 5-FU: 5-fluorouracil; MTX: methotrexate; GEM: gemcitabin; DES: diethylstilbestrol

take, suggesting that the decline in [¹⁸F]FLT uptake reflects the growth inhibition by cisplatin⁹. Francis et al.²⁶ also reported 8.3- and 14.7-fold increases in [¹⁸F]FLT uptake in colorectal cancer cell lines respectively 1 and 2 days after 5-fluorouracil treatment. Preliminary results from Yeo et al.²⁷, however, demonstrated that 2, 6 and 24 h after adriamycin treatment, A549 lung cancer cells showed, respectively, a 21%, 32% and 42% reduction in the uptake of [¹⁸F]FLT compared with control. In 9L glioma cells, [¹⁸F]FLT uptake was also decreased (80%, 48% and 80% of control). Uptake of [¹⁸F]FDG was not consistently decreased after chemotherapy.

Different types of anticancer therapies have been studied, and the results of these studies may seem inconsistent. However, as mentioned above, some chemotherapeutic agents cause an increase in TK activity by activating the DNA salvage pathway. This will lead to increased [¹⁸F]FLT uptake, whereas cellular proliferation is impaired. In contrast, other cytotoxic agents may cause a decrease in [¹⁸F]FLT uptake. The in vivo reactions on chemotherapeutic agents are most certainly even more complex. This is

illustrated by the research of Barthel et al.²⁸, who showed that, unlike in cell line studies, [¹⁸F]FLT uptake decreased in radiation-induced fibrosarcoma in mice after 5-fluorouracil treatment from 5.7% of injected dose per gram (ID/g) to 2.7% and 1.5% (after 24 and 48 h, respectively). [¹⁸F]FDG uptake decreased significantly less, from 6.1% ID/g to 4.4% and 3.2%, respectively. Although [¹⁸F]FLT uptake decreased after 5-fluorouracil treatment, suggesting low TK₁ activity, the authors showed that TK₁ protein levels increased. Their explanation was that ATP levels, as a cofactor for realizing TK₁ activity, were low. A correlation ($r=0.71$; $P=0.03$) between [¹⁸F]FLT uptake and immunostaining of proliferating cell nuclear antigen, however, proved that [¹⁸F]FLT uptake correctly followed proliferative activity of the tumors early after chemotherapy.

Another research group compared [¹⁸F]FLT-PET and [¹⁸F]FDG-PET following radiotherapy for murine prostate tumors implanted in the thighs. After 1 week, [¹⁸F]FDG uptake was increased, but after 2 and 3 weeks, [¹⁸F]FDG uptake was decreased compared with the reference. [¹⁸F]FLT uptake, however, was decreased the first week, but after 2 weeks, [¹⁸F]FLT uptake was comparable to the reference, suggesting a suppressed proliferation rate 1 week after radiotherapy which normalizes after 2 weeks²⁹. However, this suggestion was not supported by a comparison with histopathological proliferation markers.

Recently, Oyama et al.³⁰ monitored androgen ablation therapy for mice with implanted prostate cancer cells with [¹⁸F]FLT. Androgen ablation was established by either castration or diethylstilbestrol treatment. [¹⁸F]FLT uptake significantly decreased in the treated mice, but in the untreated mice, no change in [¹⁸F]FLT uptake was seen. The authors conclude that [¹⁸F]FLT is able to visualize prostate cancer and monitor androgen ablation therapy in this model. However, in translating these results to the human situation, one can imagine that the differentiation between prostate cancer and physiological uptake in the bladder region can be difficult and that for this reason the sensitivity and specificity for the detection of recurrent or residual disease might be impaired.

Bonab et al.³¹ treated tumor-bearing mice (a human ovarian xenograft) with an inhibitor of cyclin dependent kinase 2 (CDK2). MicroPET images with [¹⁸F]FLT showed that the T/NT dropped from 6.68 to 3.45 at 80 h after CDK2 treatment. At 150 h after treatment, T/NT was 4.32. In untreated animals, no change in T/NT ratio was observed. Comparable results were presented by Waldherr et al.³². Both [¹⁸F]FDG and [¹⁸F]FLT showed a significant decrease in T/NT after the treatment of 12 tumor-bearing mice with PKI-166 (an Erb1/Erb2 receptor tyrosine kinase inhibitor).

These preclinical results indicate that [¹⁸F]FLT is probably a more cancer-specific PET tracer than [¹⁸F]FDG and that [¹⁸F]FLT may be useful for evaluating early response to therapy. However, the mechanisms of change in [¹⁸F]FLT uptake are not always clear. Furthermore, both cell line studies and animal studies have certain limitations that should be taken into account before translating these results into the clinical situa-



tion. For example, changes in perfusion after therapy cannot be measured in cell line studies. In addition, it has been reported that the serum thymidine level in rodents is ten times higher than in humans³³. Endogenous thymidine may compete with [¹⁸F]FLT for the uptake transporter³⁴ and phosphorylation by TK₁³⁵, leading to lower [¹⁸F]FLT uptake in tumor cells in rodents. In one study²⁵, it was shown that administration of thymidine phosphorylase resulted in higher [¹⁸F]FLT uptake in the tumors. Thymidine phosphorylase hydrolyzes thymidine into thymine, thereby lowering the serum levels of endogenous thymidine.

Clinical studies

The most widely used PET tracer in clinical oncology is [¹⁸F]FDG. Its uptake reflects the glycolytic activity of tissues, which is increased in most cancer cells. [¹⁸F]FDG-PET is clinically used for the diagnosis, staging and re-staging of a wide variety of tumors³⁶. Although a sensitive tracer, [¹⁸F]FDG is not a highly tumor-specific tracer. Uptake is also seen in activated macrophages and other inflammatory cells, leading to false positive scans³⁷⁻³⁹.

In the search for more cancer-specific tracers, [¹⁸F]FLT was introduced as a proliferation tracer. In order to be able to answer interesting and clinically relevant research questions, the first and necessary step in the evaluation of a new PET tracer is to establish whether this tracer is taken up by the tumor at all. Therefore, most clinical [¹⁸F]FLT-PET studies have been feasibility studies directed to determine the possibility of detecting tumors, of differentiating between malignant and benign lesions or of determining the correlation with proliferation. Only a small number of patients have been scanned in each study. Therefore, the clinical relevance of these studies is limited. Future research in patients should focus on clinically relevant research questions, taking into account the strong and weak points of [¹⁸F]FLT-PET.

Physiological distribution in humans

First studies using [¹⁸F]FLT in humans have shown physiological uptake in bone marrow, liver and in the urinary tract (Fig. 3). In contrast to [¹⁸F]FDG-PET, no uptake is seen in the brain, skeletal muscles or myocardium. Uptake in the liver is increased because of the glucuronidation of [¹⁸F]FLT⁴⁰.

Pulmonary nodes and lung cancer

Differentiating malignant from benign solitary pulmonary nodes (SPNs) is a well-known diagnostic problem in daily clinical practice. [¹⁸F]FDG-PET has proven to be a helpful and accurate diagnostic tool with excellent sensitivity (96.8%) and good specificity (77.8%)⁴¹. Reported false positives originate mainly from granulomatous and

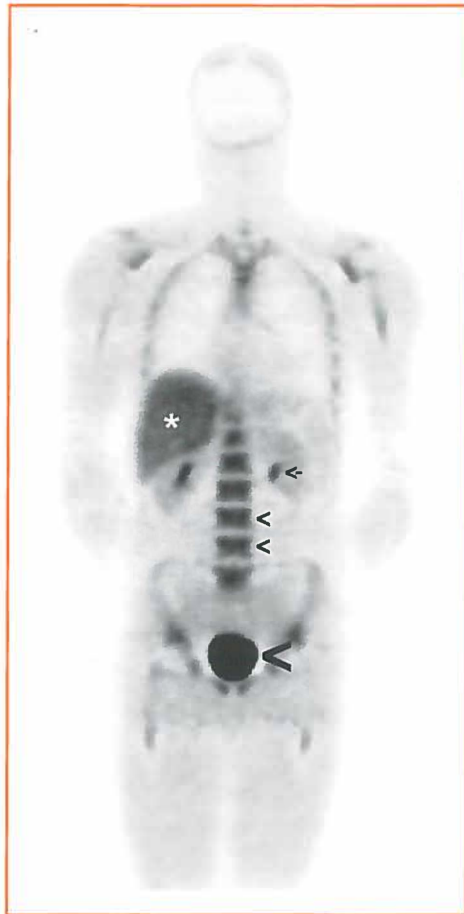


Figure 3

Physiological uptake of [¹⁸F]FLT. Coronal slice of an [¹⁸F]FLT-PET whole body scan showing the physiological uptake pattern in a 27 y old male patient. Note the uptake in the liver (asterix), bone marrow (small triangles), calices (arrow) and urinary bladder (large triangle). In the brain and myocardium, no physiological uptake is seen



inflammatory disease^{42,43}. Therefore, a more specific tracer that does not show uptake in inflammatory tissues might be useful.

The first [¹⁸F]FLT-PET scan of a patient with non-small cell lung cancer (NSCLC) showed that [¹⁸F]FLT is able to visualize NSCLC⁴⁰ with low background activity. Subsequently, [¹⁸F]FLT-PET has been studied by a number of groups in patients with SPNs. Buck et al.⁴⁴ investigated 30 patients with SPNs and reported [¹⁸F]FLT uptake in 86% of malignant lesions with a mean standardized uptake value (SUV) of 2.8. Benign lesions did not show



[¹⁸F]FLT uptake (100% specificity). Furthermore, a significant correlation ($r=0.87$) was found between SUV and Ki-67 index. Vesselle et al. ⁴⁵ also found a strong correlation between [¹⁸F]FLT uptake and Ki-67 index ($r=0.84$). Recent data comparing [¹⁸F]FDG and [¹⁸F]FLT showed significantly less uptake of [¹⁸F]FLT in thoracic tumors. [¹⁸F]FDG proved to be more sensitive (92% vs. 56%) in detecting malignancy, while the specificity was higher for [¹⁸F]FLT (64% vs. 100%) ⁴⁶⁻⁴⁸.

In a recent study, Buck et al. ⁴⁹ compared [¹⁸F]FDG-PET and [¹⁸F]FLT-PET for lung tumors. Mean uptake in tumors was higher for [¹⁸F]FDG than for [¹⁸F]FLT (4.1 vs 1.8), but [¹⁸F]FLT SUV correlated better with Ki-67 proliferation index than did [¹⁸F]FDG SUV ($r=0.92$ and $r=0.59$, respectively). [¹⁸F]FDG-PET was false negative in 1 of 18 patients with malignant lesions, while [¹⁸F]FLT-PET missed 3 of 18 lesions. [¹⁸F]FDG-PET however was false positive in four of eight patients with benign lesions. Recently, Cobben et al. ⁵⁰ investigated the value of [¹⁸F]FLT-PET as compared with [¹⁸F]FDG-PET for the staging of NSCLC. Uptake of [¹⁸F]FLT was significantly lower than [¹⁸F]FDG uptake. As compared with clinical staging, [¹⁸F]FLT-PET staged only 8 out of 17 patients correctly. Therefore the authors concluded that [¹⁸F]FLT-PET is not useful for the staging of NSCLC.

These data support the hypothesis that [¹⁸F]FLT is a more specific tracer for malignant tissues. Good correlations with proliferation rates could make [¹⁸F]FLT-PET a prognostic tool for patients with NSCLC but low sensitivity could result in false negative scans and understaging of patients. All patients included in these studies had suspicious pulmonary nodes or proven lung cancer and had not received any treatment at the time of the PET scans. It is well thinkable that sensitivity and specificity can be different in a group of patients who have undergone treatment.

Breast cancer

Breast cancer is a very common type of cancer in women. It is responsible for a considerable number of deaths in the developed world. Early diagnosis and accurate staging and re-staging of breast cancer are believed to contribute to patient-tailored treatment and better clinical outcome. Few data are currently available on the visualization of breast cancer with [¹⁸F]FLT-PET, and all studies have been feasibility studies. First investigations in patients with breast cancer showed that [¹⁸F]FLT is taken up in breast cancer cells (SUV range 4.4-12.5). Even axillary lymph node metastases and liver metastases could be visualized, despite high physiological uptake in liver tissue ⁵¹. In another study ⁵², a 1.3-2.3 times higher [¹⁸F]FLT uptake was reported in primary breast cancers as compared with [¹⁸F]FDG uptake. After the initial course of chemotherapy, [¹⁸F]FDG uptake decreased by a mean of 4.6%, while [¹⁸F]FLT uptake decreased by a mean of 23.9%. Recently, Smyczek-Gargya et al. ⁵³ investigated 12 patients with breast cancer with [¹⁸F]FLT-PET. In six patients, a comparison was made with [¹⁸F]FDG-PET. With [¹⁸F]FLT-PET, one small tumor was missed. Surprisingly, no correlation was found between Ki-67 index and [¹⁸F]FLT uptake. However, Ki-67 index was performed in core

biopsy specimens, which could be responsible for underestimation of this index. [¹⁸F]FDG uptake was higher than [¹⁸F]FLT uptake in tumors and lymph node metastases.

Pio et al.⁵⁴ compared [¹⁸F]FLT and [¹⁸F]FDG uptake with CA27.29 tumor marker levels after a single course of chemotherapy. The mean change in [¹⁸F]FLT uptake showed a close correlation with the mean change in CA27.29 tumor marker level ($r=0.78$), but for [¹⁸F]FDG there was no correlation ($r=0.18$). After completing all courses of chemotherapy, the correlations between tracer uptake and tumor marker levels increased for both tracers ($r=0.94$ for [¹⁸F]FLT, $r=0.74$ for [¹⁸F]FDG). [¹⁸F]FLT uptake predicted tumor marker response to chemotherapy better than did [¹⁸F]FDG ($r=0.77$ and $r=0.28$, respectively). CA27.29 is a reliable tumor marker for breast cancer⁵⁵, but it is not a quantitative proliferation marker. There is need for data that show a correlation between response to chemotherapy (as measured by a true proliferation marker such as SPF, Ki-67 index or TK₁ activity) and decreased [¹⁸F]FLT uptake.

It is still unclear what will be the role for [¹⁸F]FLT-PET in patients with breast cancer. Physiological uptake in bone marrow and liver will hamper the detection of bone and liver metastases. The sensitivity for detection of axillary lymph node metastases has not yet been evaluated, but with sentinel lymph node biopsies even micrometastases can be found^{56,57}. Measuring the early response to (neoadjuvant) chemotherapy for locally advanced breast cancer is probably the most interesting research question for future [¹⁸F]FLT-PET studies in patients with breast cancer.

Brain tumors

Conventional imaging techniques offer excellent anatomical information of the brain. In the management of brain tumors, PET could give information on the tumor grade and help in assessing the optimal site for biopsy. PET could also assist in the evaluation of anticancer treatment. In contrast to [¹⁸F]FDG, [¹⁸F]FLT background uptake in normal brain tissue is low, probably owing to slow proliferation rate. This offers the opportunity to visualize brain tumors with high T/NT contrast.

Proliferation in the brain has been visualized before using the salvage pathway of DNA synthesis^{58,59}. In these studies, labeled thymidine was used. Labeled thymidine, however, is readily metabolized and images should be corrected for these metabolites. Dohmen et al.⁶⁰ used [¹⁸F]FLT-PET for the detection of brain tumors and compared the results with L-methyl-[¹¹C]-methionine ([¹¹C]MET). As compared with [¹¹C]MET, [¹⁸F]FLT showed higher tumor contrast (T/NT ratio 5.4 vs 2.4) and a correlation with tumor grade of $r=0.44$. Absolute SUV, however, was higher for [¹¹C]MET. Another study showed that [¹⁸F]FLT can distinguish between recurrent tumor and radiation necrosis. Low-grade brain tumors, however, were poorly visualized⁶¹. Recent preliminary results from Garlip et al.⁶² comparing [¹⁸F]FLT uptake ratios in gliomas with [¹¹C]MET uptake ratios showed a higher uptake for [¹⁸F]FLT than for [¹¹C]MET. In grade II astrocytoma,



uptake ratios were 2.9 vs. 2.1, and in glioblastoma 12.7 vs. 4.3. Nitzsche et al.⁶³ found [¹⁸F]FLT to be superior to [¹⁸F]FDG for the detection of recurrent brain tumors after brachytherapy. [¹⁸F]FLT-PET detected recurrent disease before [¹⁸F]FDG did in 9 out of 18 patients. In the other nine patients, [¹⁸F]FLT and [¹⁸F]FDG detected recurrent disease at the same time.

Until now, only small studies have been published. [¹⁸F]FLT-PET offers images with excellent T/NT contrast, but little or no anatomical information is provided. Only a weak correlation has been found between [¹⁸F]FLT uptake and tumor grade. Therefore, future research will have to answer the question of whether [¹⁸F]FLT-PET can differentiate between benign and malignant tissue and between residual tumor and radiation necrosis. If [¹⁸F]FLT proves to be a sensitive and specific tracer for brain malignancies, it may be very useful (in combination with CT or MRI) for establishing the best site for tumor biopsy or for planning of radiotherapy in a heterogeneous tumor.

Colorectal carcinoma

[¹⁸F]FDG-PET has been evaluated for the detection of primary, recurrent and metastatic colorectal cancer (CRC). PET could play a role in selecting patients with recurrent CRC who might benefit from curative surgery. [¹⁸F]FDG-PET has proven to be very sensitive (sensitivity >90%). Specificity for recurrent disease has reported to be 76%⁶⁴.

A study by Francis et al.⁶⁵ comparing [¹⁸F]FDG-PET and [¹⁸F]FLT-PET in CRC showed good visualization of primary tumors for both tracers. Of six lung metastases, [¹⁸F]FLT was able to visualize five. All peritoneal lesions were seen with both tracers. [¹⁸F]FLT showed high background uptake in the liver. As a result, only 34% of liver metastases were seen with [¹⁸F]FLT while [¹⁸F]FDG revealed 97% of liver metastases. One peritoneal inflammatory lesion showed increased [¹⁸F]FDG uptake but no [¹⁸F]FLT uptake. Another recent study by the same group showed a close correlation ($r=0.8$, $P<0.01$) between [¹⁸F]FLT uptake and Ki-67 index. For [¹⁸F]FDG no such correlation was found⁶⁶.

It can be concluded that [¹⁸F]FLT uptake shows a good correlation with proliferation in CRC. High physiological uptake in the liver, however, makes [¹⁸F]FLT-PET unsuitable for the detection of hepatic metastatic disease. Possible indications for [¹⁸F]FLT-PET are non-invasively evaluation of tumor grade and measurement of early response to therapy.

Lymphoma

[¹⁸F]FDG-PET is a sensitive method for the visualization of high-grade lymphoma. For the end-of-treatment evaluation, [¹⁸F]FDG-PET is the best imaging tool⁶⁷. However, for indolent lymphoma, the value of [¹⁸F]FDG-PET is unclear. [¹⁸F]FLT-PET could have additional value as a tracer of proliferative tissues.

Recent data comparing [¹⁸F]FLT and [¹⁸F]FDG in nine patients with histologically proven lymphoma indicated that both tracers detected a comparable number of lesions.

[¹⁸F]FLT SUV ranged from 6 to 16. A close relation between proliferation and SUV was seen for eight of nine patients ($r=0.94$). One lesion with 90% Ki-67 positive cells had an SUV of only 6. Histopathological examination of this lesion showed >30% fibrosis, explaining the discrepancy⁶⁸. Preliminary data from Buck et al.⁶⁹ comparing [¹⁸F]FLT and [¹⁸F]FDG in 26 patients with non-Hodgkin's lymphoma showed similar visualization by either tracer. Mean [¹⁸F]FLT SUV was 4.5, mean [¹⁸F]FDG SUV was 5. A significant correlation was found between [¹⁸F]FLT uptake and Ki-67 proliferation index ($r=0.9$, $P<0.0001$).

The sensitivity for [¹⁸F]FDG and [¹⁸F]FLT for lymphoma seems comparable. In contrast to [¹⁸F]FDG, [¹⁸F]FLT uptake in lymphoma is closely correlated with the rate of proliferation. However, in lymphoma, proliferation is not always correlated with prognosis⁷⁰. In the end-of-treatment evaluation, [¹⁸F]FLT could be more specific in detecting residual tissue with high proliferation rate.

Sarcoma

Differentiation between a large lipoma and a liposarcoma relies mainly on histopathological examination of tumor tissue, which has been obtained at incision biopsy. Cobben et al.⁷¹ investigated [¹⁸F]FLT-PET in soft tissue sarcomas of the extremity. Correlations were found between SUV and T/NT and mitotic score, Ki-67 and the French and Japanese grading systems ($r=0.55-0.75$). Visualization of tumors was good, with high-contrast images with mean SUVs of 0.9 and 2.8 for low- and high-grade tumors, respectively. Mean T/NT was 1.9 and 6.0 for low- and high-grade tumors, respectively. [¹⁸F]FLT-PET was able to differentiate between low- and high-grade soft tissue sarcoma according to the French grading system. However, no differentiation could be made between benign and low-grade malignant soft tissue tumors.

These results show that [¹⁸F]FLT-PET is able to differentiate between low-grade and high-grade soft tissue sarcomas and could therefore non-invasively predict which patients could benefit from hyperthermic isolated limb perfusion (HILP). Another possible indication for [¹⁸F]FLT-PET could be the evaluation of HILP for locally advanced soft tissue sarcoma of the extremity (Fig. 4). Van Ginkel et al.^{72,73} previously evaluated HILP with [¹⁸F]FDG-PET and [¹¹C]tyrosine-PET ([¹¹C]TYR-PET). [¹⁸F]FDG-PET before HILP could predict the probability of complete response after therapy, but after HILP, images suffered interference from inflammatory tissue response. [¹¹C]TYR-PET after HILP, however, gave a good indication of pathological response. The predictive value of [¹⁸F]FLT-PET before and after HILP is currently under evaluation.

Melanoma

[¹⁸F]FDG-PET has been evaluated for staging primary cutaneous melanoma and has proven to be useful in stage III and IV disease⁷⁴⁻⁷⁶. Sensitivity for detection of metastatic melanoma with [¹⁸F]FDG-PET is 92% and specificity is 83%⁷⁷. However, for small re-



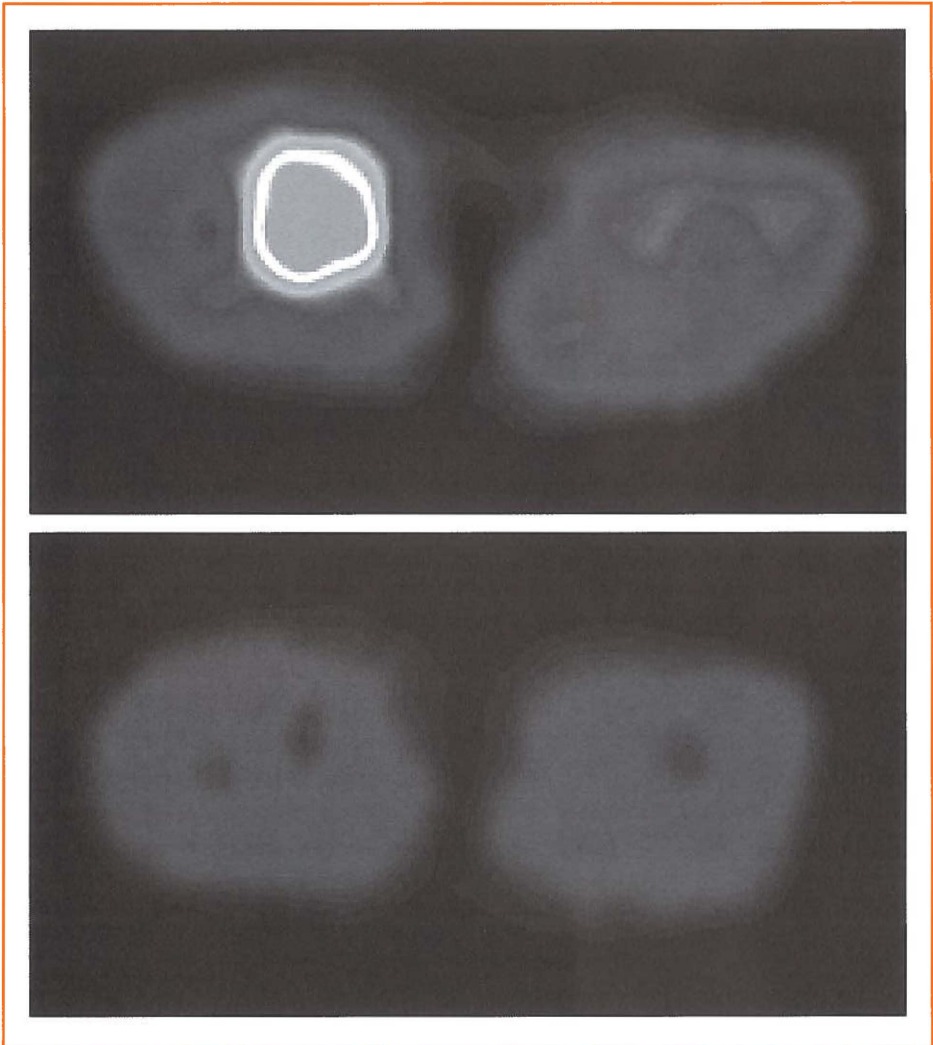


Figure 4

Evaluation of HILP with [¹⁸F]FLT-PET. [¹⁸F]FLT-PET image of a 63y old patient with a soft tissue sarcoma of his right upper leg before (top) and after (bottom) HILP. Histopathological examination of the resected specimen showed >75% necrosis after HILP

gional metastases, sentinel lymph node biopsies are superior to [¹⁸F]FDG-PET ⁷⁸. Cobben et al. ⁷⁹ studied the feasibility of using [¹⁸F]FLT-PET for visualization of metastatic melanoma in ten patients (Fig. 5). When compared with histopathologic evaluation, [¹⁸F]FLT-PET had a sensitivity of 88% and a specificity of 60%.

These data show that sensitivity and specificity of [¹⁸F]FLT for metastatic melanoma are lower than those of [¹⁸F]FDG. Very small lesions (<4 mm) will not be visualized by



Figure 5
Whole body [¹⁸F]FLT-PET of a patient with metastatic melanoma. This 34 y old male patient presented with axillary node metastases 2 months after resection of the primary melanoma of the back. [¹⁸F]FLT-PET showed uptake in both axillary regions and in a supraclavicular lymph node (arrows)

either PET tracer because of the limited spatial resolution of the PET cameras. For this indication the sentinel lymph node procedure is superior.

Laryngeal cancer

The gold standard for diagnosing and staging laryngeal cancer is laryngoscopy with biopsies and CT scanning of the neck region. PET could serve as a non-invasive imaging tool to diagnose and stage laryngeal cancer. Cobben et al.⁸⁰ studied patients with primary and recurrent laryngeal carcinoma. CT, [¹⁸F]FDG-PET and [¹⁸F]FLT-PET were compared with histopathological results. Sensitivity was 100%, 88% and 82%, respectively. Specificity was 100% for all modalities. Mean SUV was significantly higher for [¹⁸F]FDG than for [¹⁸F]FLT (2.7 vs. 1.2).



The authors concluded that for the staging of laryngeal cancer, CT is more accurate than PET. [¹⁸F]FDG-PET is more sensitive than [¹⁸F]FLT-PET. A possible indication for [¹⁸F]FLT-PET lies in the detection of recurrent or residual tumor after radiotherapy.

General discussion and future perspectives

PET is increasingly becoming a routinely used functional imaging tool. For oncological practice, [¹⁸F]FDG is the most widely used PET tracer. [¹⁸F]FDG-PET has a wide variety of indications, and cost-effectiveness studies have proven or will prove the true value of this imaging modality.

In recent years, several new tracers have been developed as imaging agents for different metabolic pathways of cancer cells. One of these tracers, [¹⁸F]FLT, was introduced as a proliferation tracer ⁴⁰. [¹⁸F]FLT is a pyrimidine analogue and it uses the salvage pathway of DNA synthesis for imaging proliferation. This could provide us with the opportunity to differentiate between benign and malignant tissues, to measure tumor aggressiveness and to monitor response to treatment.

In this article, we discussed the current status of research data of [¹⁸F]FLT. Several research groups have investigated the feasibility of using the tracer, and preclinical and clinical studies are still being performed. Three different aspects of [¹⁸F]FLT-PET have been investigated in these studies:

Firstly, the ability of [¹⁸F]FLT to visualize malignant tumors has been addressed as the first and necessary step in the evaluation of a new tracer. Most early clinical studies have shown the feasibility of using [¹⁸F]FLT-PET to visualize malignant tumors. However, in comparison with [¹⁸F]FDG, [¹⁸F]FLT uptake is lower in nearly all cases, resulting in a lower sensitivity. A number of reasons can be given for this low [¹⁸F]FLT uptake in tumors. Firstly, it has been shown that the halogen substitution in the 3' position of [¹⁸F]FLT results in a decreased affinity for the pyrimidine transporter as compared with thymidine ⁸¹. Secondly, the affinity of [¹⁸F]FLT for TK₁ is reported to be 30% lower than the affinity of thymidine ⁸². Both mechanisms lead to a preferable uptake and phosphorylation of thymidine and this may explain the low [¹⁸F]FLT uptake in tumor cells. Furthermore, as mentioned previously, the relative contributions of the salvage pathway and the de novo pathway may also influence the uptake of [¹⁸F]FLT. It has been shown that some tumor cells rely chiefly on de novo synthesis of DNA precursors, resulting in little or no uptake of thymidine and [¹⁸F]FLT. Based on these data, it can be concluded that [¹⁸F]FLT is not superior to [¹⁸F]FDG with respect to the detection of tumors. Furthermore, physiological uptake in the liver and bone marrow will also hamper the detection of liver and bone metastases.

Secondly, [¹⁸F]FLT has been investigated as a proliferation tracer. As mentioned earlier in this article, [¹⁸F]FLT can be seen as a proliferation tracer because it is phosphor-

ylated by TK₁. TK₁ activity is high in the S phase of non-malignant proliferating cells and even higher throughout the cell cycle in malignant cells. Therefore, [¹⁸F]FLT is probably more tumor specific than many other PET tracers. Several research groups have reported strong correlations between [¹⁸F]FLT uptake and histopathological proliferation markers. By visualizing and quantifying the proliferation rate of tumors, [¹⁸F]FLT-PET could serve as a non-invasive tool for establishing tumor grade. Therefore, [¹⁸F]FLT could be able to select patients who might benefit from adjuvant treatment. Furthermore, [¹⁸F]FLT-PET can visualize the heterogeneity within tumors. In combination with CT or MRI, [¹⁸F]FLT could help define the optimum site for biopsy in these tumors (for example in brain tumors).

Thirdly, as [¹⁸F]FLT-PET is a potentially more cancer-specific PET tracer, another promising indication could be the evaluation and measurement of the response to anti-cancer therapy, since no uptake is expected in inflammatory cells that are present during or shortly after therapy. This has been subject to a number of preclinical and clinical investigations. These studies have shown that [¹⁸F]FLT uptake is sometimes decreased after therapy, whereas it may be increased after other types of therapy. At first sight, this seems inconsistent, but it can be explained by the intracellular changes that are induced by these agents. For example, in the study by Dittmann et al.⁸, 5-fluorouracil treatment resulted in increased [¹⁸F]FLT uptake after 72 h of incubation. This agent causes S phase accumulation and shuts down the de novo pathway of DNA synthesis, resulting in increased TK₁ activity and a compensatory upregulation of the salvage pathway. The in vivo changes after therapy (especially after a combination of chemotherapeutic agents) are expected to be even more complex and need further investigation. If future research demonstrates that [¹⁸F]FLT is accurate in showing the response to therapy at an early stage, non-responders could be detected earlier and they could be switched to second-line treatment.

There are several ways to measure tumor proliferation, all of which target different aspects of proliferation. In daily clinical practice, the Ki-67 index is the most widely used marker and in preclinical research, SPF and thymidine labelling index are used frequently. It is not evident which is the ideal proliferation marker, and the relation between these markers and TK₁ activity is not always clear. With [¹⁸F]FLT-PET, the proliferation rate of tumors can be non-invasively measured in vivo, but in this article it has been shown that the relation between proliferation and TK₁ activity is not always fully understood. Furthermore, other pyrimidine analogues such as 2'-fluoro-5-methyl-1-beta-D-arabinofuranosyluracil (FMAU) and 2'-deoxy-2'-fluoro-5-bromo-1-beta-D-arabinofuranosyluracil (FBAU) are being developed⁸³⁻⁸⁵. These tracers offer the potential advantage over [¹⁸F]FLT of showing uptake in DNA and therefore reflecting DNA synthesis directly. However, these tracers are also substrate for TK₁ and, therefore, some of the limitations of [¹⁸F]FLT will also apply for FMAU and FBAU. A direct comparison



between these tracers together with histopathological markers should be performed to understand the strong and weak sides of each of these proliferation markers.

In conclusion, in the past years several research groups have investigated different aspects of [¹⁸F]FLT, and the published reports show promising results. However, some research groups have reported difficulties in the interpretation of [¹⁸F]FLT uptake in tumors. These difficulties have been mentioned in this review article, for example the low overall uptake in tumors, the changes in [¹⁸F]FLT uptake after anti-tumor therapy and the indirect mechanism of visualizing proliferation. Future research will have to focus on trying to clarify these problems and establishing the true value of [¹⁸F]FLT alongside other tracers for PET imaging in oncology.

Acknowledgements

This work was supported by the Dutch Cancer Society (grant no. 2000-2299).

References

1. Munch-Petersen B, Cloos L, Jensen HK, and Tyrsted G. Human thymidine kinase 1. Regulation in normal and malignant cells. *Adv Enzyme Regul* 1995;35:69-89.
2. Boothman DA, Davis TW, and Sahijdak WM. Enhanced expression of thymidine kinase in human cells following ionizing radiation. *Int J Radiat Oncol Biol Phys* 1994;30:391-398.
3. Kauffman MG and Kelly TJ. Cell cycle regulation of thymidine kinase: residues near the carboxyl terminus are essential for the specific degradation of the enzyme at mitosis. *Mol Cell Biol* 1991;11:2538-2546.
4. Rasey JS, Grierson JR, Wiens LW, Kolb PD, and Schwartz JL. Validation of FLT uptake as a measure of thymidine kinase-1 activity in A549 carcinoma cells. *J Nucl Med* 2002;43:1210-1217.
5. Bardot V, Dutrillaux AM, Delattre JY, Vega F, Poisson M, Dutrillaux B et al. Purine and pyrimidine metabolism in human gliomas: relation to chromosomal aberrations. *Br J Cancer* 1994;70:212-218.
6. Cole PD, Smith AK, and Kamen BA. Osteosarcoma cells, resistant to methotrexate due to nucleoside and nucleobase salvage, are sensitive to nucleoside analogs. *Cancer Chemother Pharmacol* 2002;50:111-116.
7. Schwartz JL, Tamura Y, Jordan R, Grierson JR, and Krohn KA. Monitoring tumor cell proliferation by targeting DNA synthetic processes with thymidine and thymidine analogs. *J Nucl Med* 2003;44:2027-2032.
8. Dittmann H, Dohmen BM, Kehlbach R, Bartusek G, Pritzkow M, Sarbia M et al. Early changes in [¹⁸F]FLT uptake after chemotherapy: an experimental study. *Eur J Nucl Med Mol Imaging* 2002;29:1462-1469.
9. Mirjolef JF, Barberi-Heyob M, Merlin JL, Marchal S, Etienne MC, Milano G et al. Thymidylate synthase expression and activity: relation to S-phase parameters and 5-fluorouracil sensitivity. *Br J Cancer* 1998;78:62-68.

10. Tsurusawa M, Niwa M, Katano N, and Fujimoto T. Flow cytometric analysis by bromodeoxyuridine/DNA assay of cell cycle perturbation of methotrexate-treated mouse L1210 leukemia cells. *Cancer Res* 1988;48:4288-4293.
11. Scholzen T and Gerdes J. The Ki-67 protein: from the known and the unknown. *J Cell Physiol* 2000;182:311-322.
12. Spyrtatos F, Ferrero-Pous M, Trassard M, Hacene K, Phillips E, Tubiana-Hulin M et al. Correlation between MIB-1 and other proliferation markers: clinical implications of the MIB-1 cutoff value. *Cancer* 2002;94:2151-2159.
13. Hartmann H, Vogt MW, Durno AG, Hirsch MS, Hunsmann G, and Eckstein F. Enhanced in vitro inhibition of HIV-1 replication by 3'-fluoro-3'-deoxythymidine compared to several other nucleoside analogs. *AIDS Res Hum Retroviruses* 1988;4:457-466.
14. Flexner C, van der HC, Jacobson MA, Powderly W, Duncanson F, Ganes D et al. Relationship between plasma concentrations of 3'-deoxy-3'-fluorothymidine (alovudine) and antiretroviral activity in two concentration-controlled trials. *J Infect Dis* 1994;170:1394-1403.
15. Grierson JR and Shields AF. Radiosynthesis of 3'-deoxy-3'-[¹⁸F]fluorothymidine: [¹⁸F]FLT for imaging of cellular proliferation in vivo. *Nucl Med Biol* 2000;27:143-156.
16. Martin SJ, Eisenbarth JA, Wagner-Utermann U, Mier W, Haberkorn U, and Eisenhut M. [¹⁸F]FLT: ¹⁸F labeling of 3-BOC-1-(2-deoxy-3-O-nosyl-5-O-trityl-beta-D-lyxofuranosyl)thymine and other thymine derivatives. *J Nucl Med* 2000;41:255P.
17. Mosdzianowski C, Nader M, Korenjak C, Martin S. J., and Eisenbarth J. A. Automated FLT syntheses using 3-N-Boc-1-(5-O-(4,4'-dimethoxytrityl)-3-O-nosyl-2-deoxy-beta-D-lyxofuranosyl)thymidine as precursor. *Eur J Nucl Med Mol Imaging* 2001; 28: 1228 [abstract].
18. Yun M, Oh SJ, Ha HJ, Ryu JS, and Moon DH. High radiochemical yield synthesis of 3'-deoxy-3'-[¹⁸F]fluorothymidine using (5'-O-dimethoxytrityl-2'-deoxy-3'-O-nosyl-beta-D-threo pentofuranosyl)thymine and its 3-N-BOC-protected analogue as a labeling precursor. *Nucl Med Biol* 2003;30:151-157.
19. Moon BS, Shim A. Y., Kim D. W., Kim S. E., Yand S. D., and Chi D. Y. New synthetic method for [¹⁸F]-3'-deoxy-3'-fluorothymidine using a nosylate precursor in ionic liquid ([bmim][OTf]). *J Labelled Cpd Radiopharm* 2003; 46: S122 [abstract].
20. Machulla HJ, Blochler A, Kuntzsch M, Piert M, Wei R, and Grierson JR. Simplified labeling approach for synthesizing 3'-deoxy-3'-[¹⁸F]fluorothymidine (¹⁸F)FLT). *Journal of Radioanalytical and Nuclear Chemistry* 2000;243:843-846.
21. Cleij MC, Steel C. J., Brady F., and Ell P. J. An improved synthesis of 3'-deoxy-3'-[¹⁸F]fluorothymidine (¹⁸F)FLT and the fate of the precursor, 2,3'-anhydro-5'-O-(4,4'-dimethoxytrityl)-thymidine. *J Labelled Cpd Radiopharm* 2001; 44: S871-S873 [abstract].
22. Seitz U, Wagner M, Neumaier B, Wawra E, Glatting G, Leder G et al. Evaluation of pyrimidine metabolising enzymes and in vitro uptake of 3'- [¹⁸F]fluoro-3'-deoxythymidine ([¹⁸F]FLT) in pancreatic cancer cell lines. *Eur J Nucl Med Mol Imaging* 2002;29:1174-1181.
23. Carter EA, McKuster K, Syed S. Z., and Thompkins R. G. Comparison of ¹⁸FLT with ¹⁸FDG for differentiation between tumor and focal sites of infection in rats [abstract]. *J Nucl Med* 2002; 43: 266P [abstract].
24. Lee TS, Shim A. Y., Hwang W. T., Ahn S. H., Sung H. D., Chung H. K., Lee J. C., Song O. R., Woo K. S., Chung W. S., Cheon G. J., Choi C. W., Lim S. M., and Hong S. W. Comparison of FDG, FET and FLT for differentiation between tumor and abscess in rats [abstract]. *SNM 50th Annual Meeting* 2003, 2003; [abstract].
25. Van Waarde A, Cobben DCP, Suurmeijer AJH, Maas B, Vaalburg W, De Vries EFJ et al. Selectivity of 3'-deoxy-3'-[¹⁸F]fluorothymidine (FLT) and 2-[¹⁸F]fluoro-2-deoxy-D-glucose (FDG) for tumor versus inflammation in a rodent model. *J Nucl Med* 2004;45:695-700.
26. Francis DL, Loizidou M., Visvikis D, DeVos S., Luthra S. K., and Taylor I. Monitoring 5-fluorouracil chemotherapy response in colorectal cancer using positron emission tomography. *Eur J Surg Oncol* 2003; 29: 789 [abstract].



27. Yeo JS, Lim S. J, Oh S. J., Ryu J. S., Yun M. K., and Moon D. H. Comparison of F-¹⁸ FLT uptake with F-18 FDG for early evaluation of chemotherapy response in human cancer cell lines. *J Nucl Med* 2003; 44: 81P [abstract].
28. Barthel H, Cleij MC, Collingridge DR, Hutchinson OC, Osman S, He Q et al. 3'-deoxy-3'-[¹⁸F]fluorothymidine as a new marker for monitoring tumor response to antiproliferative therapy in vivo with positron emission tomography. *Cancer Res* 2003;63:3791-3798.
29. Huang SC, McBride W., Stout D., Sitko J, Liao Y. P., Daigle J, Chatziioannou A, Satyamurthy N., Barrio J. R., and Phelps M. E. Post-irradiation temporal changes in glucose metabolism and cell proliferation in implanted murine tumors as measured by FDG and FLT PET [abstract]. *J Nucl Med* 2002; 43: 25P [abstract].
30. Oyama N, Ponde DE, Dence C, Kim J, Tai YC, and Welch MJ. Monitoring of therapy in androgen-dependent prostate tumor model by measuring tumor proliferation. *J Nucl Med* 2004;45:519-525.
31. Bonab AA, Weise S. W., Syed S. Z., Martyn F. S., Carter E. A., and Fischman A. J. Monitoring treatment with a CDK2 inhibitor by microPET with ¹⁸F-FLT in a nude mouse tumor model [abstract]. *SNM 50th Annual Meeting* 2003, 2003; Abstract 1313 [abstract].
32. Waldherr C, Safaei A, Mellinghoff I, Tran C, Stout D, Vranjesevic D et al. MicroPET with ¹⁸F-FLT and ¹⁸F-FDG for monitoring targeted tumor therapy in SCID mice [abstract]. *J Nucl Med* 2003;44:80P-81P.
33. Nottebrock H and Then R. Thymidine concentrations in serum and urine in different animal species and man. *Biochemical Pharmacology* 1977;26:2175-2179.
34. Kong XB, Zhu QY, Vidal PM, Watanabe KA, Polsky B, Armstrong D et al. Comparisons of anti-human immunodeficiency virus activities, cellular transport, and plasma and intracellular pharmacokinetics of 3'-fluoro-3'-deoxythymidine and 3'-azido-3'-deoxythymidine. *Antimicrob Agents Chemother* 1992;36:808-818.
35. Munch-Petersen B, Cloos L, Tyrsted G, and Eriksson S. Diverging substrate specificity of pure human thymidine kinases 1 and 2 against antiviral dideoxynucleosides. *J Biol Chem* 1991;266:9032-9038.
36. Jerusalem G, Hustinx R, Beguin Y, and Fillet G. PET scan imaging in oncology. *Eur J Cancer* 2003;39:1525-1534.
37. Minn H, Clavo AC, Grenman R, and Wahl RL. In vitro comparison of cell proliferation kinetics and uptake of tritiated fluorodeoxyglucose and L-methionine in squamous-cell carcinoma of the head and neck. *J Nucl Med* 1995;36:252-258.
38. Higashi K, Clavo AC, and Wahl RL. In vitro assessment of 2-fluoro-2-deoxy-D-glucose, L-methionine and thymidine as agents to monitor the early response of a human adenocarcinoma cell line to radiotherapy. *J Nucl Med* 1993;34:773-779.
39. Haberkorn U, Ziegler SI, Oberdorfer F, Trojan H, Haag D, Peschke P et al. FDG uptake, tumor proliferation and expression of glycolysis associated genes in animal tumor models. *Nucl Med Biol* 1994;21:827-834.
40. Shields AF, Grierson JR, Dohmen BM, Machulla HJ, Stayanoff JC, Lawhorn-Crews JM et al. Imaging proliferation in vivo with [¹⁸F]FLT and positron emission tomography. *Nat Med* 1998;4:1334-1336.
41. Gould MK, Maclean CC, Kuschner WG, Rydzak CE, and Owens DK. Accuracy of positron emission tomography for diagnosis of pulmonary nodules and mass lesions: a meta-analysis. *JAMA* 2001;285:914-924.
42. Croft DR, Trapp J, Kernstine K, Kirchner P, Mullan B, Galvin J et al. FDG-PET imaging and the diagnosis of non-small cell lung cancer in a region of high histoplasmosis prevalence. *Lung Cancer* 2002;36:297-301.
43. Cerfolio RJ, Ojha B, Bryant AS, Bass CS, Bartalucci AA, and Mountz JM. The role of FDG-PET scan in staging patients with nonsmall cell carcinoma. *Ann Thorac Surg* 2003;76:861-866.

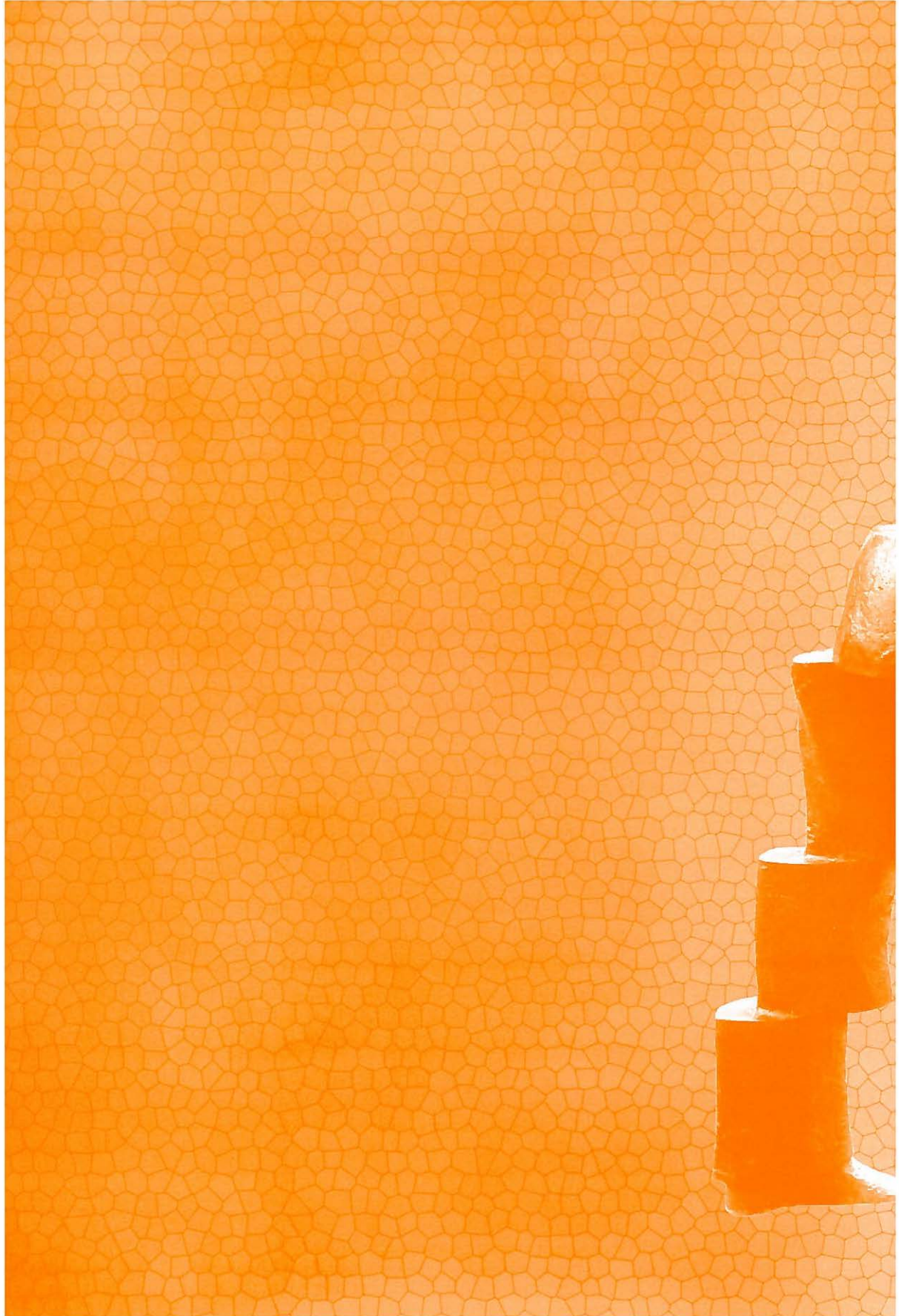
44. Buck AK, Schirrmeister H, Hetzel M, Von Der HM, Halter G, Glatting G et al. 3-deoxy-3-[(¹⁸F)]fluorothymidine-positron emission tomography for noninvasive assessment of proliferation in pulmonary nodules. *Cancer Res* 2002;62:3331-3334.
45. Vesselle H, Grierson J, Muzi M, Pugsley JM, Schmidt RA, Rabinowitz P et al. In Vivo Validation of 3'-deoxy-3'-[(¹⁸F)]fluorothymidine ([(¹⁸F)]FLT) as a Proliferation Imaging Tracer in Humans: Correlation of [(¹⁸F)]FLT Uptake by Positron Emission Tomography with Ki-67 Immunohistochemistry and Flow Cytometry in Human Lung Tumors. *Clin Cancer Res* 2002;8:3315-3323.
46. Dittmann H, Dohmen B. M., Paulsen F, Wehrmann M., and Bares R. [¹⁸F]FLT PET for diagnosis and staging of thoracic tumors. *J Nucl Med* 2003; 44: 134P [abstract].
47. Yap CS, Schiepers C., Quon A., Silverman D. H., Satyamurthy N., Phelps M. E., and Czernin J. A comparison between [F-¹⁸]Fluorodeoxyglucose (FDG) and [F-¹⁸] 3'-deoxy-3'-fluorothymidine (FLT) uptake in solitary pulmonary nodules and lung cancer. *J Nucl Med* 2003; 44: 123P [abstract].
48. Dittmann H, Dohmen BM, Paulsen F, Eichhorn K, Eschmann SM, Horger M et al. [(¹⁸F)]FLT PET for diagnosis and staging of thoracic tumours. *Eur J Nucl Med Mol Imaging* 2003;30:1407-1412.
49. Buck AK, Halter G, Schirrmeister H, Kotzerke J, Wurzigler I, Glatting G et al. Imaging proliferation in lung tumors with PET: ¹⁸F-FLT versus ¹⁸F-FDG. *J Nucl Med* 2003;44:1426-1431.
50. Cobben DC, Elsinga PH, Hoekstra HJ, Suurmeijer AJ, Vaalburg W, Maas B et al. Is ¹⁸F-3'-fluoro-3'-deoxy-L-thymidine useful for staging and restaging of patients with non-small cell lung cancer? *J Nucl Med* 2004.
51. Shields AF, Dohmen BM, Mangner TJ, Lawhorn-Crews JM, Machulla HJ, Muzik O et al. Imaging of thoracic tumors with ¹⁸F-FLT. *J Nucl Med* 2000;41:74P.
52. Silverman DH, Pio B. S., Satyamurthy N., Park C. K., Chap L., Pegram M, Czernin J., and Phelps M. E. Monitoring effects of breast cancer chemotherapy with fluorodeoxyglucose and fluoro-L-thymidine [abstract]. *J Nucl Med* 2002; 43: 311P [abstract].
53. Smyczek-Gargya B, Fersis N, Dittmann H, Vogel U, Reischl G, Machulla HJ et al. PET with [(¹⁸F)]fluorothymidine for imaging of primary breast cancer: a pilot study. *Eur J Nucl Med Mol Imaging* 2004;31:720-724.
54. Pio BS, Park C. K., Satyamurthy N., Chap L., Pegram M, Czernin J, Phelps M. E., and Silverman D. H. Monitoring early and long-term effects of breast cancer chemotherapy with fluorodeoxyglucose and fluoro-L-thymidine [abstract]. *ASCO conference 2003* 2003; [abstract].
55. Hou MF, Chen YL, Tseng TF, Lin CM, Chen MS, Huang CJ et al. Evaluation of serum CA27.29, CA15-3 and CEA in patients with breast cancer. *Kaohsiung J Med Sci* 1999;15:520-528.
56. Giuliano AE, Jones RC, Brennan M, and Statman R. Sentinel lymphadenectomy in breast cancer. *J Clin Oncol* 1997;15:2345-2350.
57. Veronesi U, Galimberti V, Zurrada S, Pigatto F, Veronesi P, Robertson C et al. Sentinel lymph node biopsy as an indicator for axillary dissection in early breast cancer. *Eur J Cancer* 2001;37:454-458.
58. Vander BT, Pauwels S, Lambotte L, Labar D, De Maeght S, Stroobandt G et al. Brain tumor imaging with PET and 2-[carbon-11]thymidine. *J Nucl Med* 1994;35:974-982.
59. Eary JF, Mankoff DA, Spence AM, Berger MS, Olshen A, Link JM et al. 2-[C-11]thymidine imaging of malignant brain tumors. *Cancer Res* 1999;59:615-621.
60. Dohmen BM, Shields AF, Grierson JR, Kuntzsch M, Reimold M, Sloan A et al. [¹⁸F]FLT-PET in brain tumors; SNM 2000 [abstract]. *J Nucl Med* 2000;41(suppl):216P.
61. Bendaly EA, Sloan AE, Dohmen BM, Mangner TJ, Machulla HJ, Bares R et al. Use of ¹⁸F-FLT-PET to assess the metabolic activity of primary and metastatic brain tumors [abstract]. *J Nucl Med* 2002;111P.
62. Garlip G, Dittmar C, Kracht L, Thomas AV, Herholz K, Heiss WD et al. Identification of DNA and amino acid metabolism in human gliomas by PET. *J Nucl Med* 2003;44:167P.

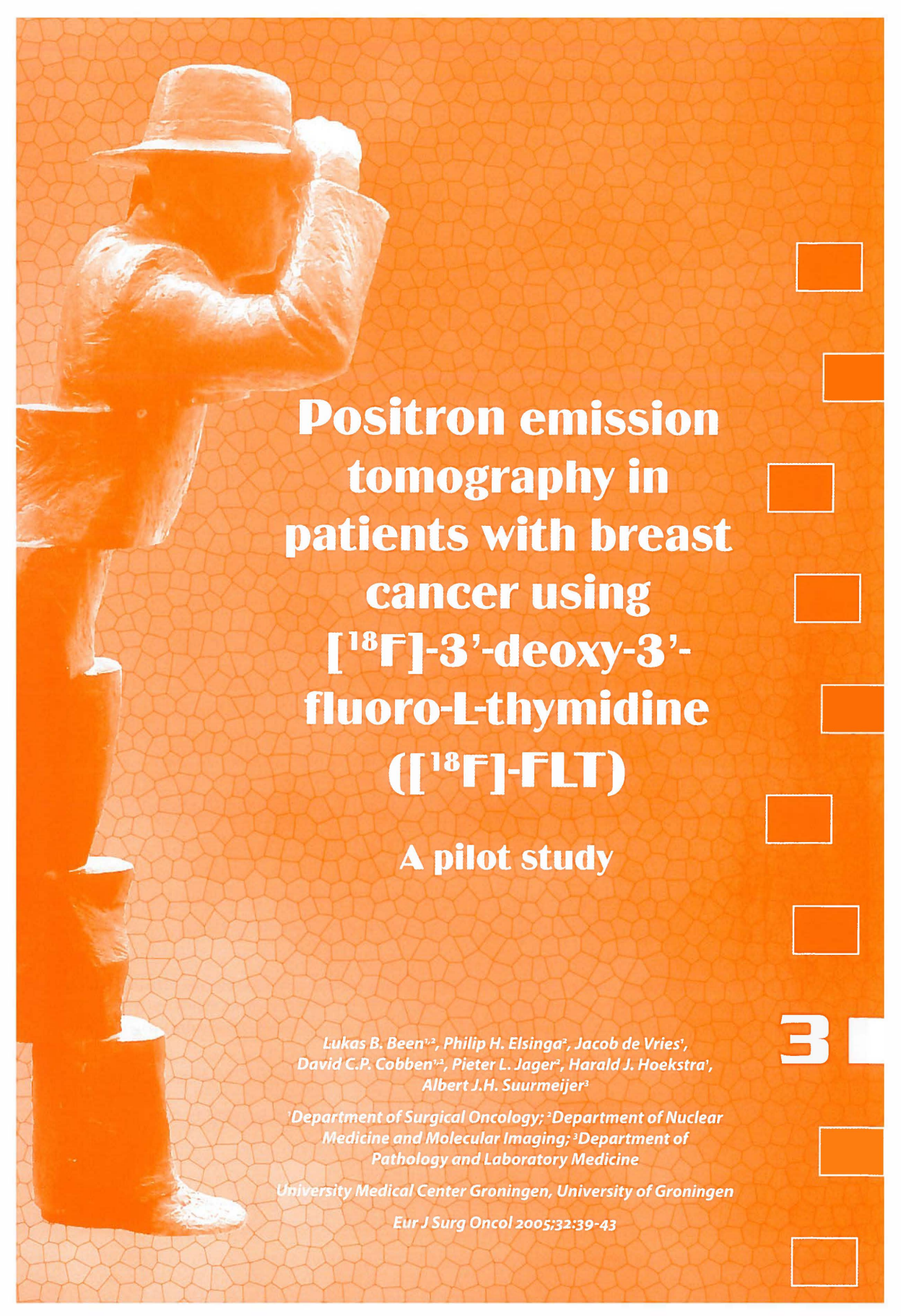


63. Nitzsche EU, Walter MA, Schirp U, Machulla H. J., and Mueller J. Combined PET maging of proliferation and glycolysis for follow up of brachytherapy in brain tumors. [abstract]. SNM 50th Annual Meeting 2003, 2003; [abstract].
64. Huebner RH, Park KC, Shepherd JE, Schwimmer J, Czernin J, Phelps ME et al. A meta-analysis of the literature for whole-body FDG PET detection of recurrent colorectal cancer. *J Nucl Med* 2000;41:1177-1189.
65. Francis DL, Visvikis D, Costa DC, Arulampalam TH, Townsend C, Luthra SK et al. Potential impact of [¹⁸F]3'-deoxy-3'-fluorothymidine versus [¹⁸F]fluoro-2-deoxy-D-glucose in positron emission tomography for colorectal cancer. *Eur J Nucl Med Mol Imaging* 2003;30:988-994.
66. Francis DL, Freeman A, Visvikis D, Costa DC, Luthra SK, Novelli M et al. In vivo imaging of cellular proliferation in colorectal cancer using positron emission tomography. *Gut* 2003;52:1602-1606.
67. Jerusalem G, Beguin Y, Fassotte MF, Najjar F, Paulus P, Rigo P et al. Whole-body positron emission tomography using ¹⁸F-fluorodeoxyglucose for posttreatment evaluation in Hodgkin's disease and non-Hodgkin's lymphoma has higher diagnostic and prognostic value than classical computed tomography scan imaging. *Blood* 1999;94:429-433.
68. Wagner M, Seitz U, Buck A, Neumaier B, Schultheiss S, Bangerter M et al. 3'-[¹⁸F]fluoro-3'-deoxythymidine (¹⁸F)-FLT) as positron emission tomography tracer for imaging proliferation in a murine B-Cell lymphoma model and in the human disease. *Cancer Res* 2003;63:2681-2687.
69. Buck AK, Pitterle K, Schirrmeister H., Bommer M., Glatting G., Neumaier B., and Reske S. N. [¹⁸F]FLT positron emission tomography for imaging Non-Hodgkin's lymphoma and assessment of proliferative activity. *J Nucl Med* 2003; 44: 188P-189P [abstract].
70. Tominaga K, Yamaguchi Y, Nozawa Y, Abe M, and Wakasa H. Proliferation in non-Hodgkin's lymphomas as determined by immunohistochemical double staining for Ki-67. *Hematol Oncol* 1992;10:163-169.
71. Cobben DC, Elsinga PH, Suurmeijer AJ, Vaalburg W, Maas B, Jager PL et al. Detection and grading of soft tissue sarcomas of the extremities with (¹⁸F)-3'-fluoro-3'-deoxy-L-thymidine. *Clin Cancer Res* 2004;10:1685-1690.
72. van Ginkel RJ, Hoekstra HJ, Pruim J, Nieweg OE, Molenaar WM, Paans AM et al. FDG-PET to evaluate response to hyperthermic isolated limb perfusion for locally advanced soft-tissue sarcoma. *J Nucl Med* 1996;37:984-990.
73. van Ginkel RJ, Kole AC, Nieweg OE, Molenaar WM, Pruim J, Koops HS et al. L-[1-¹¹C]-tyrosine PET to evaluate response to hyperthermic isolated limb perfusion for locally advanced soft-tissue sarcoma and skin cancer. *J Nucl Med* 1999;40:262-267.
74. Cobben DC, Koopal S, Tiebosch AT, Jager PL, Elsinga PH, Wobbes T et al. New diagnostic techniques in staging in the surgical treatment of cutaneous malignant melanoma. *Eur J Surg Oncol* 2002;28:692-700.
75. Rinne D, Baum RP, Hor G, and Kaufmann R. Primary staging and follow-up of high risk melanoma patients with whole- body ¹⁸F-fluorodeoxyglucose positron emission tomography: results of a prospective study of 100 patients. *Cancer* 1998;82:1664-1671.
76. Macfarlane DJ, Sondak V, Johnson T, and Wahl RL. Prospective evaluation of 2-[¹⁸F]-2-deoxy-D-glucose positron emission tomography in staging of regional lymph nodes in patients with cutaneous malignant melanoma. *J Clin Oncol* 1998;16:1770-1776.
77. Holder WD, Jr., White RL, Jr., Zuger JH, Easton EJ, Jr., and Greene FL. Effectiveness of positron emission tomography for the detection of melanoma metastases. *Ann Surg* 1998;227:764-769.
78. Havenga K, Cobben DC, Oyen WJ, Nienhuijs S, Hoekstra HJ, Ruers TJ et al. Fluorodeoxyglucose-positron emission tomography and sentinel lymph node biopsy in staging primary cutaneous melanoma. *Eur J Surg Oncol* 2003;29:662-664.
79. Cobben DC, Jager PL, Elsinga PH, Maas B, Suurmeijer AJ, and Hoekstra HJ. 3'-(¹⁸F)-Fluoro-3'-Deoxy-L-Thymidine: A New Tracer for Staging Metastatic Melanoma? *J Nucl Med* 2003;44:1927-1932.
80. Cobben DC, van der Laan BF, Maas B, Vaalburg W, Suurmeijer AJ, Hoekstra HJ et al. ¹⁸F-FLT PET for Visualization of Laryngeal Cancer: Comparison with (¹⁸F)-FDG PET. *J Nucl Med* 2004;45:226-231.

81. Gati WP, Misra HK, Knaus EE, and Wiebe LI. Structural modifications at the 2'- and 3'-positions of some pyrimidine nucleosides as determinants of their interaction with the mouse erythrocyte nucleoside transporter. *Biochem Pharmacol* 1984;33:3325-3331.
82. Eriksson S, Kierdaszuk B, Munch-Petersen B, Oberg B, and Johansson NG. Comparison of the substrate specificities of human thymidine kinase 1 and 2 and deoxycytidine kinase toward antiviral and cytostatic nucleoside analogs. *Biochem Biophys Res Commun* 1991;176:586-592.
83. Bergstrom M, Lu L, Fasth KJ, Wu F, Bergstrom-Pettermann E, Tolmachev V et al. In vitro and animal validation of bromine-76-bromodeoxyuridine as a proliferation marker. *J Nucl Med* 1998;39:1273-1279.
84. Conti PS, Alauddin MM, Fissekis JR, Schmall B, and Watanabe KA. Synthesis of 2'-fluoro-5-[¹⁴C]-methyl-1-beta-D-arabinofuranosyluracil ([¹⁴C]-FMAU): a potential nucleoside analog for in vivo study of cellular proliferation with PET. *Nucl Med Biol* 1995;22:783-789.
85. Mangner TJ, Klecker RW, Anderson L, and Shields AF. Synthesis of 2'-deoxy-2'-[¹⁸F]fluoro-beta-D-arabinofuranosyl nucleosides, [¹⁸F]FAU, [¹⁸F]FMAU, [¹⁸F]FBAU and [¹⁸F]FIAU, as potential PET agents for imaging cellular proliferation. Synthesis of [¹⁸F]labelled FAU, FMAU, FBAU, FIAU. *Nucl Med Biol* 2003;30:215-224.







**Positron emission
tomography in
patients with breast
cancer using
[¹⁸F]-3'-deoxy-3'-
fluoro-L-thymidine
([¹⁸F]-FLT)**

A pilot study

*Lukas B. Been^{1,2}, Philip H. Elsinga², Jacob de Vries¹,
David C.P. Cobben^{1,2}, Pieter L. Jager², Harald J. Hoekstra¹,
Albert J.H. Suurmeijer³*

*¹Department of Surgical Oncology; ²Department of Nuclear
Medicine and Molecular Imaging; ³Department of
Pathology and Laboratory Medicine*

University Medical Center Groningen, University of Groningen

Eur J Surg Oncol 2005;32:39-43

3

Abstract

This pilot study investigated the feasibility of [¹⁸F]-3'-deoxy-3'-fluoro-L-thymidine ([¹⁸F]FLT) as a positron emission tomography (PET) tracer for the visualisation of breast cancer.

Methods

Patients with breast cancer underwent [¹⁸F]FLT-PET prior to surgery. The uptake of [¹⁸F]FLT was determined in the primary tumor and in the axilla.

Results

Eight tumors were visualized by [¹⁸F]FLT-PET with a mean uptake value (SUV_{mean}) of 1.7 and mean tumor to non-tumor ratio (T/NT) of 5.0. In seven patients, axillary lymph-node metastases were found at pathological examinations, however, [¹⁸F]FLT-PET showed uptake in only two large (and clinically evident) lymph-node metastases.

Conclusions

[¹⁸F]FLT shows uptake in most primary breast tumors and in large axillary lymph node metastases.

Introduction

Positron emission tomography (PET) is a non-invasive imaging modality that offers the possibility to visualize different metabolic cellular processes. Several studies have investigated the diagnostic accuracy of PET using [¹⁸F]-fluoro-2'-deoxy-D-glucose ([¹⁸F]FDG) in breast cancer patients ¹⁻⁶. [¹⁸F]FDG uptake reflects glucose metabolism, which is often increased in malignant tissues. In advanced stages, [¹⁸F]FDG-PET has proven to be an accurate tool to visualize and stage breast cancer ⁷. However, the limited sensitivity for small lesions makes [¹⁸F]FDG-PET unsuitable for the exclusion of early stage disease.^{1,8} In a recent study, Buck et al. ⁶ investigated the correlation between [¹⁸F]FDG uptake in breast cancer and several prognostic parameters and found a correlation ($r^2=0.39$) with proliferative activity (Ki-67 index). Possible clinical applications for [¹⁸F]FDG-PET may include monitoring response to therapy in locally advanced breast cancer (LABC), but further research is needed. [¹⁸F]FDG is not a highly selective tracer for imaging cancer, since [¹⁸F]FDG is also taken up by activated macrophages and other inflammatory cells.

Shields et al. ⁹ developed [¹⁸F]-3'-deoxy-3'-fluoro-L-thymidine ([¹⁸F]FLT) as a new PET tracer. [¹⁸F]FLT is a pyrimidine analogue and after its uptake into the cell, [¹⁸F]FLT is phosphorylated by thymidine kinase 1 (TK₁) into [¹⁸F]FLT-monophosphate. This causes intracellular entrapment of the radioactivity. TK₁ is a principal enzyme in the salvage pathway of DNA synthesis. Its activity is increased during the S phase of the cell cycle. Therefore, [¹⁸F]FLT uptake reflects the proliferation rate of malignant tissues ¹⁰.

Several research groups worldwide are investigating the clinical use of [¹⁸F]FLT-PET for detecting and staging different tumor types ¹¹⁻¹⁷. The aim of this study was to investigate the feasibility of [¹⁸F]FLT-PET for the visualization of breast cancer and lymph-node metastases.

Materials and methods

Patients

Patients with proven breast cancer were included in this prospective study to undergo [¹⁸F]FLT-PET. Diagnosis was suspected by palpation, mammography and ultrasonography of the breast and proven by fine needle aspiration cytology or core biopsy histology. Patients should not have undergone surgical treatment shortly before PET imaging nor should they have received radiotherapy or chemotherapy prior to PET imaging. Patients with abnormal liver and kidney functions and abnormal hematological parameters (white blood cells, red blood cells and thrombocytes) were excluded from the study because of toxicity data of therapeutic doses of unlabeled



31



FLT (alovudine), ¹⁸ although no side-effects are expected at tracer doses. Furthermore, pregnant patients were excluded from the study. All patients gave written informed consent and the study protocol was approved by the Medical Ethics Committee of the University Medical Center Groningen.

Tracer synthesis

Synthesis of [¹⁸F]FLT was performed according to the method of Machulla et al. ¹⁹ [¹⁸F]FLT was produced by fluorination with [¹⁸F]-fluoride of the 4,4'-dimethoxytrityl protected anhydrothymidine, followed by a deprotection step. After purification by reversed phase high performance liquid chromatography, the product was made isotonic and passed through a 0.22 µm filter. [¹⁸F]FLT was produced with a radiochemical purity of >95% and specific activity of >10 TBq/mmol. The radiochemical yield was 8.8% ± 3.7% (decay corrected).

[¹⁸F]FLT-PET studies

For this study, an ECAT HR+ PET camera (Siemens/CTI, Knoxville, TN, USA) was used. To establish the optimal time interval between injection and scanning, the first three patients were scanned at 30, 120, 180 and 240 min after injection of [¹⁸F]FLT. These patients received 411 MBq (range 390-420) of [¹⁸F]FLT, which accounts for a radiation dose of approximately 12 mSv ²⁰. Based on these results (Fig. 1), all other patients were scanned only at 120 min after injection. These patients were injected with 200 MBq (range 160-250 MBq) of [¹⁸F]FLT, which accounts for a radiation dose of approximately 6 mSv ²⁰. After injection, patients were instructed to drink 500 mL of water for optimal hydration and to stimulate excretion of [¹⁸F]FLT. Patients were placed in prone position on a custom-made mattress, allowing free exposure of both breasts. The arms of the patients were placed alongside the head. Scanning was performed in emission-transmission-transmission-emission mode over two bed positions for 7 min per bed position (2 min transmission, 5 min emission) from the seventh cervical vertebra downwards. Data from both bed positions were iteratively reconstructed (ordered subset expectation maximization) ²¹. The liver was not scanned, partly because no liver metastases were anticipated in these early stage breast cancer patients and partly because the sensitivity of [¹⁸F]FLT for detecting liver metastases in the literature is low ¹³.

Data analysis

All PET images were analyzed by a clinical investigator (LBB) and an experienced nuclear medicine specialist (PLJ), blinded for other clinical and histopathological data. [¹⁸F]FLT-PET images were scored for presence or absence of areas of increased [¹⁸F]FLT uptake. Also lesions outside the location of the primary tumor were scored, blinded for other clinical information.

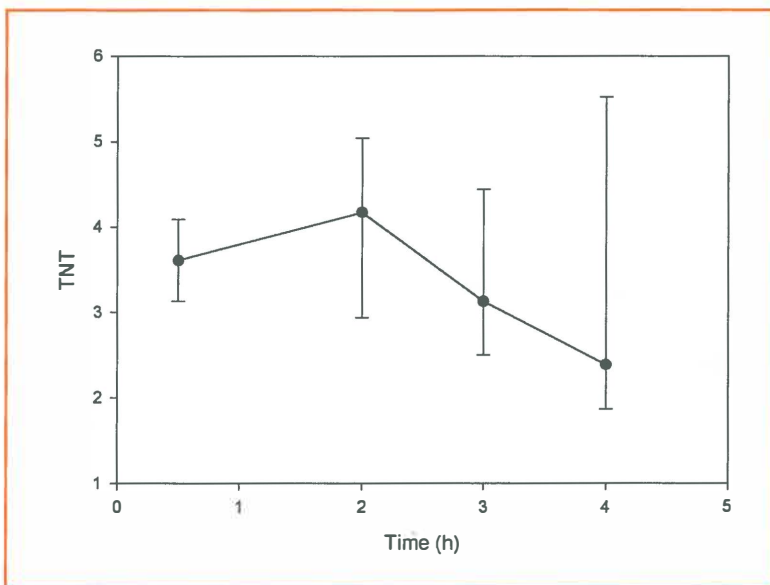


Figure 1
Tumor-non-tumor (TNT) ratios measured in three patients at various time intervals. TNT values expressed as median and range

After visual analysis, semiquantitative evaluation of the PET scans was performed by analyzing areas with increased [¹⁸F]FLT uptake on transverse sections. The plane with the highest standardized uptake value (SUV) was selected for region of interest (ROI) analysis. A ROI was placed at the 70% isocontour of the SUV_{max} in the tumor to determine the SUV_{mean}. A manually drawn ROI around contralateral breast tissue was applied for measuring background activity (SUV_{bgr}). The SUV_{mean} in the ROI of the tumor was divided by the SUV_{bgr} to produce the tumor to non-tumor ratio (T/NT). After calculating the SUVs and TNTs, the PET data were correlated with the histopathological findings.

Surgery

After PET, patients underwent either breast conserving surgical treatment or a mastectomy. Furthermore, patients underwent a sentinel lymph node biopsy using a combination of patent blue dye and ^{99m}Tc-nanocolloid particles. In case of the presence of a metastatic lymph node at SLNB, an axillary lymph node dissection was performed.



Results

Patients

Ten patients (mean age 45.4 years, range 31-72 years) were included in the study and all patients underwent [¹⁸F]FLT-PET.

Seven patients had an invasive ductal carcinoma, two patients had an invasive lobular carcinoma and one patient had a ductal carcinoma in situ.

PET imaging

In eight patients, [¹⁸F]FLT uptake was demonstrated in the primary tumor, in two patients no increased uptake was seen (Figs. 2 and 3 for examples). The mean SUV_{mean} was 1.7 (range 0.3-4.4). Mean SUV_{bgr} was 0.3 (range 0.2-0.4) and mean T/NT was 5.0 (range 1.0-11.5). There were no additional areas of increased tracer uptake in the breasts.

In two patients, additional lesions were seen in the axilla. In both patients, palpable axillary lymph nodes had been detected at the time of diagnosis. In the remaining eight patients, [¹⁸F]FLT-PET showed no uptake in the axilla. The [¹⁸F]FLT-PET findings of all patients are summarized in Table 1.

Histopathological examination of the resected tumor specimens showed seven invasive ductal carcinomas, two invasive lobular carcinomas and one ductal carcinoma in situ. Mean tumor size was 25.6 mm (range 11-50 mm). Three tumors were graded as grade 1 tumors, 2 tumors were grade 2 tumors and 4 tumors were grade 3 tumors. The ductal carcinoma in situ was a high-grade tumor.

Two patients had clinically apparent lymph node metastases at the time of diagnosis. The size of these lymph-node metastases was approximately 20 mm. In the remaining eight patients, SLNB and/or ALND showed metastatic lymph nodes in five patients. The size of these lymph node metastases ranged from isolated tumor cells (<0.1 mm) to 11 mm.

Discussion

We have studied the feasibility of [¹⁸F]FLT to visualize breast cancer in ten patients. [¹⁸F]FLT-PET offers the possibility to non-invasively visualize malignancies and measure the rate of proliferation. Several research groups have reported a strong correlation between [¹⁸F]FLT uptake and Ki-67 proliferation index in lung tumors^{12,14,22}.

We have shown that [¹⁸F]FLT uptake can be demonstrated and measured in primary malignant breast tumors and even in some large axillary lymph-node metastases. However, two out of 10 tumors showed no [¹⁸F]FLT uptake. Furthermore, small axillary lymph node metastases were not seen on [¹⁸F]FLT-PET.

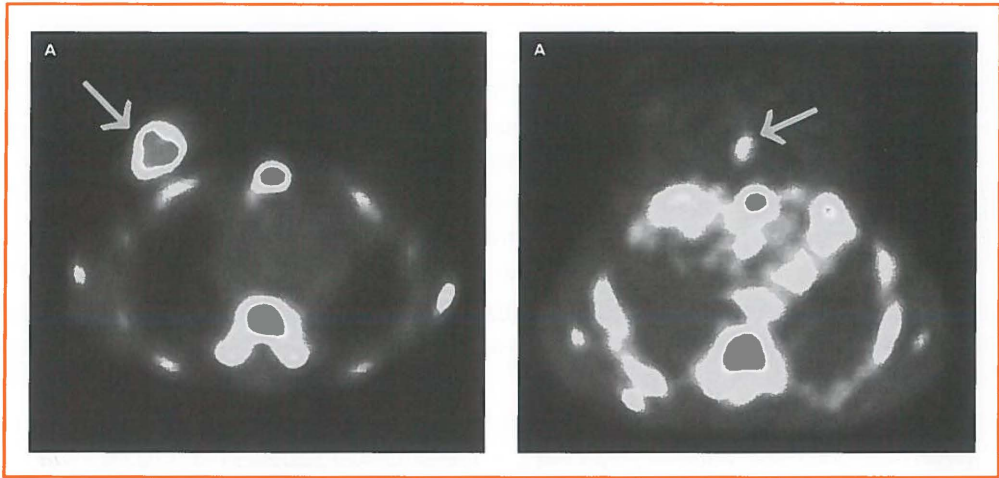


Figure 2
 Transverse slice of a [¹⁸F]FLT-PET scan of patient 9 diagnosed with a large tumor (45 mm) in the right breast. TNT was 10.9

Figure 3
 Transverse slice of a [¹⁸F]FLT-PET scan of patient 1 diagnosed with a small tumor (15 mm) medially in the left breast. TNT was 2.4

Table 1
 PET findings

| Pt no | Visualisation tumor | Visualisation LN | SUV _{max} tumor | SUV _{mean} tumor | TNT |
|-------|---------------------|------------------|--------------------------|---------------------------|------|
| 1 | yes | no | 1.01 | 0.79 | 2.4 |
| 2 | yes | no | 1.22 | 0.91 | 5.1 |
| 3 | no | no | n.a. | n.a. | 1.0* |
| 4 | yes | no | 0.47 | 0.33 | 1.2 |
| 5 | no | no | n.a. | n.a. | 1.0* |
| 6 | yes | no | 1.76 | 1.31 | 5.0 |
| 7 | yes | no | 1.31 | 0.96 | 4.2 |
| 8 | yes | yes | 5.64 | 4.36 | 11.5 |
| 9 | yes | yes | 4.42 | 3.26 | 10.9 |
| 10 | yes | no | 2.04 | 1.54 | 7.3 |

* no visible tumor
 LN = lymph node; n.a. = not applicable



In a recent study by Smyczek-Gargya et al.²³, [¹⁸F]FLT uptake was measured in patients with primary breast cancer. The results of this small feasibility study show that 13 out of 14 breast tumors and seven out of eight histologically proven axillary lymph node metastases could be visualized with [¹⁸F]FLT-PET. These investigators are somewhat more optimistic about the opportunities of [¹⁸F]FLT-PET in detecting primary breast cancer and staging the axilla. However, in their study, patients with larger tumors were included (mean size 33 mm vs. 26 mm in our study), being a possible explanation for the higher SUV values in their study. It is clear that future studies with larger patient numbers are needed to establish the true value of [¹⁸F]FLT-PET in detecting and staging breast cancer.

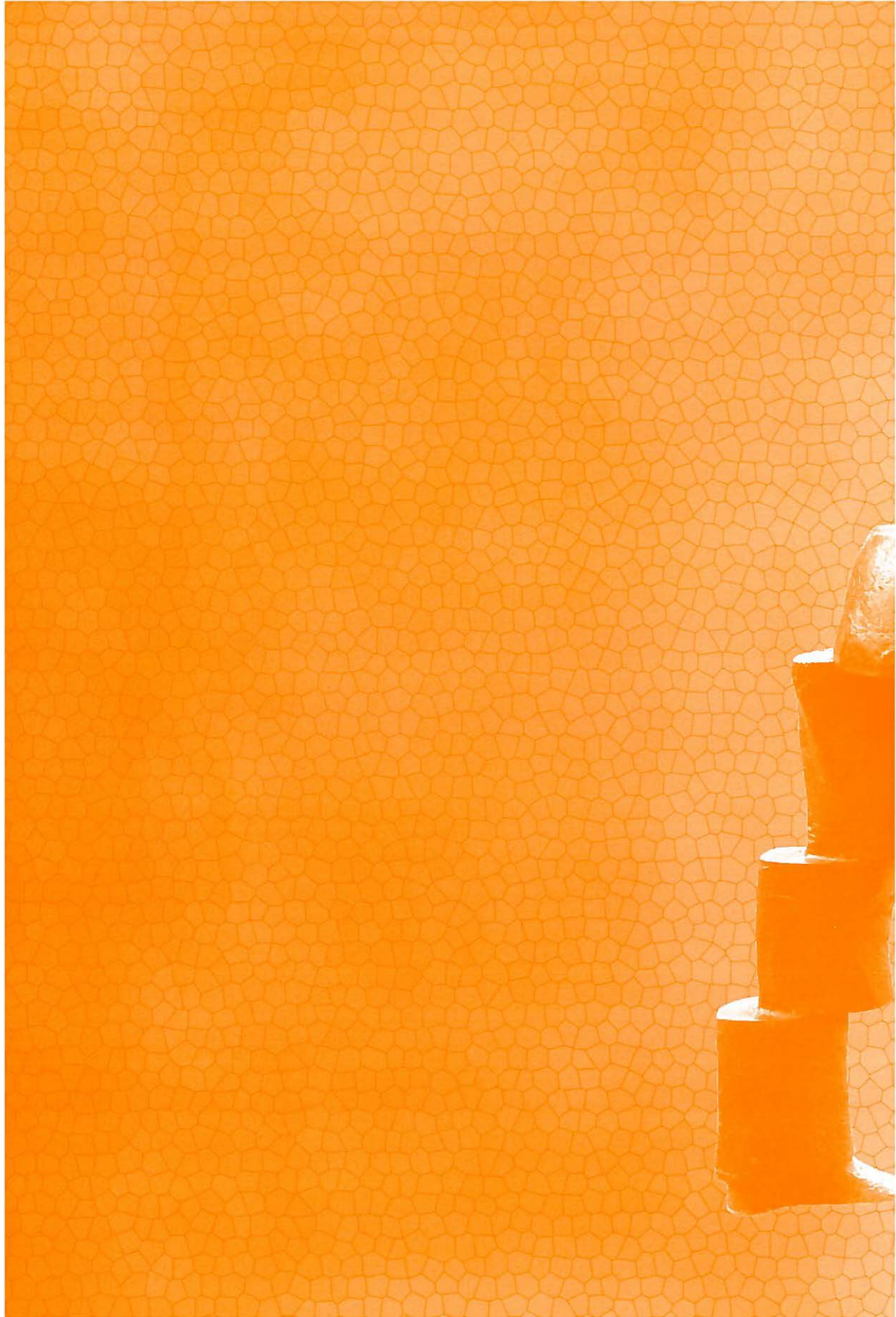
In conclusion, this pilot study shows that primary breast tumors can be visualized by [¹⁸F]FLT-PET. The true value of [¹⁸F]FLT-PET in breast cancer patients need to be investigated in larger patient series. The recently reviewed [¹⁸F]FLT-PET literature indicates that [¹⁸F]FLT is probably not an ideal tracer for detection and staging tumors, but that it shows potential in measuring the response to therapy at an early stage²⁴. Since large tumors with high proliferation rate probably are visualized with [¹⁸F]FLT-PET, future research will need to be focused on measuring the response to neoadjuvant chemotherapy in patients with locally advanced breast cancer. [¹⁸F]FDG-PET has been evaluated in patients with LABC by a number of research groups (for review see Krak et al.)²⁵, showing promising results with regard to measuring response to chemotherapy. However, [¹⁸F]FDG also shows uptake in inflammatory cells, sometimes hampering the interpretation during or shortly after therapy. We, therefore, think that [¹⁸F]FLT could be a better tracer for measuring the response to chemotherapy, since it shows no uptake in inflammatory tissues²⁶.

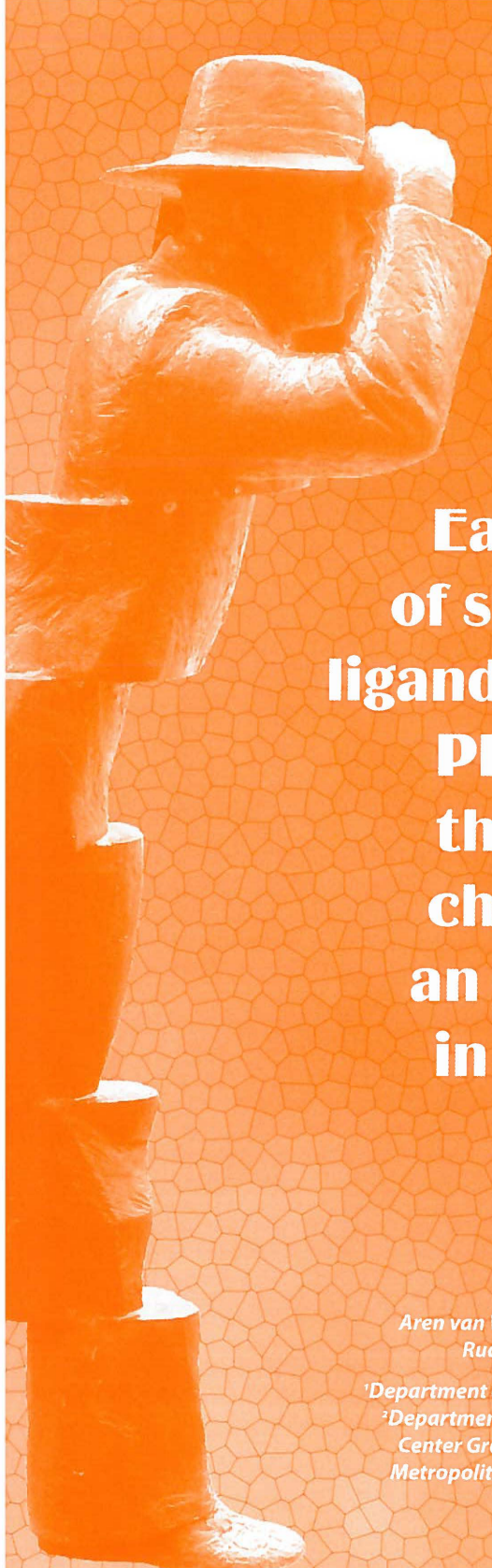
References

1. Avril N, Rose CA, Schelling M, Dose J, Kuhn W, Bense S et al. Breast imaging with positron emission tomography and fluorine-18 fluorodeoxyglucose: use and limitations. *J Clin Oncol* 2000;18:3495-3502.
2. Avril N, Bense S, Ziegler SI, Dose J, Weber W, Laubenbacher C et al. Breast imaging with fluorine-18-FDG PET: quantitative image analysis. *J Nucl Med* 1997;38:1186-1191.
3. Crippa F, Seregini E, Agresti R, Chiesa C, Pascali C, Bogni A et al. Association between [¹⁸F]fluorodeoxyglucose uptake and postoperative histopathology, hormone receptor status, thymidine labelling index and p53 in primary breast cancer: a preliminary observation. *Eur J Nucl Med* 1998;25:1429-1434.
4. Adler LP, Crowe JP, al Kaisi NK, and Sunshine JL. Evaluation of breast masses and axillary lymph nodes with [¹⁸F] 2-deoxy-2-fluoro-D-glucose PET. *Radiology* 1993;187:743-750.
5. Dose J, Bleckmann C, Bachmann S, Bohuslavizki KH, Berger J, Jenicke L et al. Comparison of fluorodeoxyglucose positron emission tomography and "conventional diagnostic procedures" for the detection of distant metastases in breast cancer patients. *Nucl Med Commun* 2002;23:857-864.
6. Buck A, Schirmeister H, Kuhn T, Shen C, Kalker T, Kotzerke J et al. FDG uptake in breast cancer: correlation with biological and clinical prognostic parameters. *Eur J Nucl Med Mol Imaging* 2002;29:1317-1323.

7. van der Hoeven JJ, Krak NC, Hoekstra OS, Comans EF, Boom RP, van Geldere D et al. 18F-2-fluoro-2-deoxy-d-glucose positron emission tomography in staging of locally advanced breast cancer. *J Clin Oncol* 2004;22:1253-1259.
8. Hoh CK and Schiepers C. ¹⁸F-DG imaging in breast cancer. *Semin Nucl Med* 1999;29:49-56.
9. Shields AF, Grierson JR, Dohmen BM, Machulla HJ, Stayanoff JC, Lawhorn-Crews JM et al. Imaging proliferation in vivo with [¹⁸F]FLT and positron emission tomography. *Nat Med* 1998;4:1334-1336.
10. Rasey JS, Grierson JR, Wiens LW, Kolb PD, and Schwartz JL. Validation of FLT uptake as a measure of thymidine kinase-1 activity in A549 carcinoma cells. *J Nucl Med* 2002;43:1210-1217.
11. Dittmann H, Dohmen BM, Paulsen F, Eichhorn K, Eschmann SM, Horger M et al. [¹⁸F]FLT PET for diagnosis and staging of thoracic tumors. *Eur J Nucl Med Mol Imaging* 2003;30:1407-1412.
12. Vesselle H, Grierson J, Muzi M, Pugsley JM, Schmidt RA, Rabinowitz P et al. In Vivo Validation of 3'-deoxy-3'-[¹⁸F]fluorothymidine ([¹⁸F]FLT) as a Proliferation Imaging Tracer in Humans: Correlation of [¹⁸F]FLT Uptake by Positron Emission Tomography with Ki-67 Immunohistochemistry and Flow Cytometry in Human Lung Tumors. *Clin Cancer Res* 2002;8:3315-3323.
13. Francis DL, Visvikis D, Costa DC, Arulampalam TH, Townsend C, Luthra SK et al. Potential impact of [¹⁸F]3'-deoxy-3'-fluorothymidine versus [¹⁸F]fluoro-2-deoxy-D-glucose in positron emission tomography for colorectal cancer. *Eur J Nucl Med Mol Imaging* 2003;30:988-994.
14. Buck AK, Halter G, Schirrmeyer H, Kotzerke J, Wurziger I, Glatting G et al. Imaging proliferation in lung tumors with PET: ¹⁸F-FLT versus ¹⁸F-FDG. *J Nucl Med* 2003;44:1426-1431.
15. Cobben DC, Jager PL, Elsinga PH, Maas B, Suurmeijer AJ, and Hoekstra HJ. 3'-[¹⁸F]-Fluoro-3'-Deoxy-L-Thymidine: A New Tracer for Staging Metastatic Melanoma? *J Nucl Med* 2003;44:1927-1932.
16. Cobben DC, van der Laan BF, Maas B, Vaalburg W, Suurmeijer AJ, Hoekstra HJ et al. ¹⁸F-FLT PET for Visualization of Laryngeal Cancer: Comparison with (¹⁸F)-FDG PET. *J Nucl Med* 2004;45:226-231.
17. Cobben DC, Elsinga PH, Suurmeijer AJ, Vaalburg W, Maas B, Jager PL et al. Detection and grading of soft tissue sarcomas of the extremities with (¹⁸F)-3'-fluoro-3'-deoxy-L-thymidine. *Clin Cancer Res* 2004;10:1685-1690.
18. Flexner C, van der HC, Jacobson MA, Powderly W, Duncanson F, Ganes D et al. Relationship between plasma concentrations of 3'-deoxy-3'-fluorothymidine (alovudine) and antiretroviral activity in two concentration-controlled trials. *J Infect Dis* 1994;170:1394-1403.
19. Machulla HJ, Blochler A, Kuntzsch M, Piert M, Wei R, and Grierson JR. Simplified labeling approach for synthesizing 3'-deoxy-3'-[¹⁸F]fluorothymidine ([¹⁸F]FLT). *Journal of Radioanalytical and Nuclear Chemistry* 2000;243:843-846.
20. Vesselle H, Grierson J, Peterson LM, Muzi M, Mankoff DA, and Krohn KA. ¹⁸F-Fluorothymidine radiation dosimetry in human PET imaging studies. *J Nucl Med* 2003;44:1482-1488.
21. Lonneux M, Borbath I, Bol A, Coppens A, Sibomana M, Bausart R et al. Attenuation correction in whole-body FDG oncological studies: the role of statistical reconstruction. *Eur J Nucl Med* 1999;26:591-598.
22. Buck AK, Schirrmeyer H, Hetzel M, Von Der HM, Halter G, Glatting G et al. 3-deoxy-3'-[¹⁸F]fluorothymidine-positron emission tomography for noninvasive assessment of proliferation in pulmonary nodules. *Cancer Res* 2002;62:3331-3334.
23. Smyczek-Gargya B, Fersis N, Dittmann H, Vogel U, Reischl G, Machulla HJ et al. PET with [¹⁸F]fluorothymidine for imaging of primary breast cancer: a pilot study. *Eur J Nucl Med Mol Imaging* 2004;31:720-724.
24. Been LB, Suurmeijer AJ, Cobben DC, Jager PL, Hoekstra HJ, and Elsinga PH. [¹⁸F]FLT-PET in oncology; current status and opportunities. *Eur J Nucl Med Mol Imaging* 2004;in press.
25. Krak NC, Hoekstra OS, and Lammertsma AA. Measuring response to chemotherapy in locally advanced breast cancer: methodological considerations. *Eur J Nucl Med Mol Imaging* 2004.
26. Van Waarde A, Cobben DCP, Suurmeijer AJH, Maas B, Vaalburg W, De Vries EFJ et al. Selectivity of 3'-deoxy-3'-[¹⁸F]fluorothymidine (FLT) and 2-[¹⁸F]fluoro-2-deoxy-D-glucose (FDG) for tumor versus inflammation in a rodent model. *J Nucl Med* 2004;45:695-700.







**Early response
of sigma receptor
ligands and metabolic
PET tracers to
three forms of
chemotherapy:
an in vitro study
in glioma cells**

4

*Aren van Waarde¹, Lukas B. Been^{1,2}, Kiichi Ishiwata³
Rudi A. Dierckx¹ and Philip H. Elsinga¹*

*¹Department of Nuclear Medicine and Molecular Imaging;
²Department of Surgical Oncology, University Medical
Center Groningen; ³Positron Medical Center, Tokyo
Metropolitan Institute of Gerontology, Tokyo, Japan*

J Nucl Med 2006;47:1538-1545

Abstract

The significant presence of nontumor cell populations within tumors can complicate the assessment of in vivo tumor metabolism during therapy. To more clearly define the impact of cytotoxic agents, we compared early changes in the uptake of six PET tracers in cultured glioma cells. Doxorubicin (1 $\mu\text{mol/L}$), cisplatin (10 $\mu\text{mol/L}$), and 5-fluorouracil (10 mmol/L) were selected to target different aspects of cellular metabolism.

The tracers were two extracellular sigma receptor ligands: [^{18}F]FE-SA5845 (nonsubtype selective) and [^{11}C]SA4503 (sigma-1), the nucleoside [^{18}F]-fluoro-3'-deoxy-3'-L-fluorothymidine [^{18}F]FLT, [^{11}C]choline, [^{11}C]methionine and [^{18}F]FDG. C6 glioma cells were grown as monolayers and exposed to cytotoxic agents at concentrations at least 1 order of magnitude higher than the concentration for 50% growth inhibition of this cell line. Effects on cellular parameters were measured after 0, 1, 2, 3, 4, and 24 h.

All treatments resulted in a decline of cell numbers within 24 h. The binding of the sigma ligands [^{11}C]SA4503 and [^{18}F]FE-SA5845 and the uptake of [^{11}C]choline (normalized for the number of viable cells) were strongly increased. The uptake of [^{18}F]FDG showed little change, and cellular accumulation of [^{18}F]FLT and [^{11}C]methionine was decreased. Uptake of [^{18}F]FLT and [^{11}C]methionine was related to the fraction of cells in S-phase, but not under all conditions: (a) doxorubicin caused a more rapid decline in [^{18}F]FLT uptake than in the S-phase fraction because of depletion of cellular ATP, and (b) cisplatin inhibited the transport of [^{11}C]methionine across the tumor cell membrane.

Increased binding of sigma ligands and an increased uptake of [^{11}C]choline after chemotherapy may reflect active membrane repair in damaged cells. [^{18}F]FLT and [^{11}C]methionine behaved as proliferation markers. However, the accumulation of [^{18}F]FDG reflected not the proliferation rate but, rather, the number of viable cells per well.

Introduction

Although the most widely used radiopharmaceutical in clinical oncology is [^{18}F]FDG, this glucose analog is not useful under all circumstances. High physiological uptake of glucose in the healthy brain and strong accumulation of radioactivity in the urinary bladder limit the use of [^{18}F]FDG for tumor detection in the central nervous system ¹ and in the lower part of the abdomen ². A high rate of false-positive lesions further restricts the use of [^{18}F]FDG for certain applications ^{3,4}. [^{18}F]FDG is not tumor cell specific and it can also accumulate in other cells – for example, active macrophages ⁵. This lack of specificity is a pitfall in the monitoring of therapy control with [^{18}F]FDG-PET after chemotherapy ⁶. Thus, there is opportunity for the development of alternative imaging agents that lack some of the disadvantages of [^{18}F]FDG.

[^{11}C]- and [^{18}F]-labeled amino acids, nucleosides, and cholines have been developed as radiopharmaceuticals to target elevated synthesis of proteins, DNA, and biomembranes in malignant tissue ⁷⁻¹¹. Sigma receptor ligands, which have been proposed as novel radiopharmaceuticals for tumor imaging, are also proliferation markers ¹². These radiotracers track the synthesis of cell membrane lipids ¹³.

Oncologic tracers can be used not only for tumor detection, but also for evaluation of the tumor response to treatment. Metabolic changes induced by chemotherapy precede the morphologic changes. Radiolabeled compounds that track different aspects of cell metabolism may show different uptake kinetics after therapy. The uptake of an ideal tracer would show a rapid change in responding tumors and the magnitude of this change would correspond to the final therapy outcome.

Various radiopharmaceuticals have been examined, comparatively, as early response indicators of chemotherapy. Sato et al. ¹⁴ measured uptake changes of two nucleosides ([^{18}F]-5-fluoro-2'-deoxyuridine, [^{14}C]thymidine), one amino acid ([^{14}C]methionine) and a glucose analog ([^3H]deoxyglucose) in rat glioma after in vivo chemotherapy with 1-(4-amino-2-methyl-5-pyrimidinyl)methyl-3-(2-chloroethyl)-3-nitrosourea (ACNU). Schaidler et al. ¹⁵ monitored the uptake of two amino acids ([^3H]- α -aminoisobutyric acid and L-[^{14}C]methyl]methionine), a nucleoside ([^3H]thymidine) and a glucose analog ([^{18}F]FDG) in a human colon carcinoma cell line during in vitro chemotherapy with dinaline. Takeda et al. ¹⁶ measured sequential changes in DNA synthesis, glucose use, protein synthesis, and peripheral benzodiazepine receptor density in C6 tumors within rat brain in vivo during chemotherapy with nitrosoureas. To the best of our knowledge, treatment responses of sigma receptor ligands have never been compared with those of established PET tracers ([^{18}F]FDG, [^{18}F]FLT, [^{11}C]methionine) and of [^{11}C]choline. Therefore, we decided to measure changes in the uptake of the sigma-1 ligand [^{11}C]SA4503 and the nonsubtype-selective sigma ligand [^{18}F]FESA5845, [^{18}F]FLT, [^{11}C]choline, [^{11}C]methionine, and [^{18}F]FDG during three forms of chemotherapy in vitro.



A considerable (and unknown) fraction of the total mass of in vivo tumors consists of normal cells. Human breast cancers have been reported to contain 19%-64% of macrophages¹⁷ and up to 10% of lymphocytes¹⁸. Thus, nontumor cells may contribute significantly to the radioactive signal being measured and their presence complicates the assessment of changes in tumor metabolism during therapy. In vitro models contain only tumor cells. Changes in tracer uptake in these models are a more direct reflection of metabolic impact within tumor cells. Thus, in vitro data can be more easily interpreted than results from in vivo studies.

For our own in vitro chemotherapy model we used cisplatin, doxorubicin, and 5-fluorouracil, compounds which interact with DNA¹⁹, topoisomerase II²⁰ and thymidylate synthetase²¹, respectively. The agents were administered to C6 glioma cells in concentrations that were >1 order of magnitude greater than the concentration for 50% growth inhibition (GIC₅₀) values²². The C6 line was chosen because it had also been used in our previous work on sigma ligands^{23,24}.

Materials and methods

Culture media and drugs

Cisplatin (cis-diammineplatinum (II) dichloride) was a product of Sigma. Fluracedyl (5-fluorouracil solution 50 mg/mL) and doxorubicin were obtained from Pharmachemie. Dulbecco's Minimum Essential Medium (DMEM), fetal calf serum (FCS) and trypsin were from Invitrogen.

Radiopharmaceuticals

[¹¹C]methionine, [¹¹C]choline, [¹⁸F]FLT, and [¹⁸F]FDG were prepared by standard procedures reported in the literature. [¹⁸F]FE-SA5845 and [¹¹C]SA4503 were prepared by reaction of [¹⁸F]fluoroethyl tosylate and [¹¹C]methyl iodide, respectively, with the appropriate 4-O-methyl compound²⁵. All radiochemical purities were >95%.

Cell culture and treatment with cytostatic agents

C6 rat glioma cells obtained from the American Type Culture Collection were cultured in monolayers in DMEM supplemented with 5% FCS in a humidified atmosphere of 5% CO₂/95% air at 37°C. Before each experiment, the cells were seeded in 12-well plates (Costar) with 1.3 mL of DMEM supplemented with 5% FCS per well. After 24 h at 37°C, monolayers were established. Cytotoxic agents (final concentration in culture medium: 1 μmol/L doxorubicin, 10 μmol/L cisplatin, 10 mmol/L 5-fluorouracil) were then added to the wells 24, 4, 3, 2 and 1 h before addition of radiotracer.

Incubation with radiotracer

Experiments were performed in quadruplicate. Studies of radiotracer uptake were performed in monolayers grown at the bottom of 12-well plates. At time zero, 2 MBq of a radiotracer ($[^{14}\text{C}]$ methionine, $[^{14}\text{C}]$ choline, $[^{14}\text{C}]$ SA4503, $[^{18}\text{F}]$ FDG, $[^{18}\text{F}]$ FLT, or $[^{18}\text{F}]$ FE-SA5845) in 50 μL of saline was added to each well. At the end of incubation (60 min), the medium was quickly removed and the monolayer was washed 3 times with chilled phosphate-buffered saline (PBS). Cells were then treated with 0.2 mL of trypsin. When the cells had detached from the bottom of the well, 1 mL of DMEM was added to stop the proteolytic action. Cell clumps were removed by repeated (at least 10-fold) pipetting of the trypsin/DMEM mixture. Radioactivity in the cell suspension (1.2 mL) was assessed using a gamma counter (Compugamma 1282 CS, LKB-Wallac). A 50- μL sample of the suspension was mixed with 50 μL of trypan blue (0.4% solution in PBS) and used for cell counting. Cell numbers were manually determined, using a phase-contrast microscope (Olympus), a Bürker bright-line chamber (depth 0.1 mm; 0.0025- mm^2 squares), and a hand-tally counter.

Propidium Iodine (PI) staining and flow cytometric analysis

C6 cells were grown and harvested as described; two wells from a 12-wells plate were pooled. The cell samples were washed twice with PBS containing 5 mmol/L MgCl_2 . After each washing step, a cell pellet was collected by short centrifugation (5 min, 2000 rpm; Hettich tabletop centrifuge). The washed cells were fixed in 2 mL 80% ethanol:acetone (1:1 v/v) at 4°C for at least 18 h. Fixed cells were washed once with 5 mL PBS containing 5 mmol/L MgCl_2 and the pellet was resuspended in 20 μL DNase-free RNase A (Sigma) and incubated for 30 min at 37°C. At the end of the incubation, 400 μL PI (Sigma) was added (a solution of 10 $\mu\text{g}/\text{mL}$ in PBS with 5 mmol/L MgCl_2) and the mixture was stored in the refrigerator (4°C) for at least 18 h. Cellular DNA content was determined with a FACSCalibur (Becton Dickinson). Data were plotted using CellQuest software; at least 5,000 events were analysed for each sample.

Thymidine Kinase assay

C6 cells were grown and harvested as described; four wells from a 12-wells plate were pooled. A cell pellet was collected by a short centrifugation (as above). The pellet was resuspended in 0.5 mL of ice-cold lysis buffer (20 mmol/L Tris-HCl, pH 8.1, 40 mmol/L KCl, 1 mmol/L EDTA, 10% glycerol, 1 mmol/L dithiothreitol (DTT), 1 mmol/L phenylmethylsulfonyl fluoride (PMSF), 1 $\mu\text{g}/\text{mL}$ aprotinin). The cells were lysed by repeated sonication 0°C. Cell and membrane fragments were removed from the lysate by centrifugation (Hettich Mikrofuge, 5 min, 12,000 $\times g$).

The enzyme reaction mixture (ERM) contained 80 mmol/L potassium phosphate buffer pH 7.6, 160 mmol/L KCl, 100 mmol/L NaF, 4 mg/mL bovine serum albumin (BSA), 20 mmol/L (ATP)- MgCl_2 and 4 mmol/L DTT. Equal volumes of cell lysate (0.5 mL) and ERM

**41**

(0.5 mL) were mixed and incubated with 2 MBq [^{18}F]FLT in a closed glass vial for 60 min at 37°C. Two samples (50 μL) were taken from each vial and pipetted onto Whatman DE-81 filters. One filter remained untreated; the other was washed 3 times with a 4 mmol/L ammonium formate solution and 3 times with ethanol. Radioactivity on the filters was determined with a gamma counter (as above). Activity on the washed filter represented [^{18}F]FLT-phosphates, whereas the activity on the untreated filter represented [^{18}F]FLT-phosphates plus unreacted [^{18}F]FLT. A blank incubation (0.5 mL lysis buffer without C6 cells) was run in parallel during each experiment.

Preliminary experiments indicated that the thymidine kinase assay was linear for incubation times up to 90 min. Therefore, an incubation time of 60 min was chosen in subsequent experiments. Radioactivity in blank incubations was <3% of that in cell lysates after 60 min.

ATP assay

Cellular ATP was measured with a kit based on firefly (*Photinus pyralis*) luciferase (ATPlite Luminescence ATP Detection Assay System; Perkin-Elmer). The bioluminescence was quantified using a Lumicount microplate luminometer (Packard Instruments Co.). A reaction blank and a standard curve with 7 concentrations of ATP were run in parallel. The assay was linear over a large range of ATP concentrations (5×10^{-9} mol/L to 10^{-6} mol/L) and of cell numbers in the assay. Samples were diluted to ensure that the concentration of ATP was within the range of the calibration curve.

Statistics

Differences between groups were examined using one-way ANOVA. A p -value <0.05 was considered statistically significant.

Results

Cell number

The number of viable cells per well decreased as a result of chemotherapy. The three cytostatic agents inhibited cellular proliferation with different time courses (Fig. 1). The effect of doxorubicin (1 $\mu\text{mol/L}$) was relatively rapid. A statistically significant cell loss was already observed after 3 h of incubation, and a progressive decline (to $64\% \pm 2\%$ of control, $P < 0.0001$) occurred between 3 and 24 h. Cisplatin (10 $\mu\text{mol/L}$) caused no significant decline of cell numbers during the initial 4 h, but a highly significant cell loss (to $63\% \pm 3\%$ of control, $P < 0.0001$) occurred between 4 and 24 h. Incubation of cells with 5-fluorouracil (10 mmol/L) caused a very rapid cell loss. Cell numbers declined already within 1 h and a very strong decrease (to $15\% \pm 2\%$ of control, $P < 0.0001$) was observed after 24 h.

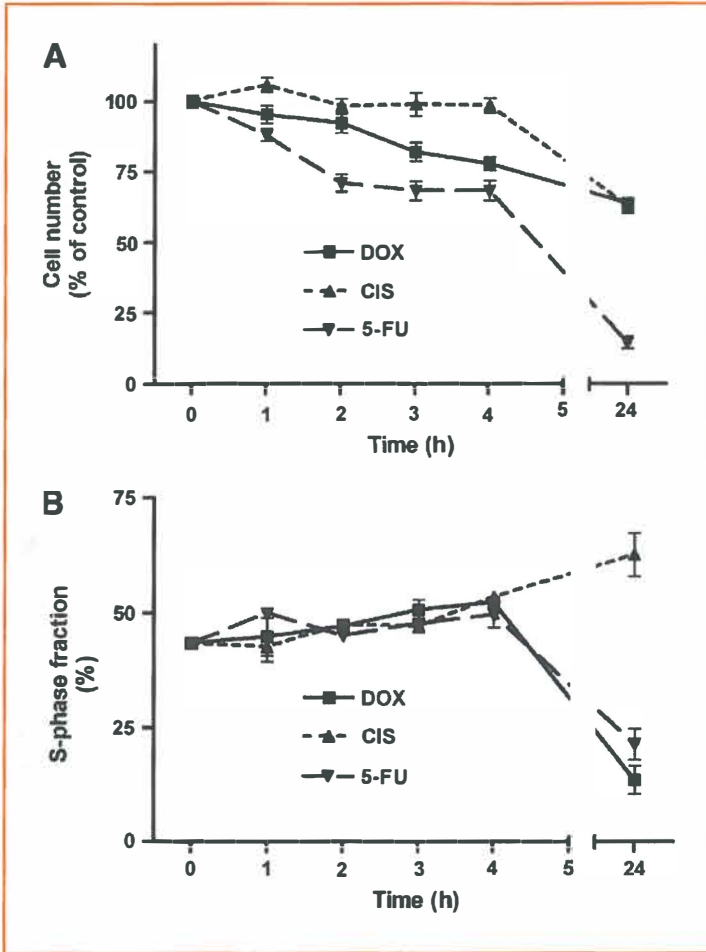


Figure 1
Declines of cell number (upper panel) and changes in S-phase fraction (lower panel) after the onset of chemotherapy. Data plotted as mean \pm SEM

Fraction of cells in S-phase

The three cytostatic agents also had different effects on the fraction of cells in S-phase (Fig. 1). During the first 4 h of treatment, all compounds caused a slight increase in this parameter. However, whereas doxorubicin and 5-fluorouracil caused a significant decrease in the relative numbers of cells in S-phase after 24 h, cisplatin had the opposite effect (Fig. 1). The S-phase fraction was changed from $43\% \pm 1\%$ at time zero to $14 \pm 3\%$ (doxorubicin; $P < 0.0001$), $63\% \pm 5\%$ (cisplatin; $P < 0.0005$), and $21\% \pm 3\%$ (5-fluorouracil; $P < 0.0001$) after 24 h of treatment.

[¹¹C]SA4503

Cytostatic agents caused an increase of the binding of the sigma-1 ligand [¹¹C]SA4503 to C6 cells (Fig. 2). A statistically significant increase of tracer binding was already noticed within 1 h of treatment with doxorubicin or 5-fluorouracil and within 2 h of incubation with cisplatin. After 24 h of treatment, SA4503 uptake per cell was increased to 168% ± 9% (doxorubicin; P=0.0005); 206% ± 20% (cisplatin; P=0.002), and 272% ± 7% of control (5-fluorouracil; P<0.0001).

[¹⁸F]FE-SA5845

Cellular binding of the non-subtype selective sigma ligand [¹⁸F]FE-SA5845 responded less strongly than that of the sigma-1 agonist [¹¹C]SA4503 to chemotherapy. During 24 h of treatment of cells with doxorubicin, the binding of [¹⁸F]FE-SA5845 per cell did not show any change (Fig. 2). However, a significant increase of [¹⁸F]FE-SA5845 binding was observed after 3, 4 and 24 h of treatment with cisplatin, and after 24h of incubation with 5-fluorouracil. [¹⁸F]FE-SA5845 binding was increased to 157% ± 5% (cisplatin; P=0.0001) and 217% ± 32% of control (5-fluorouracil; P=0.01) after 24 h of treatment.

[¹¹C]choline

During the initial 4 h of treatment with doxorubicin and cisplatin, uptake of [¹¹C]choline per viable cell remained constant, but a rapid increase (within 1 h) was induced by 5-fluorouracil (Fig. 3). [¹¹C]choline uptake was significantly increased by all treatments after 24 h, to 132% ± 7% (doxorubicin; P<0.01), 164% ± 10% (cisplatin; P<0.001), and 203% ± 16% of control (5-fluorouracil; P<0.005; Fig. 3).

[¹⁸F]FDG

During treatment of C6 cells with doxorubicin and cisplatin, uptake of [¹⁸F]FDG per cell remained constant throughout the entire study period (Fig. 3). After treatment with 5-fluorouracil, [¹⁸F]FDG uptake remained constant during the initial 4 h. However, this cytostatic agent induced a small decrease in [¹⁸F]FDG uptake after 24 h (to 79% ± 5% of control, P<0.005; Fig. 3).

[¹¹C]methionine

The uptake of [¹¹C]methionine per cell was depressed by chemotherapy although this was a relatively late effect (Fig. 4). During the initial 4 h of treatment with all cytostatic agents, cellular uptake of the amino acid remained constant. A statistically significant decline occurred after 24 h, to 62% ± 4% (doxorubicin; P<0.002), 91% ± 3% (cisplatin; P=0.05), and 71% ± 3% of control (5-fluorouracil; P<0.005).

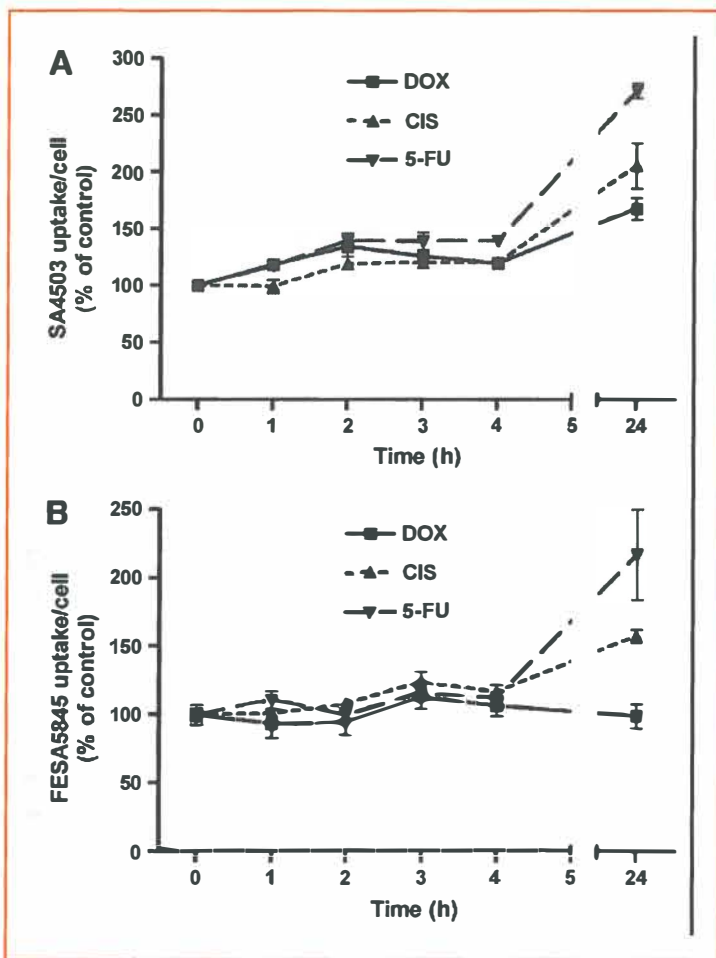


Figure 2
Cellular binding of the sigma ligands [¹¹C]SA4503 (upper panel) and [¹⁸F]-FE-SA5845 (lower panel) during 24 h of chemotherapy

[¹⁸F]FLT

Uptake of the nucleoside [¹⁸F]FLT showed the strongest response to chemotherapy of all studied PET tracers (Fig. 4). A rapid and significant decrease (within 1 h) was observed after treatment of cells with doxorubicin; after 24 h of treatment [¹⁸F]FLT uptake was almost completely suppressed (1.3% ± 0.2% of control; P<0.0001). A less rapid decrease occurred during chemotherapy with cisplatin. [¹⁸F]FLT uptake was not significantly altered during the initial 4 h of cisplatin treatment, but a strong decrease (to 49% ± 4% of control; P<0.0001) occurred after 24 h. Incubation of cells with 5-fluorouracil had a biphasic effect on cellular [¹⁸F]FLT uptake. During the initial 4 h of treatment,

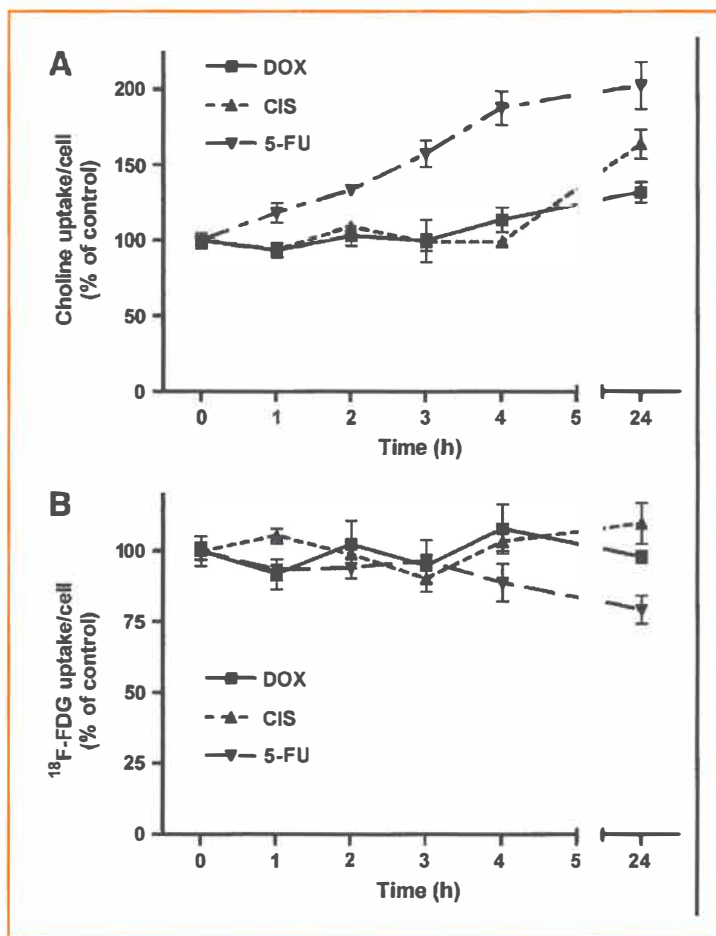


Figure 3
Uptake of [¹⁴C]choline (upper panel) and of [¹⁸F]FDG per cell (lower panel) during 24 h of chemotherapy

uptake of the nucleoside was significantly increased (from 100% ± 6 to 143% ± 10%; P=0.01), but it was strongly depressed after 24 h (to 32% ± 7% of control; P=0.0001).

Activity of cellular thymidine kinase

The activity of cellular thymidine kinase (normalized for the number of viable cells) showed a similar pattern of changes after 24 h of treatment with cytostatic agents as the fraction of cells in S-phase (Fig. 5). Doxorubicin and 5-fluorouracil caused a significant decrease in cellular thymidine kinase activity after 24 h (P<0.0002 in both cases), whereas cisplatin caused an increase (P<0.005; Fig. 5). There was much variability in

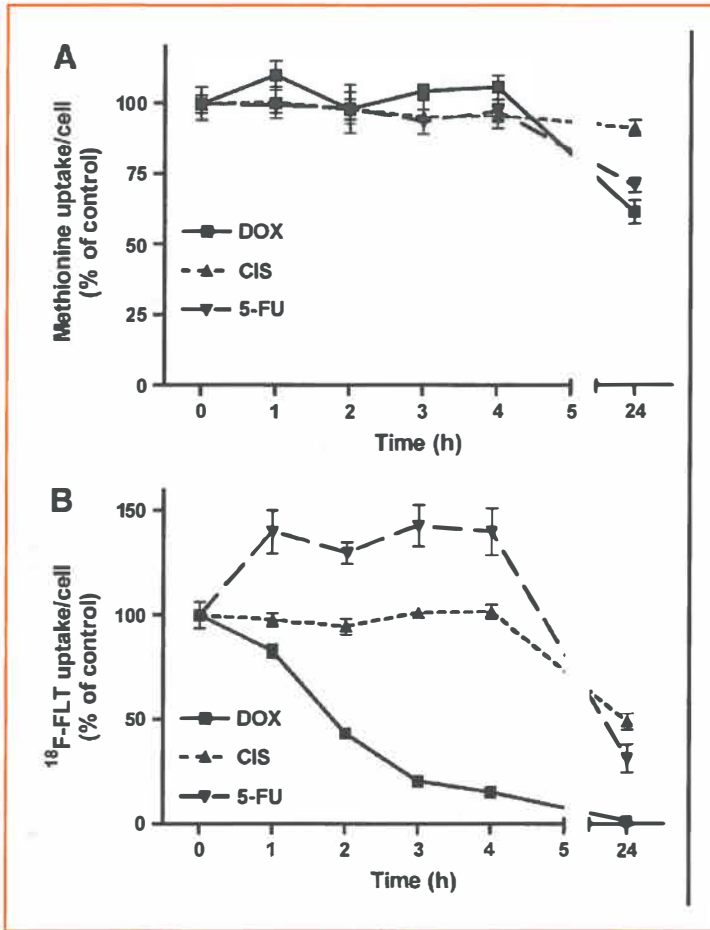


Figure 4
 Uptake of [¹⁴C]methionine (upper panel) and of [¹⁸F]FLT per cell (lower panel) during 24 h of chemotherapy. NB On some curves, error bars are within the size of the data symbols and therefore not visible

the enzyme data after 2 to 4 h of treatment. 5-Fluorouracil induced a transient increase in enzyme activity during this period ($P < 0.0001$), followed by a subsequent decline ($P < 0.0002$; Fig. 5).

Cellular ATP content

The amount of ATP per cell was decreased during 24 h of treatment with doxorubicin (to $60\% \pm 2\%$ of control; $P < 0.01$), but was virtually unchanged after treatment with cisplatin and 5-fluorouracil (Fig. 5).



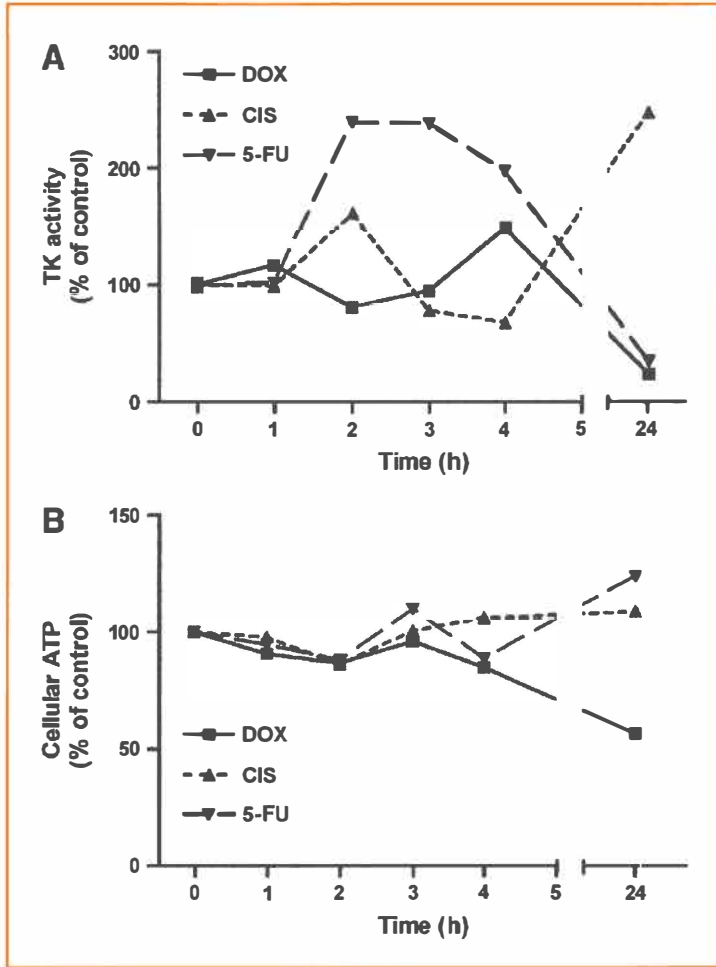


Figure 5
Effect of chemotherapy on the activity of cellular thymidine kinase (upper panel) and on cellular ATP content (lower panel). Error bars within size of data symbols

Discussion

Cell numbers

On the basis of the doses used, we expected a reduction in cell numbers after treatment of C6 cells with cytostatic agents. The dose of doxorubicin that we administered was >7 times higher than the $GI_{C_{50}}$ for this cell line²⁶. Doses of cisplatin and 5-fluorouracil were also an order of magnitude higher than those required for 50% growth inhibition^{27,28}. The reduction in the number of viable C6 cells that we observed after

24 h of treatment with cytostatic agents (Fig. 1) is very similar to values reported in the literature ^{29,30}.

S-phase fraction

In our in vitro chemotherapy model, cytostatic agents had different effects on the fraction of cells in S-phase after 24 h. Doxorubicin and 5-fluorouracil decreased the S-phase fraction, in contrast to cisplatin (Fig. 1). Reports in the literature have indicated that doxorubicin and 5-fluorouracil induce G₂-M arrest ³¹ and combined G₁/G₂ arrest ³², respectively, with corresponding decreases of the fraction of cells in S-phase. In contrast, cisplatin initially blocks C6 cells in the S-phase, resulting in a transient increase of the S-phase fraction. Only after longer periods of treatment with cisplatin (≥ 3 d), a fair number of cells is blocked at the premitotic G₂-phase of the cell cycle ³³.

Tracer response to treatment

Three responses of tracer uptake to chemotherapy were observed in the current study: (a) increased uptake (sigma ligands [¹¹C]SA4503 and [¹⁸F]FE-SA5845, [¹¹C]choline; Figs. 2 and 3), (b) relatively little change in cell-specific uptake ([¹⁸F]FDG; Fig. 3), and (c) decreased uptake ([¹¹C]methionine, [¹⁸F]FLT; Fig. 4).

To our knowledge, there are no published reports about changes in uptake of sigma ligands in tumors or tumor cells after chemotherapy. Our data indicate that the cellular uptake of these tracers is initially increased (Figs. 2 and 3). The increased uptake of sigma ligands (and of [¹¹C]choline) may be related to an enhancement of lipid synthesis caused by repair mechanisms ¹⁵. [¹¹C]SA4503 and [¹⁸F]FE-SA5845 have different subtype selectivities and, therefore, may show different tracer kinetics. [¹¹C]SA4503 binds to the sigma-1 subtype only, whereas [¹⁸F]FE-SA5845 has considerable affinity to both sigma-1 and sigma-2 receptors ³⁴. The stronger increase of [¹¹C]SA4503 uptake than of [¹⁸F]FE-SA5845 uptake after chemotherapy (Fig. 2) suggests that the sigma-1 and sigma-2 receptor populations respond differently to treatment with cytostatic agents.

A study in the literature has indicated that radiolabeled choline is not very suitable for evaluation of cytotoxic effects as the uptake of [³H]choline (and also of [¹⁸F]FDG) in prostate tumor cells did not show any decrease after treatment of the cells with 2-methoxyestradiol ³⁵. Our own data indicate that uptake of [¹¹C]choline in C6 cells is increased after 24 h of antitumor therapy in contrast to that of the proliferation marker [¹⁸F]FLT (Figs. 3 and 4).

A relatively small response of [¹⁸F]FDG uptake to chemotherapy, compared with the response of radiolabeled nucleosides, has often been reported. In murine RIF-1 tumors, the 5-fluorouracil-induced reduction in [¹⁸F]FLT uptake was more rapid and significantly more pronounced than that of [¹⁸F]FDG ³⁶. Similar observations were made in a hormone-responsive rat tumor model, using radioiodinated 5'-iodo-2'-deoxyuridine and [³H]deoxyglucose ³⁷. In OSC-1 tumor cells grown in vitro, cisplatin induced a signifi-



cant and dose-dependent reduction in the uptake of [^{18}F]FLT, whereas the uptake of [^{18}F]FDG was unchanged after 24 h ³⁸. Fleischmannova et al. ³⁹ observed a 54% decline of the uptake of [^3H]thymidine in C6 rat glioma cells after 20 h of treatment with 10 μg cisplatin/mL, close to the value that we observed for [^{18}F]FLT (Fig. 4).

Because the uptake of [^{18}F]FDG per cell showed little change during most forms of chemotherapy (Fig. 3), [^{18}F]FDG appeared to trace the number of viable cells per well rather than the proliferative rate of the cells. Higashi et al. ⁴⁰ reached the same conclusion in a human ovarian adenocarcinoma cell line. [^{18}F]FDG uptake was largely unchanged as carcinoma cells progressed through the growth cycle, but cellular [^3H]thymidine uptake declined when they progressed from lag to plateau phase. The authors concluded that, in their cell line, [^{18}F]FDG measured a substantially different parameter (viable cell number) than [^3H]thymidine (proliferative rate). Rasey et al. ⁴¹ reported a much greater variation of the uptake of [^{18}F]FLT than of [^{14}C]deoxyglucose as a function of growth rate in human lung carcinoma cells.

Sato et al. ¹⁴ studied changes in the uptake of two radiolabeled nucleosides, one amino acid and a glucose analogue in a rat glioma (KEG-1) after chemotherapy. They observed an immediate, sharp fall of nucleoside uptake ([^{18}F]-5'-fluoro-2'-deoxyuridine and [^{14}C]thymidine), a moderate fall of the uptake of [^{14}C]methionine and only after a long interval (> 1 wk), any decline in the uptake of [^3H]deoxyglucose following treatment of the animals with ACNU. These findings are very similar to our own in vitro observations (Fig. 3 and 4).

S-phase fraction and tracer uptake

We observed a significant correlation between the uptake of [^{11}C]methionine after treatment of cells with doxorubicin or 5-fluorouracil and the fraction of cells in S-phase ($n=11$, $r=0.94$; $P<0.0001$). However, this correlation did not hold for [^{11}C]methionine uptake after cisplatin treatment. The increase of the S-phase fraction after cisplatin treatment was not accompanied by an increased cellular uptake of [^{11}C]methionine (compare Figs. 1 and 4). The aberrant behavior of [^{11}C]methionine uptake after cisplatin treatment can be attributed to the fact that cisplatin inhibits not only cell division but also the transport of amino acids across the tumor cell membrane. This side effect of cisplatin treatment has been noted previously, using [^{14}C]methionine and L1210 murine leukemia cells ⁴² or C6 and P388 tumors grown in rats in vivo ^{43,44}.

[^{18}F]FLT uptake after 0, 1, 2, 4, and 24 h of treatment of cells with 5-fluorouracil and after 24 h of treatment with doxorubicin showed also a significant relationship with the fraction of cells in S-phase ($n=7$, $r=0.99$; $P<0.0001$). This observation is in accordance with studies in the literature which reported close, or fairly close, correlations between the fraction of tumor cells in S-phase and the cellular uptake of [^{18}F]FLT ^{45,46}. However, we did not observe any correlation between [^{18}F]FLT uptake and S-phase fraction after treatment of C6 cells with cisplatin, or after 1, 2, 3 or 4 h of incubation

with doxorubicin. Under such conditions, uptake of the nucleoside was reduced in contrast to the S-phase fraction, which remained high (compare Figs. 1 and 4). Cellular trapping of [¹⁸F]FLT is dependent on the activity of thymidine kinase 1 (TK₁)^{47,48}. The activity of this enzyme is not only determined by the fraction of cells in S-phase and the corresponding level of TK₁ expression, but also by the availability of the cofactor ATP⁴⁹. Decreased trapping of [¹⁸F]FLT in the presence of a continuing high expression of the TK₁ protein may occur in tumor cells when cellular ATP levels fall⁵⁰. A bioluminescence assay that we performed indicated that cellular ATP content was decreased after treatment of C6 cells with doxorubicin but not after treatment with cisplatin or 5-fluorouracil (Fig. 5). Thus, the effect of doxorubicin on [¹⁸F]FLT uptake may be related to depletion of the cellular ATP pool in the presence of the cytostatic agent, but the mechanism of the cisplatin effect is as yet unknown. Cisplatin may interfere not only with amino acid transport but also with the transport of nucleosides across the tumor cell membrane⁵¹.

No correlation was observed between cellular uptake of [¹¹C]choline, [¹¹C]SA4503, [¹⁸F]FDG, or [¹⁸F]FE-SA5845 and the fraction of cells in S-phase under the conditions of this study.

Conclusion

The six PET tracers that we studied showed different uptake kinetics after therapy. Increased binding of sigma ligands and an increased uptake of [¹¹C]choline may reflect active membrane repair in damaged cells. Uptake of [¹⁸F]FLT and of [¹¹C]methionine showed a decline; these tracers acted as proliferation markers. Accumulation of [¹⁸F]FDG reflected not proliferation, but the number of viable cells per well.

Cellular uptake of the nucleoside [¹⁸F]FLT and binding of the sigma receptor ligand [¹¹C]SA4503 showed the most rapid changes after the onset of chemotherapy. On the basis of these data from an in vitro model, [¹⁸F]FLT appears more suitable as an early predictor of therapeutic response than [¹⁸F]FDG. If rapid increases in the binding of [¹¹C]SA4503 are also observed in vivo and are related to the final therapy outcome, [¹¹C]SA4503 may be useful for therapy monitoring and may provide information complementary to [¹⁸F]FLT.

Acknowledgements

We thank Geert Mesander (Pathology and Laboratory Medicine, University Medical Center Groningen) for skilful assistance during the flow cytometric analysis, and An-



41



nelies Draaisma (Pharmacokinetics and Drug Delivery, University Medical Center Groningen) for help with the bioluminescent ATP assay.

References

1. Weber WA, Avril N, and Schwaiger M. Relevance of positron emission tomography (PET) in oncology. *Strahlenther Onkol* 1999;175:356-373.
2. De Jong IJ, Pruim J, Elsinga PH, Vaalburg W, and Mensink HJ. Visualization of prostate cancer with ¹¹C-choline positron emission tomography. *Eur Urol* 2002;42:18-23.
3. Strauss LG. Fluorine-18 deoxyglucose and false-positive results: a major problem in the diagnostics of oncological patients. *Eur J Nucl Med* 1996;23:1409-1415.
4. Kubota K. From tumor biology to clinical Pet: a review of positron emission tomography (PET) in oncology. *Ann Nucl Med* 2001;15:471-486.
5. Kubota K. From tumor biology to clinical Pet: a review of positron emission tomography (PET) in oncology. *Ann Nucl Med* 2001;15:471-486.
6. Lorenzen J, de Wit M, Buchert R, Igel B, and Bohuslavizki KH. [Granulation tissue: pitfall in therapy control with F-¹⁸-FDG PET after chemotherapy]. *Nuklearmedizin* 1999;38:333-336.
7. Kubota K, Yamada K, Fukada H, Endo S, Ito M, Abe Y et al. Tumor detection with carbon-11-labelled amino acids. *Eur J Nucl Med* 1984;9:136-140.
8. Kubota K. From tumor biology to clinical Pet: a review of positron emission tomography (PET) in oncology. *Ann Nucl Med* 2001;15:471-486.
9. Shields AF, Lim K, Grierson J, Link J, and Krohn KA. Utilization of labeled thymidine in DNA synthesis: studies for PET. *J Nucl Med* 1990;31:337-342.
10. Shields AF, Grierson JR, Dohmen BM, Machulla HJ, Stayanoff JC, Lawhorn CJ et al. Imaging proliferation in vivo with [F-¹⁸]FLT and positron emission tomography. *Nat Med* 1998;4:1334-1336.
11. Shinoura N, Nishijima M, Hara T, Haisa T, Yamamoto H, Fujii K et al. Brain tumors: detection with C-¹¹ choline PET. *Radiology* 1997;202:497-503.
12. Wheeler KT, Wang LM, Wallen CA, Childers SR, Cline JM, Keng PC et al. Sigma-2 receptors as a biomarker of proliferation in solid tumours. *British Journal Of Cancer* 2000;82:1223-1232.
13. Hayashi T and Su TP. The potential role of sigma-1 receptors in lipid transport and lipid raft reconstitution in the brain: implication for drug abuse. *Life Sci* 2005;77:1612-1624.
14. Sato K, Kameyama M, Ishiwata K, Katakura R, and Yoshimoto T. Metabolic changes of glioma following chemotherapy: an experimental study using four PET tracers. *J Neurooncol* 1992;14:81-89.
15. Schaidt H, Haberkorn U, Berger MR, Oberdorfer F, Morr I, and Van Kaick G. Application of α -aminoisobutyric acid, L-methionine, thymidine and 2-fluoro-2-deoxy-D-glucose to monitor effects of chemotherapy in a human colon carcinoma cell line. *Eur J Nucl Med* 1996;23:55-60.
16. Takeda N, Diksic M, and Yamamoto YL. The sequential changes in DNA synthesis, glucose utilization, protein synthesis, and peripheral benzodiazepine receptor density in C6 brain tumors after chemotherapy to predict the response of tumors to chemotherapy. *Cancer* 1996;77:1167-1179.
17. Steele RJ, Brown M, and Eremin O. Characterisation of macrophages infiltrating human mammary carcinomas. *Br J Cancer* 1985;51:135-138.
18. Whitford P, Mallon EA, George WD, and Campbell AM. Flow cytometric analysis of tumour infiltrating lymphocytes in breast cancer. *Br J Cancer* 1990;62:971-975.
19. Reedijk J and Lohman PHM. Cisplatin - Synthesis, Antitumour Activity and Mechanism of Action. *Pharmaceutisch Weekblad-Scientific Edition* 1985;7:173-180.
20. Zunino F and Capranico G. Dna Topoisomerase-Ii As the Primary Target of Antitumor Anthracyclines. *Anti-Cancer Drug Design* 1990;5:307-317.

21. Parker WB and Cheng YC. Metabolism and Mechanism of Action of 5-Fluorouracil. *Pharmacology & Therapeutics* 1990;48:381-395.
22. Wolff JE, Trilling T, Molenkamp G, Egeler RM, and Jurgens H. Chemosensitivity of glioma cells in vitro: a meta analysis. *J Cancer Res Clin Oncol* 1999;125:481-486.
23. Van Waarde A, Buursma AR, Hospers GA, Kawamura K, Kobayashi T, Ishii K et al. Tumor Imaging with 2 [sigma]-Receptor Ligands, ¹⁸F-FE-SA5845 and ¹¹C-SA4503: A Feasibility Study. *J Nucl Med* 2004;45:1939-1945.
24. Van Waarde A, Jager PL, Ishiwata K, Dierckx RA, and Elsinga PH. Comparison of Sigma-Ligands and Metabolic PET Tracers for Differentiating Tumor from Inflammation. *J Nucl Med* 2006;47:150-154.
25. Kawamura K, Elsinga PH, Kobayashi T, Ishii S, Wang WF, Matsuno K et al. Synthesis and evaluation of (¹¹C)- and (¹⁸F)-labeled 1-[2-(4-alkoxy-3-methoxyphenyl)ethyl]-4-(3-phenylpropyl)piperazines as sigma receptor ligands for positron emission tomography studies. *Nucl Med Biol* 2003;30:273-284.
26. Schott B and Robert J. Comparative cytotoxicity, DNA synthesis inhibition and drug incorporation of eight anthracyclines in a model of doxorubicin-sensitive and -resistant rat glioblastoma cells. *Biochem Pharmacol* 1989;38:167-172.
27. Wolff JE, Trilling T, Molenkamp G, Egeler RM, and Jurgens H. Chemosensitivity of glioma cells in vitro: a meta analysis. *J Cancer Res Clin Oncol* 1999;125:481-486.
28. Mineura K and Kowada M. Enhancement of 5-fluorouracil cytotoxicity by cisplatin in brain tumour cell lines. *Cell Biol Int* 1996;20:355-357.
29. Wolff JE, Trilling T, Molenkamp G, Egeler RM, and Jurgens H. Chemosensitivity of glioma cells in vitro: a meta analysis. *J Cancer Res Clin Oncol* 1999;125:481-486.
30. Mares V, Giordano PA, Mazzini G, Lisa V, Pellicciari C, Scherini E et al. Influence of cis-dichlorodiamineplatinum on glioma cell morphology and cell cycle kinetics in tissue culture. *Histochem J* 1987;19:187-194.
31. Fornari FA, Jr., Jarvis DW, Grant S, Orr MS, Randolph JK, White FK et al. Growth arrest and non-apoptotic cell death associated with the suppression of c-myc expression in MCF-7 breast tumor cells following acute exposure to doxorubicin. *Biochem Pharmacol* 1996;51:931-940.
32. Yoshikawa R, Kusunoki M, Yanagi H, Noda M, Furuyama JI, Yamamura T et al. Dual antitumor effects of 5-fluorouracil on the cell cycle in colorectal carcinoma cells: a novel target mechanism concept for pharmacokinetic modulating chemotherapy. *Cancer Res* 2001;61:1029-1037.
33. Mares V, Giordano PA, Mazzini G, Lisa V, Pellicciari C, Scherini E et al. Influence of cis-dichlorodiamineplatinum on glioma cell morphology and cell cycle kinetics in tissue culture. *Histochem J* 1987;19:187-194.
34. Kawamura K, Elsinga PH, Kobayashi T, Ishii S, Wang WF, Matsuno K et al. Synthesis and evaluation of (¹¹C)- and (¹⁸F)-labeled 1-[2-(4-alkoxy-3-methoxyphenyl)ethyl]-4-(3-phenylpropyl)piperazines as sigma receptor ligands for positron emission tomography studies. *Nucl Med Biol* 2003;30:273-284.
35. Davoodpour P, Bergstrom M, and Landstrom M. Effects of 2-methoxyestradiol on proliferation, apoptosis and PET-tracer uptake in human prostate cancer cell aggregates. *Nucl Med Biol* 2004;31:867-874.
36. Barthel H, Cleij MC, Collingridge DR, Hutchinson OC, Osman S, He Q et al. 3'-deoxy-3'-[¹⁸F]fluorothymidine as a new marker for monitoring tumor response to antiproliferative therapy in vivo with positron emission tomography. *Cancer Res* 2003;63:3791-3798.
37. Carnochan P and Brooks R. Radiolabelled 5'-iodo-2'-deoxyuridine: A promising alternative to [¹⁸F]-2-fluoro-2-deoxy-D-glucose for PET studies of early response to anticancer treatment. *Nucl Med Biol* 1999;26:667-672.
38. Dittmann H, Dohmen BM, Kehlbach R, Bartusek G, Pritzkow M, Sarbia M et al. Early changes in [¹⁸F]FLT uptake after chemotherapy: an experimental study. *European Journal of Nuclear Medicine and Molecular Imaging* 2002;29:1462-1469.
39. Fleischmannova V, Schmeer A., Drobnik J., Lodin Z., and Mares V. The influence of drugs with a cytostatic action on the growth and differentiation of glioma cells in tissue culture. *Physiol Bohemoslov* 1982; 31: 441 [abstract].




41





Early response of sigma receptor ligands and metabolic PET tracers

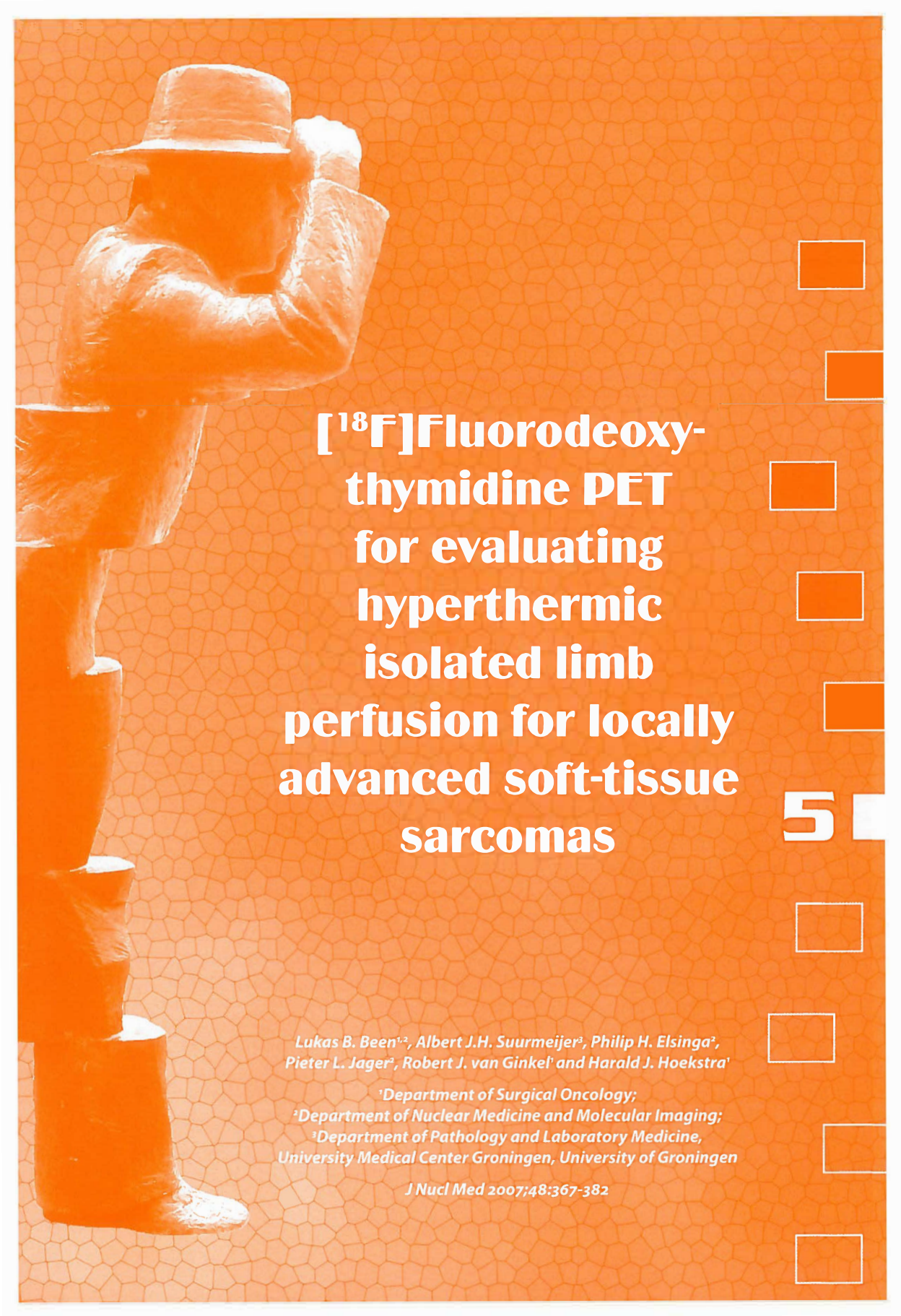
40. Higashi K, Clavo AC, and Wahl RL. Does FDG uptake measure proliferative activity of human cancer cells? In vitro comparison with DNA flow cytometry and tritiated thymidine uptake. *J Nucl Med* 1993;34:414-419.
 41. Rasey JS, Grierson JR, Wiens LW, Kolb PD, and Schwartz JL. Validation of FLT uptake as a measure of thymidine kinase-1 activity in A549 carcinoma cells. *J Nucl Med* 2002;43:1210-1217.
 42. Scanlon KJ, Safirstein RL, Thies H, Gross RB, Waxman S, and Guttenplan JB. Inhibition of amino acid transport by cis-diamminedichloroplatinum(II) derivatives in L1210 murine leukemia cells. *Cancer Res* 1983;43:4211-4215.
 43. Mineura K, Sasajima T, Sasajima H, and Kowada M. Inhibition of methionine uptake by cis-diamminedichloroplatinum (II) in experimental brain tumors. *Int J Cancer* 1996;67:681-683.
 44. Shirasaka T, Shimamoto Y, Ohshimo H, Saito H, and Fukushima M. Metabolic basis of the synergistic antitumor activities of 5-fluorouracil and cisplatin in rodent tumor models in vivo. *Cancer Chemother Pharmacol* 1993;32:167-172.
 45. Rasey JS, Grierson JR, Wiens LW, Kolb PD, and Schwartz JL. Validation of FLT uptake as a measure of thymidine kinase-1 activity in A549 carcinoma cells. *J Nucl Med* 2002;43:1210-1217.
 46. Toyohara J, Waki A, Takamatsu S, Yonekura Y, Magata Y, and Fujibayashi Y. Basis of FLT as a cell proliferation marker: comparative uptake studies with [³H]thymidine and [³H]arabinothymidine, and cell-analysis in 22 asynchronously growing tumor cell lines. *Nucl Med Biol* 2002;29:281-287.
 47. Rasey JS, Grierson JR, Wiens LW, Kolb PD, and Schwartz JL. Validation of FLT uptake as a measure of thymidine kinase-1 activity in A549 carcinoma cells. *J Nucl Med* 2002;43:1210-1217.
 48. Kong XB, Zhu QY, Vidal PM, Watanabe KA, Polsky B, Armstrong D et al. Comparisons of anti-human immunodeficiency virus activities, cellular transport, and plasma and intracellular pharmacokinetics of 3'-fluoro-3'-deoxythymidine and 3'-azido-3'-deoxythymidine. *Antimicrob Agents Chemother* 1992;36:808-818.
 49. Barthel H, Cleij MC, Collingridge DR, Hutchinson OC, Osman S, He Q et al. 3'-deoxy-3'-[¹⁸F]fluorothymidine as a new marker for monitoring tumor response to antiproliferative therapy in vivo with positron emission tomography. *Cancer Res* 2003;63:3791-3798.
 50. Barthel H, Cleij MC, Collingridge DR, Hutchinson OC, Osman S, He Q et al. 3'-deoxy-3'-[¹⁸F]fluorothymidine as a new marker for monitoring tumor response to antiproliferative therapy in vivo with positron emission tomography. *Cancer Res* 2003;63:3791-3798.
 51. Rasey JS, Grierson JR, Wiens LW, Kolb PD, and Schwartz JL. Validation of FLT uptake as a measure of thymidine kinase-1 activity in A549 carcinoma cells. *J Nucl Med* 2002;43:1210-1217.
- 



41







**[¹⁸F]Fluorodeoxy-
thymidine PET
for evaluating
hyperthermic
isolated limb
perfusion for locally
advanced soft-tissue
sarcomas**

*Lukas B. Been^{1,2}, Albert J.H. Suurmeijer³, Philip H. Elsinga²,
Pieter L. Jager², Robert J. van Ginkel¹ and Harald J. Hoekstra¹*

¹Department of Surgical Oncology;

²Department of Nuclear Medicine and Molecular Imaging;

*³Department of Pathology and Laboratory Medicine,
University Medical Center Groningen, University of Groningen*

J Nucl Med 2007;48:367-382

Abstract

Locally advanced soft-tissue sarcomas of an extremity can be treated either by amputation of the limb or by hyperthermic isolated limb perfusion (HILP) followed by resection of the tumor. In this study, the response to HILP was measured by PET with [¹⁸F]fluorodeoxythymidine ([¹⁸F]FLT).

Methods

Ten patients with primary nonresectable soft-tissue sarcoma of an extremity underwent HILP with tumor necrosis factor- α and melphalan. Before and after HILP, all patients underwent PET scanning with [¹⁸F]FLT for response evaluation.

Results

Before HILP, all tumors were clearly visible on [¹⁸F]FLT-PET; for the maximum standardized uptake value (SUV_{max}), the mean was 3.5 (range 1.0-6.7), and for the mean standardized uptake value (SUV_{mean}), the mean was 1.9 (range 0.7-2.7). After HILP, all but one tumor showed necrosis, ranging from 10% to 95%. [¹⁸F]FLT-PET after HILP revealed significantly decreased uptake of the tracer. The mean SUV_{max} decreased to 1.7 ($P=0.008$), and mean SUV_{mean} decreased to 0.8 ($P=0.002$). One small axillary lymph-node metastasis was not visible on [¹⁸F]FLT-PET.

Conclusion

[¹⁸F]FLT-PET revealed high uptake in soft-tissue sarcomas. [¹⁸F]FLT uptake was correlated with the mitotic index of the tumors ($r=0.82$ and $P=0.004$ for SUV_{max} and $r=0.87$ and $P=0.001$ for SUV_{mean} , respectively). After HILP, the uptake of [¹⁸F]FLT decreased significantly ($P=0.008$ and $P=0.002$ for SUV_{max} and SUV_{mean} , respectively). Tumors with initially high [¹⁸F]FLT uptake showed a better response to HILP ($r=0.64$, $P<0.05$). Software fusion of PET images with conventional imaging modalities revealed the heterogeneity of the tumors before and after HILP. Such data can help a surgeon in planning the resection of the tumor.

Introduction

Soft-tissue sarcomas are relatively rare, accounting for fewer than 1% of all cancers in adults, but they are responsible for approximately 2% of all cancer-related deaths. The numbers of patients presenting with soft-tissue sarcomas each year are approximately 8,300 in the United States and about 500-600 in the Netherlands ¹. The majority of soft-tissue sarcomas occur in the upper or lower extremities. The usual treatment protocols include limb-saving surgery, often followed by adjuvant radiotherapy ². Locally advanced soft-tissue sarcomas of the extremities may require ablative surgical procedures (amputation of the limb). Hyperthermic isolated limb perfusion (HILP) with cytostatic agents has the potential to render the majority of these tumors resectable, thereby preventing the need for amputation. With HILP, chemotherapeutic tissue concentrations up to 20 times higher than those achieved with systemic chemotherapy can be achieved ³. HILP with tumor necrosis factor- α (TNF α) and melphalan has resulted in overall response rates of 63-91% and limb salvage rates of 73-86% ⁴⁻⁸. However, HILP with TNF α and melphalan is an expensive and intensive treatment with possible serious side effects ⁹.

Positron emission tomography (PET) is an imaging modality that offers the possibility of visualizing and quantifying metabolic pathways in a non-invasive way. [¹⁸F]FDG is the most widely used PET tracer in oncology. [¹⁸F]FDG uses the increased glycolytic activity of cancer cells for PET visualization. [¹⁸F]FDG also shows increased uptake in inflammatory cells, a property that limits the specificity of this tracer in monitoring cancer therapy.

In 1998, a new PET tracer, [¹⁸F]fluorodeoxythymidine ([¹⁸F]FLT) was developed ^{10,11}. [¹⁸F]FLT is a pyrimidine analogue that uses the salvage pathway of DNA synthesis for PET visualization. [¹⁸F]FLT is taken up through facilitated transport and diffusion and is phosphorylated by thymidine kinase 1 (TK₁) into [¹⁸F]FLT-monophosphate. TK₁ is a cell cycle regulated enzyme, and its activity is high in the S phase of normal cells. TK₁ activity is higher in malignant cells than in normal cells and is present throughout the cell cycle, leading to increased phosphorylation of [¹⁸F]FLT in malignant tissues. After phosphorylation, [¹⁸F]FLT is trapped intracellularly; therefore, uptake of [¹⁸F]FLT is a reflection of the proliferation activity of tissues. In a previous study, we showed that [¹⁸F]FLT-PET clearly visualizes soft-tissue sarcomas and has the potential to differentiate between low-grade and high-grade soft-tissue sarcomas ¹².

Recent research data on the use of [¹⁸F]FLT-PET for the visualization of different tumor types indicated that the sensitivity of [¹⁸F]FLT-PET for most tumor types is lower than that of [¹⁸F]FDG-PET. However, we showed that the specificity of [¹⁸F]FLT in a tumor/inflammation animal model is higher than that of [¹⁸F]FDG ¹³. To date, conventional imaging techniques (CT and MRI) have been used to monitor the response to HILP in



patients with locally advanced soft-tissue sarcomas. With these imaging modalities, excellent anatomical information can be obtained and the growth or shrinkage of soft-tissue sarcomas can be monitored. However, images of CT or MRI provide only scant information about tumor aggressiveness and biological response to therapy. In this study, the potential of [¹⁸F]FLT-PET to measure the metabolic response to treatment in patients with soft-tissue sarcomas was investigated.

Materials and methods

Patients

In this prospective study, ten consecutive patients with locally advanced soft-tissue sarcomas of an extremity were included between May 2002 through November 2004. All tumors were considered nonresectable because of size, multicentricity or localization near bone or neurovascular structures on MRI. To render these tumors resectable, patients were treated by use of HILP with TNF α and melphalan followed by delayed resection. All patients were treated in the University Medical Center Groningen and gave written informed consent. For patients to be included in the study, hematological parameters and liver and kidney function tests had to be within normal limits. Pregnant patients and patients with psychiatric disorders were excluded from the study. This study protocol was approved by the Medical Ethics Committee of the University Medical Center Groningen.

HILP

The perfusion technique used in the University Medical Center Groningen is based on the technique developed by Creech et al.¹⁴. The major artery and vein of the limb are clamped, and cannulas are inserted and connected to an extracorporeal circuit. A tourniquet is applied to minimize leakage to the systemic circulation. Leakage is measured continuously during perfusion using [¹³¹I]-albumin and a precordial scintillation detector, as previously described by Daryanani et al.¹⁵. The limb is wrapped in a thermal blanket to reduce heat loss and to achieve mild hyperthermia (39°C-40°C). Perfusion is performed with a roller pump, a DIDECO 902 (DIDECO) membrane oxygenator and a heat exchanger. The perfusate consists of 250 mL of dextran 40 in saline 0.9% (NPBI International BV), 250 mL white cell-reduced (filtered) packed red cells, 30 mL of 8.4% NaHCO₃ and 0.5 mL of heparin (5000 IU/mL). Subsequently, TNF α (Boehringer-Ingelheim GmbH) at 3 mg (upper limb) or 4 mg (lower limb) and melphalan (GlaxoSmithKline) at 10 mg/L (leg volume) or 13 mg/L (arm volume) are administered intraarterially. After 60-90 min of perfusion, the limb is extensively flushed with 4-6 L of saline and then filled with 250 mL of white cell-reduced packed red cells. After another 60 min, the limb is flushed with 3000-6000 mL dextran 40 in 5% glucose and 500 mL of blood (250 mL

red cells and 250 mL plasma)¹⁶. After removal of the cannulas, the procedure is concluded with a fasciotomy to prevent compartmental syndrome. On day 1 after surgery, the patient is observed closely in an intensive care unit, because serious complications can arise, especially when leakage into the systemic circulation has occurred^{9,17}.

Histopathological examinations

The histopathological diagnosis was established after examination of either incision biopsies or true-cut biopsy specimens. Tumors were graded according to the French grading system as described by Coindre et al.¹⁸. With this system, the differentiation grade of tumors, the number of mitotic figures per 2 mm² and the amount of necrosis are scored. All tumors were divided into grade 1, grade 2 or grade 3 tumors. The mitotic index (number of mitotic figures per 2 mm²) was determined on hematoxylin- and eosin-stained sections of the tumor; the areas with the highest rates of mitosis were selected.

At 6-8 wk after HILP, patients were scheduled for local excision of their tumors. The pathologist measured tumor size and determined the percentage of tumor necrosis in the specimen resected after HILP.

PET imaging

[¹⁸F]FLT was synthesized by the method of Machulla et al.¹⁹. [¹⁸F]FLT was produced by fluorination with [¹⁸F]fluoride of the 4,4'-dimethoxytrityl-protected anhydrothymidine and then a deprotection step. After purification by reversed-phase high-performance liquid chromatography, the product was made isotonic and passed through a 0.22 μm filter. [¹⁸F]FLT was produced with a radiochemical purity of greater than 95% and specific activity of greater than 10 TBq/mmol. The radiochemical yield was 8.8 ± 3.7% (decay corrected).

PET studies were scheduled shortly before and 39 d (range, 28-49 d) after perfusion, concurrent with MRI scans. A median dose of 399 MBq (range, 320-430 MBq) of [¹⁸F]FLT was injected intravenously before perfusion, and 363 MBq (range, 120-430 MBq) was injected after perfusion. At 60 min after injection, patients were placed into an ECAT EXACT HR+ PET scanner (Siemens/CTI Inc.) for imaging of the tumor in emission-transmission-transmission-emission mode. Depending on the size of the tumor, 1-4 bed positions were used for 8 min per position (5 min for emission and 3 min for transmission). After imaging of the tumor, a whole-body scan was performed from crown to half way femur for 5 min per bed position. Data from multiple bed positions were iteratively reconstructed (ordered-subset expectation maximization)²⁰.

Data analysis

PET scans of the tumors were interpreted visually for regions of increased uptake. A 3-dimensional volume of interest was drawn around the tumor by use of the 70%



isocontour of maximum standardized uptake value (SUV) of the tumor. The maximum SUV (SUV_{max}) and the mean SUV (SUV_{mean}) within this volume of interest were determined automatically with a Leonardo workstation (Syngo Leonardo; Siemens AG). For some patients, PET images were fused with MRI images by use of fusion software on the Leonardo workstation.

Whole-body images were scored for the presence or absence of regions of increased [¹⁸F]FLT uptake, taking into account the pattern of physiological uptake of [¹⁸F]FLT.

Statistical analysis

The mean SUV_{max} and mean SUV_{mean} before and after HILP were compared by use of the paired-sample *t* test. The SUV_{max} and SUV_{mean} before HILP were correlated with the mitotic index by use of the Pearson correlation coefficient. *p*-values of less than 0.05 were considered statistically significant.

Results

Ten patients (6 men and 4 women) with a mean age of 51 y (range, 27-71 y) were studied. Patient and tumor characteristics are shown in Table 1. For 9 patients, histologic diagnosis was made from an incision biopsy; for 1 patient (patient 9) multiple true-cut biopsies were performed. Patient 10 was diagnosed with a recurrent soft-tissue sarcoma.

Before perfusion, all tumors were clearly visible on [¹⁸F]FLT-PET, with a mean SUV_{max} of 3.5 (range, 1.0-6.7) and a mean SUV_{mean} of 1.9 (range, 0.7-2.7). Both SUV_{max} and SUV_{mean} correlated with the mitotic index of tumors ($r=0.82$ and $P=0.004$ for SUV_{max} ; $r=0.87$, $P=0.001$ for SUV_{mean}) (Fig. 1).

In all but 1 tumor, necrosis was found after HILP, ranging from 10% to 95% (Table 2). The 2 grade 1 tumors (patient 9 and 10) showed little or no necrosis and the grade 2 epithelioid sarcoma showed only 10% necrosis. [¹⁸F]FLT-PET after HILP revealed significantly decreased uptake of the tracer. The SUV_{max} decreased to 1.7 ($P=0.008$), and mean SUV_{mean} decreased to 0.8 ($P=0.002$). Most tumors showed a center of very little or no [¹⁸F]FLT uptake and a rim of moderate [¹⁸F]FLT uptake. For some tumors, [¹⁸F]FLT-PET images were fused with the corresponding MR images by use of dedicated computer software. For these tumors, we were able to show that [¹⁸F]FLT-PET can identify areas of necrosis and viable tumor after HILP (Fig. 2).

No significant correlation between the percentage of necrosis and the decrease in SUV_{mean} could be demonstrated. A weak but significant correlation ($r=0.642$, $P<0.05$) between the initial SUV_{mean} and the percentage of necrosis after HILP was demonstrated (Fig. 3).

Table 1
Patient and tumor characteristics

| No/sex/age | Histology | Tumor grade | Localization | Largest diameter before HILP (cm)* | Mitotic index (per 2 mm ²) | Largest diameter after HILP (cm)* |
|------------|----------------------------|-------------|-----------------|------------------------------------|--|-----------------------------------|
| 1/F/47 | Pleomorphic leiomyosarcoma | 3 | Upper arm | 2.8 | 43 | 4.0 |
| 2/F/56 | Pleomorphic sarcoma | 3 | Upper arm | 6.0 | 22 | 5.0 |
| 3/F/58 | Pleomorphic sarcoma | 3 | Lower leg | 6.0 | 36 | 5.0 |
| 4/M/63 | Synovial sarcoma | 3 | Upper leg | 6.0 | 30 | 5.6 |
| 5/M/53 | Myxofibrosarcoma | 3 | Upper leg | 12.0 | 18 | 12.0 |
| 6/M/28 | Synovial sarcoma | 2 | Popliteal fossa | 3.0 | 6 | 1.5 |
| 7/M/70 | Pleomorphic sarcoma | 2 | Lower leg | 10.0 | 18 | 10.0 |
| 8/M/27 | Epitheloid sarcoma | 2 | Lower arm | 3.5 | 16 | 3.0 |
| 9/F/37 | Myxoid liposarcoma | 1 | Upper leg | 12.2 | 2 | 10.0 |
| 10/M/71 | Myxofibrosarcoma | 1 | Lower arm | 2.0 | 9 | 2.0 |

* established on MRI



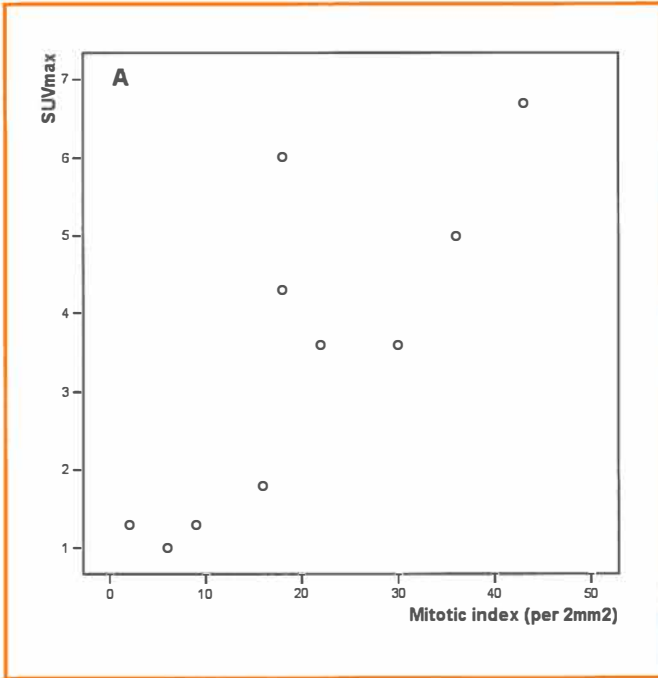


Figure 1a
Correlation between SUV_{max} and mitotic index before HILP ($r=0.87$, $P=0.001$)

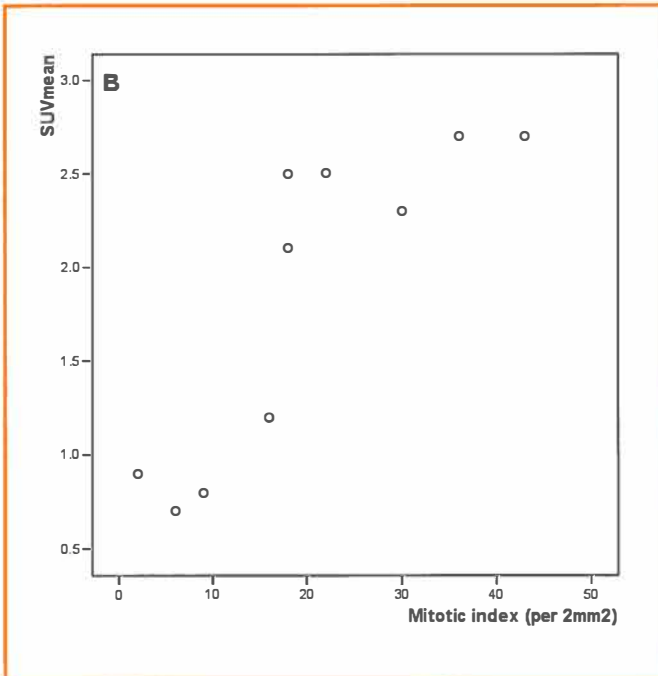


Figure 1b
Correlation between SUV_{mean} and mitotic index before HILP ($r=0.82$, $P=0.004$)

Table 2
PET results and pathologic response

| No | Before HILP | | Interval (days) | After HILP | | Δ SUV _{max} (%) | Δ SUV _{mean} (%) | Necrosis (%) |
|----|--------------------|---------------------|-----------------|--------------------|---------------------|---------------------------------|----------------------------------|--------------|
| | SUV _{max} | SUV _{mean} | | SUV _{max} | SUV _{mean} | | | |
| 1 | 6.7 | 2.7 | 28 | 6.4 | 2.0 | 5 | 24 | 75 |
| 2 | 3.6 | 2.5 | 34 | 1.2 | 1.0 | 67 | 61 | 70 |
| 3 | 5.0 | 2.7 | 30 | 1.2 | 0.7 | 77 | 73 | 90 |
| 4 | 3.6 | 2.3 | 43 | 0.9 | 0.6 | 77 | 76 | 80 |
| 5 | 4.3 | 2.1 | 49 | 2.4 | 0.5 | 44 | 77 | 80 |
| 6 | 1.0 | 0.7 | 34 | 1.0 | 0.7 | 2 | 3 | 95 |
| 7 | 6.0 | 2.5 | 41 | 1.2 | 0.7 | 79 | 71 | 95 |
| 8 | 1.8 | 1.2 | 45 | 1.2 | 0.9 | 34 | 25 | 10 |
| 9 | 1.3 | 0.9 | 47 | 0.7 | 0.5 | 45 | 45 | 10 |
| 10 | 1.3 | 0.8 | 43 | 0.8 | 0.7 | 39 | 21 | 0 |

Discussion

In this study, the value of [¹⁸F]FLT-PET to evaluate the response of locally advanced soft-tissue sarcomas to HILP was investigated. [¹⁸F]FLT is a relatively new tracer that uses one of the DNA synthesis pathways of tumor cells for PET visualization. There is considerable evidence that [¹⁸F]FLT has the potential to visualize and measure the viability of tumor cells during or early after (chemo)therapy because it does not accumulate in inflammatory cells¹³.

[¹⁸F]FLT-PET after HILP was scheduled shortly before the resection of the tumor, together with MRI for therapy evaluation. There is some evidence in the literature that [¹⁸F]FLT-PET can monitor response to therapy at an early stage²¹. However, in this study, we wished to compare the results of [¹⁸F]FLT-PET after HILP with histopathologic examinations of the resected tumors and decided to perform [¹⁸F]FLT-PET shortly before the resection.

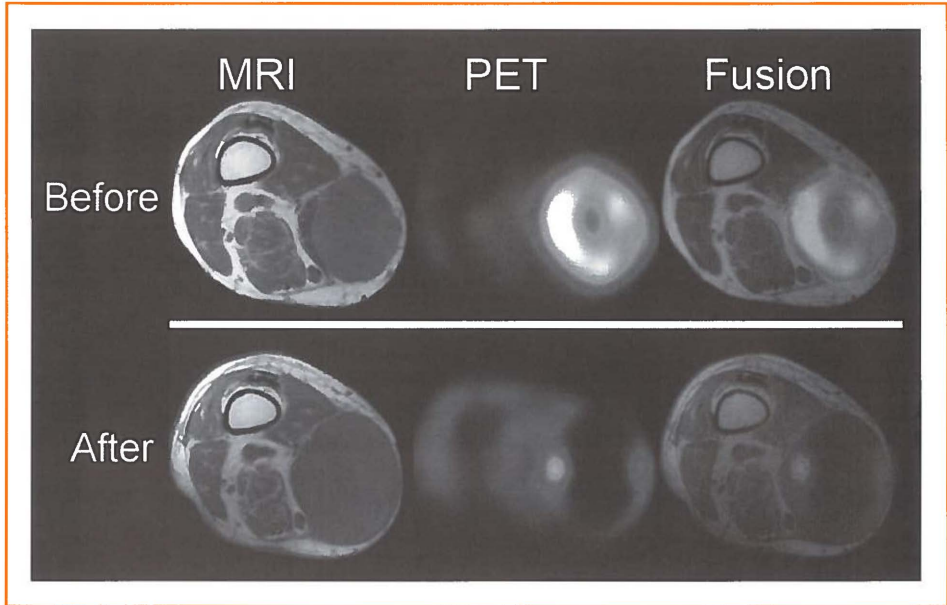


Figure 2

Example of [¹⁸F]FLT-PET, MRI and software fusion images of a high grade myxofibrosarcoma before and after HILP. After HILP, this tumor consisted of 80% necrosis. [¹⁸F]FLT-PET shows the heterogeneity of the tumor after HILP

For our group of 10 patients with locally advanced soft-tissue sarcomas, the baseline uptake of [¹⁸F]FLT correlated with the mitotic index, which is a derivative of tumor aggressiveness. Cobben et al. previously showed that [¹⁸F]FLT-PET could differentiate between high-grade tumors (Coindre grades 2 and 3) and low-grade tumors (grade 1)¹². For other tumor types, similar correlations between pathologic proliferation markers and [¹⁸F]FLT uptake have been reported²²⁻²⁴.

Furthermore, tumors with high initial [¹⁸F]FLT uptake seemed to show good pathologic response after HILP, although the studied number of patients is too small to draw strong conclusions. Three tumors in our study showed little or no necrosis after HILP. These tumors had a low initial SUV_{max} , ranging from 1.3 to 1.8, and a SUV_{mean} ranging from 0.7 to 1.2. In general, high-grade or aggressive soft-tissue sarcomas respond better to HILP than low-grade tumors²⁵. [¹⁸F]FLT-PET may therefore be able to identify patients who will benefit the most from HILP.

Cobben et al. previously investigated the value of [¹⁸F]FLT-PET for the staging of soft-tissue sarcomas¹². In the present study, besides the uptake in the area of the primary tumor, no additional areas of increased [¹⁸F]FLT uptake were found on whole-body [¹⁸F]FLT-PET; 1 patient had a proven lymph node metastasis at the time of the PET scan. For other types of cancer, the sensitivity of [¹⁸F]FLT-PET for detecting metastases has

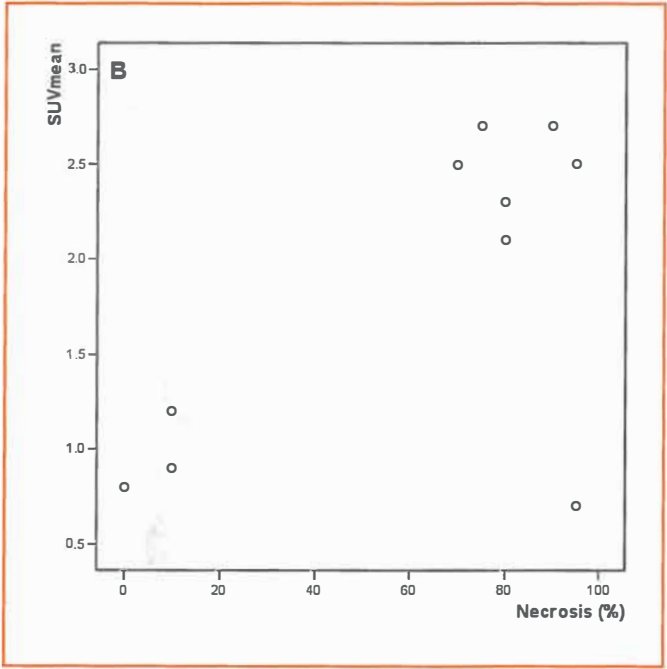


Figure 3a
 There is no significant correlation between the SUV_{max} before HILP and the percentage of necrosis after HILP ($r=0.622$, $P=0.55$)

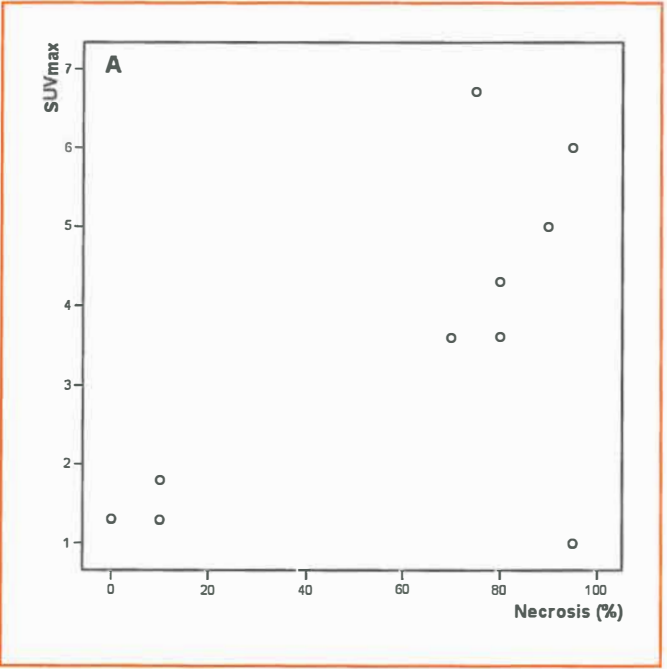


Figure 3b
 Correlation between SUV_{mean} before HILP and the percentage of necrosis ($r=0.642$, $P<0.05$). This shows that tumors with high initial $[^8]FLT$ uptake show better response to HILP



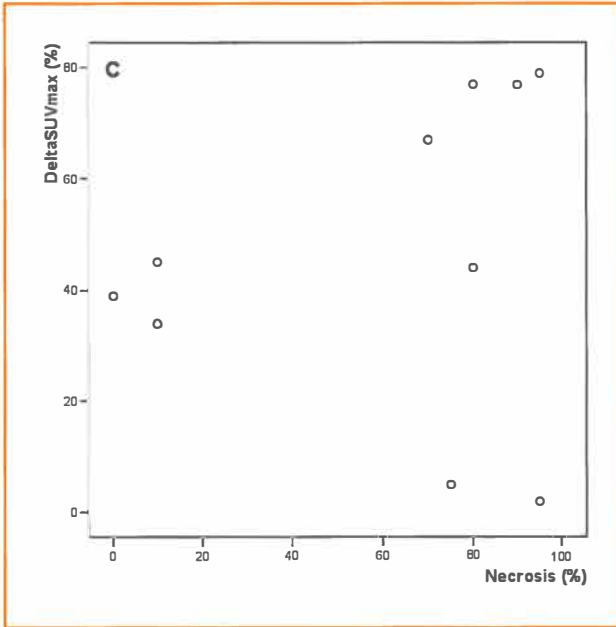


Figure 3c

No significant correlation between the decrease in SUV_{max} and the percentage of necrosis after HILP ($r=0.190$, $P=0.60$)

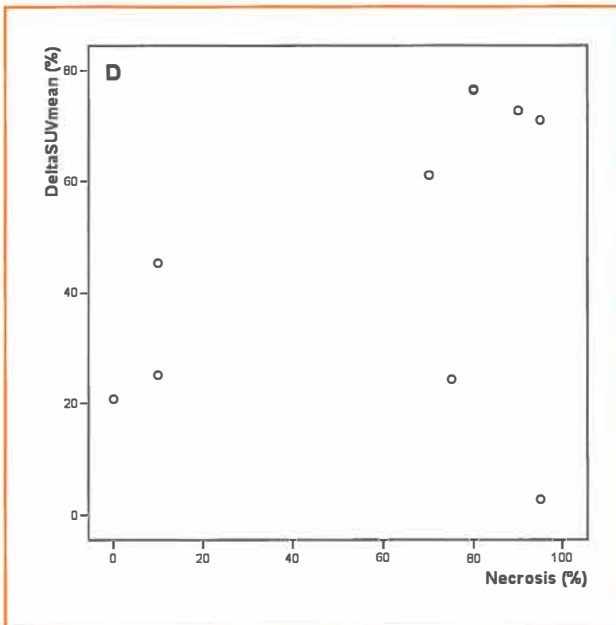


Figure 3d

No significant correlation between the decrease in SUV_{mean} and the percentage of necrosis after HILP ($r=0.404$, $P=0.25$)

been investigated by a number of research groups, and [^{18}F]FLT-PET has been shown to be probably not superior to [^{18}F]FDG¹¹. For different reasons, [^{18}F]FLT uptake is lower than [^{18}F]FDG uptake in almost all types of cancer. Bastiaannet et al. recently reviewed the literature regarding [^{18}F]FDG-PET for patients with soft-tissue sarcomas and concluded that there is no indication to use [^{18}F]FDG-PET routinely²⁶.

We believe that the true value of [^{18}F]FLT is not its capacity to detect tumors, but its capacity to evaluate the response to therapy. Van Ginkel et al. previously investigated [^{18}F]FDG-PET and [^{11}C]tyrosine-PET for patients undergoing HILP for soft-tissue sarcomas and skin cancers^{27,28}. They concluded that [^{18}F]FDG-PET was able to measure the response to HILP; however, [^{18}F]FDG could not discriminate between viable tumor cells and inflammatory tissue because [^{18}F]FDG uptake was observed in both. [^{11}C]tyrosine uptake was not observed in inflammatory cells, but the use of this tracer is limited due to its short half-life, 20.4 minutes. We believe that [^{18}F]FLT, like [^{11}C]tyrosine, also will not show uptake in inflammatory tissues, although this notion was not investigated in the present study. Recently, van Waarde et al. investigated uptake in an acute inflammation model and showed that [^{18}F]FLT did not demonstrate uptake in inflammatory tissues¹³.

Conclusion

Although [^{18}F]FLT-PET after HILP did not directly influence our decision regarding whether to perform a local resection or an amputation, we observed that the heterogeneity of [^{18}F]FLT uptake for a few tumors seemed to correspond well to areas of necrosis and viable tumor tissue in the resected specimens. This finding supports our opinion that [^{18}F]FLT-PET could be valuable in the future for guiding surgeons in planning resections or radiotherapists in planning conformal radiotherapy.

References

1. Weir HK, Thun MJ, Hankey BF, Ries LA, Howe HL, Wingo PA et al. Annual report to the nation on the status of cancer, 1975-2000, featuring the uses of surveillance data for cancer prevention and control. *J Natl Cancer Inst* 2003;95:1276-1299.
2. Ham SJ, van der Graaf WT, Pras E, Molenaar WM, van den BE, and Hoekstra HJ. Soft tissue sarcoma of the extremities. A multimodality diagnostic and therapeutic approach. *Cancer Treat Rev* 1998;24:373-391.
3. Guchelaar HJ, Hoekstra HJ, de Vries EG, Uges DR, Oosterhuis JW, and Schraffordt KH. Cisplatin and platinum pharmacokinetics during hyperthermic isolated limb perfusion for human tumours of the extremities. *Br J Cancer* 1992;65:898-902.

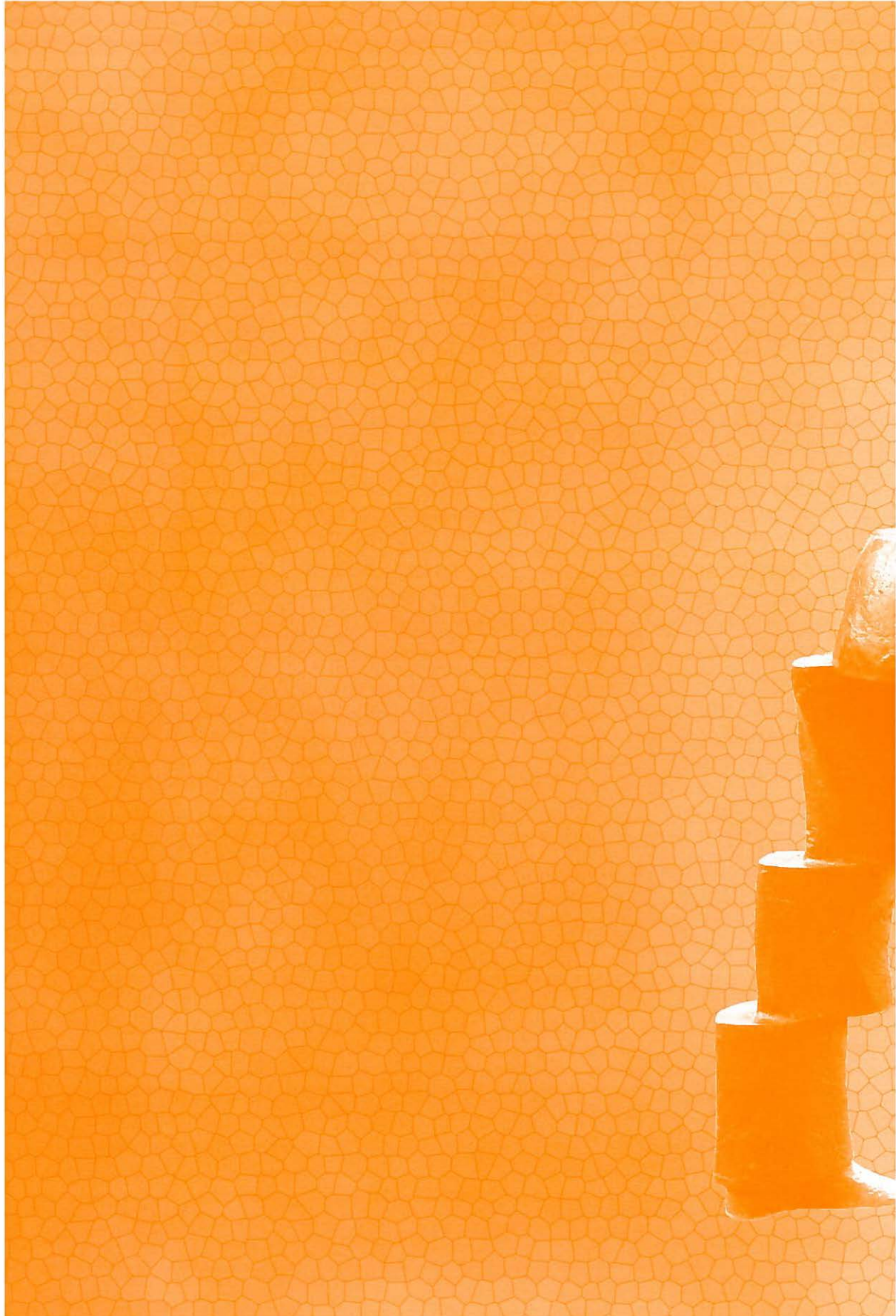
4. Noorda EM, Vrouwenraets BC, Nieweg OE, van Coevorden F, van Slooten GW, and Kroon BB. Isolated limb perfusion with tumor necrosis factor-alpha and melphalan for patients with unresectable soft tissue sarcoma of the extremities. *Cancer* 2003;98:1483-1490.
5. Lejeune FJ, Pujol N, Lienard D, Mosimann F, Raffoul W, Genton A et al. Limb salvage by neoadjuvant isolated perfusion with TNFalpha and melphalan for non-resectable soft tissue sarcoma of the extremities. *Eur J Surg Oncol* 2000;26:669-678.
6. Eggermont AM, Schraffordt KH, Klausner JM, Kroon BB, Schlag PM, Lienard D et al. Isolated limb perfusion with tumor necrosis factor and melphalan for limb salvage in 186 patients with locally advanced soft tissue extremity sarcomas. The cumulative multicenter European experience. *Ann Surg* 1996;224:756-764.
7. Gutman M, Inbar M, Lev-Shlush D, Abu-Abid S, Mozes M, Chaitchik S et al. High dose tumor necrosis factor-alpha and melphalan administered via isolated limb perfusion for advanced limb soft tissue sarcoma results in a >90% response rate and limb preservation. *Cancer* 1997;79:1129-1137.
8. Thijssens KM, van Ginkel RJ, Pras E, Suurmeijer AJ, and Hoekstra HJ. Isolated limb perfusion with tumor necrosis factor alpha and melphalan for locally advanced soft tissue sarcoma: the value of adjuvant radiotherapy. *Ann Surg Oncol* 2006;13:518-524.
9. Zwaveling JH, Maring JK, Mulder AB, Bom VJ, van Ginkel RJ, Schraffordt KH et al. Effects of hyperthermic isolated limb perfusion with recombinant tumor necrosis factor alpha and melphalan on the human fibrinolytic system. *Cancer Res* 1996;56:3948-3953.
10. Shields AF, Grierson JR, Dohmen BM, Machulla HJ, Stayanoff JC, Lawhom-Crews JM et al. Imaging proliferation in vivo with [¹⁸F]FLT and positron emission tomography. *Nat Med* 1998;4:1334-1336.
11. Been LB, Suurmeijer AJ, Cobben DC, Jager PL, Hoekstra HJ, and Elsinga PH. [¹⁸F]FLT-PET in oncology: current status and opportunities. *Eur J Nucl Med Mol Imaging* 2004;31:1659-1672.
12. Cobben DC, Elsinga PH, Suurmeijer AJ, Vaalburg W, Maas B, Jager PL et al. Detection and grading of soft tissue sarcomas of the extremities with (¹⁸F)-3'-fluoro-3'-deoxy-L-thymidine. *Clin Cancer Res* 2004;10:1685-1690.
13. Van Waarde A, Cobben DCP, Suurmeijer AJH, Maas B, Vaalburg W, De Vries EFJ et al. Selectivity of 3'-deoxy-3'-[¹⁸F]fluorothymidine (FLT) and 2-[¹⁸F]fluoro-2-deoxy-D-glucose (FDG) for tumor versus inflammation in a rodent model. *J Nucl Med* 2004;45:695-700.
14. Creech O, Jr., Kremenz ET, Ryan RF, and Winblad JN. Chemotherapy of cancer: regional perfusion utilizing an extracorporeal circuit. *Ann Surg* 1958;148:616-632.
15. Daryanani D, Komdeur R, Ter Veen J, Nijhuis PH, Piers DA, and Hoekstra HJ. Continuous leakage measurement during hyperthermic isolated limb perfusion. *Ann Surg Oncol* 2001;8:566-572.
16. Hoekstra, H. J., Daryanani, D., and Girbes, A. R. Isolated limb perfusion. In P. Van Schil (ed.), *Lung metastases and isolated lung perfusion* Hauppauge, NY: Nova Science Publishers, 2005.
17. Zwaveling JH, Hoekstra HJ, Maring JK, Ginkel RJ, Schraffordt KH, Smit AJ et al. Renal function in cancer patients treated with hyperthermic isolated limb perfusion with recombinant tumor necrosis factor-alpha and melphalan. *Nephron* 1997;76:146-152.
18. Coindre JM, Trojani M, Contesso G, David M, Rouesse J, Bui NB et al. Reproducibility of a histopathologic grading system for adult soft tissue sarcoma. *Cancer* 1986;58:306-309.
19. Machulla HJ, Blochter A, Kuntzsch M, Piert M, Wei R, and Grierson JR. Simplified labeling approach for synthesizing 3'-deoxy-3'-[¹⁸F]fluorothymidine ([¹⁸F]FLT). *Journal of Radioanalytical and Nuclear Chemistry* 2000;243:843-846.
20. Lonneux M, Borbath I, Bol A, Coppens A, Sibomana M, Bausart R et al. Attenuation correction in whole-body FDG oncological studies: the role of statistical reconstruction. *Eur J Nucl Med* 1999;26:591-598.
21. Pio BS, Park CK, Pietras R, Hsueh WA, Satyamurthy N, Pegram MD et al. Usefulness of 3'-[¹⁸F]fluoro-3'-deoxythymidine with positron emission tomography in predicting breast cancer response to therapy. *Mol Imaging Biol* 2006;8:36-42.

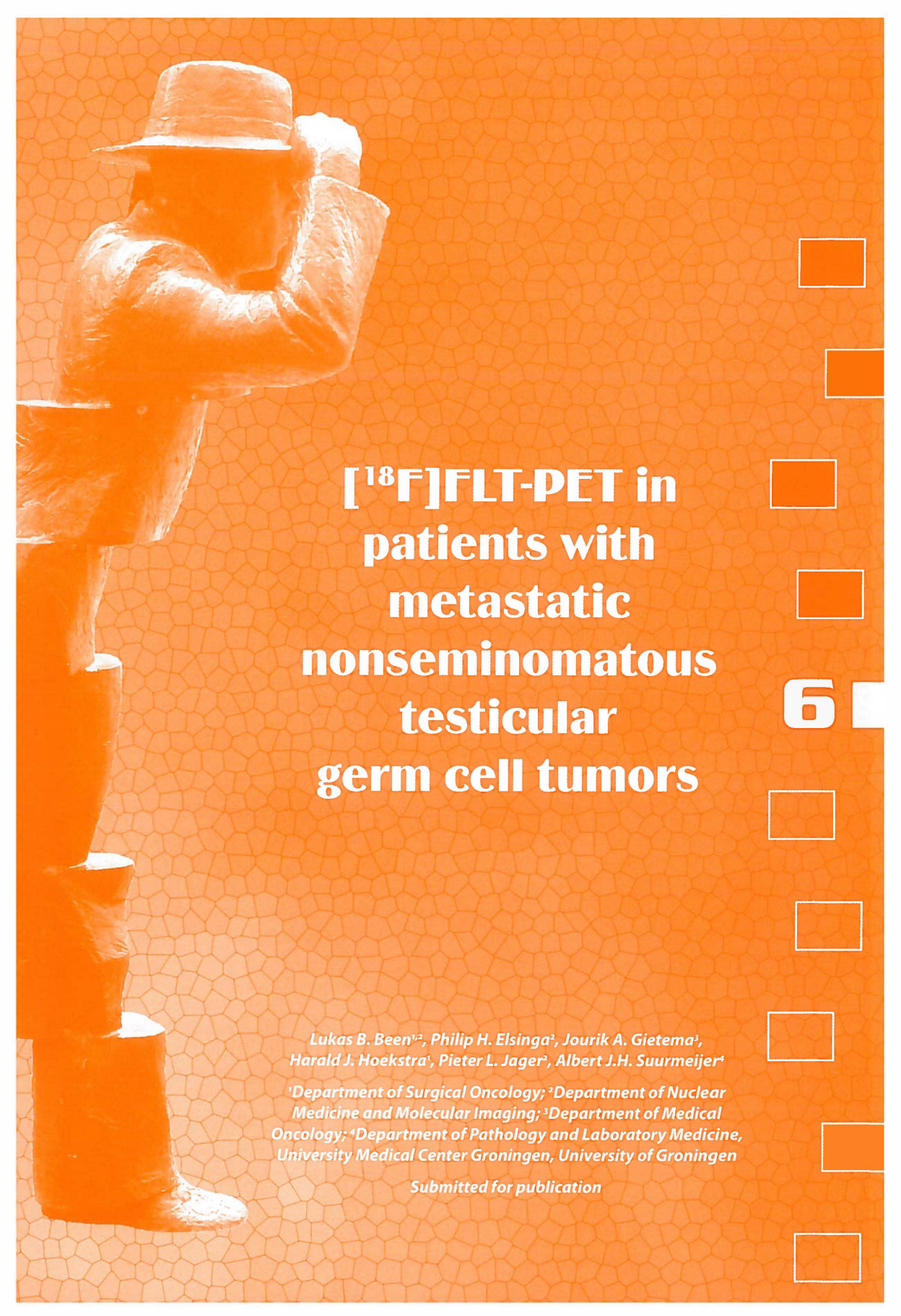
22. Buck AK, Pitterle K., Schirrmeister H., Bommer M., Glatting G., Neumaier B., and Reske S. N. [¹⁸F]FLT positron emission tomography for imaging Non-Hodgkin's lymphoma and assessment of proliferative activity. *J Nucl Med* 2003; 44: 188P-189P [abstract].
23. Vesselle H, Grierson J, Muzi M, Pugsley JM, Schmidt RA, Rabinowitz P et al. In Vivo Validation of 3'-deoxy-3'-[¹⁸F]fluorothymidine ([¹⁸F]FLT) as a Proliferation Imaging Tracer in Humans: Correlation of [¹⁸F]FLT Uptake by Positron Emission Tomography with Ki-67 Immunohistochemistry and Flow Cytometry in Human Lung Tumors. *Clin Cancer Res* 2002;8:3315-3323.
24. Wagner M, Seitz U, Buck A, Neumaier B, Schultheiss S, Bangerter M et al. 3'-[¹⁸F]fluoro-3'-deoxythymidine ([¹⁸F]-FLT) as positron emission tomography tracer for imaging proliferation in a murine B-Cell lymphoma model and in the human disease. *Cancer Res* 2003;63:2681-2687.
25. Issakov J, Merimsky O, Gutman M, Kollender Y, Lev-Chelouche D, Abu-Abid S et al. Hyperthermic isolated limb perfusion with tumor necrosis factor-alpha and melphalan in advanced soft-tissue sarcomas: histopathological considerations. *Ann Surg Oncol* 2000;7:155-159.
26. Bastiaannet E, Groen H, Jager PL, Cobben DC, van der Graaf WT, Vaalburg W et al. The value of FDG-PET in the detection, grading and response to therapy of soft tissue and bone sarcomas; a systematic review and meta-analysis. *Cancer Treat Rev* 2004;30:83-101.
27. van Ginkel RJ, Hoekstra HJ, Pruijm J, Nieweg OE, Molenaar WM, Paans AM et al. FDG-PET to evaluate response to hyperthermic isolated limb perfusion for locally advanced soft-tissue sarcoma. *J Nucl Med* 1996;37:984-990.
28. van Ginkel RJ, Kole AC, Nieweg OE, Molenaar WM, Pruijm J, Koops HS et al. L-[1-¹⁴C]-tyrosine PET to evaluate response to hyperthermic isolated limb perfusion for locally advanced soft-tissue sarcoma and skin cancer. *J Nucl Med* 1999;40:262-267.



51







[¹⁸F]FLT-PET in patients with metastatic nonseminomatous testicular germ cell tumors

6

*Lukas B. Been^{1,2}, Philip H. Elsinga², Jourik A. Gietema³,
Harald J. Hoekstra¹, Pieter L. Jager³, Albert J.H. Suurmeijer⁴*

*¹Department of Surgical Oncology; ²Department of Nuclear
Medicine and Molecular Imaging; ³Department of Medical
Oncology; ⁴Department of Pathology and Laboratory Medicine,
University Medical Center Groningen, University of Groningen*

Submitted for publication

Abstract

Staging patients with NSTGCT and evaluating the response to chemotherapy relies mainly on CT scanning and tumor marker levels. Until now, no PET tracer has been routinely used in patients with NSTGCT. In this study, [¹⁸F]FLT uptake was determined in patients with metastatic NSTGCT before and after chemotherapy.

Methods

Ten patients with metastatic NSTGCT were included. Before and after chemotherapy, [¹⁸F]FLT-PET was performed. According to current treatment protocols, six patients underwent resections of residual retroperitoneal tumor mass.

Results

[¹⁸F]FLT uptake before chemotherapy was low with mean SUV of 2.3. In four patients, tumors were clearly visualized by [¹⁸F]FLT, in five tumors [¹⁸F]FLT showed moderate uptake and in one tumor no [¹⁸F]FLT uptake could be demonstrated. After chemotherapy, no [¹⁸F]FLT uptake was seen.

Conclusion

[¹⁸F]FLT uptake in retroperitoneal tumor masses is low. After chemotherapy, no uptake was seen in the retroperitoneal space, not even in two lesions containing mature teratoma.

Introduction

The introduction of cisplatin-based polychemotherapy in the late 1970s, has improved the prognosis of patients with metastatic nonseminomatous testicular germ cell tumors (NSTGCT). This has resulted in excellent long-term survival rates. After chemotherapy, approximately 40 percent of patients have residual tumor lesions despite normalization of tumor markers. Most of these masses consist of necrosis and/or fibrosis, whereas mature teratoma is found in approximately 30 percent and viable carcinoma is still present in approximately 10-20 percent of all marker-negative residual masses ¹. After surgery of residual tumor, these patients may benefit from additional chemotherapy, whereas patients with necrosis and fibrosis do not need any additional treatment. The resection of residual mature teratoma is also necessary to prevent growing teratoma or development of secondary malignancy ²⁻⁴.

Currently, computerized tomography (CT) is used for staging NSTGCT, for evaluation of the response to chemotherapy. In case of residual disease, patients need a resection. However, CT does not allow for differentiation between fibrosis, necrosis, teratoma and viable carcinoma.

A few studies have reported on the value of positron emission tomography (PET) using 2-[¹⁸F]fluoro-2-deoxy-D-glucose ([¹⁸F]FDG) in patients with metastatic NSTGCT. For staging purposes, [¹⁸F]FDG-PET has no additional value over CT because small nodes with viable carcinoma or nodes consisting of only teratoma frequently do not show [¹⁸F]FDG uptake ^{5,6}. In evaluating the response to chemotherapy, [¹⁸F]FDG-PET was able to differentiate between viable carcinoma and necrosis or fibrosis in the residual tumor mass. However, differentiation between teratoma and necrosis or fibrosis was not possible ⁶. Apparently, teratoma has normal glucose metabolism and therefore shows no increased [¹⁸F]FDG uptake. Furthermore, false positive [¹⁸F]FDG uptake has been demonstrated in inflammatory changes of benign retroperitoneal tissues after chemotherapy ⁷.

In recent years, many other PET tracers visualizing different metabolic pathway of tumors have been developed and studied in (pre)clinical trials. In this pilot study of ten patients with metastatic NSTGCT, we investigated the value of [¹⁸F]-3-deoxy-3-fluoro-L-thymidine ([¹⁸F]FLT) ⁸. [¹⁸F]FLT is a proliferation tracer that uses the salvage pathway of DNA synthesis for PET imaging. Its ability to visualize different tumor types has been established in the past few years. Some studies indicate that [¹⁸F]FLT is potentially more cancer specific than [¹⁸F]FDG because of selective uptake in viable tumor and not in fibrosis, necrosis or post chemotherapy inflammation ⁹.

We performed [¹⁸F]FLT-PET scans before chemotherapy to establish whether [¹⁸F]FLT shows uptake in retroperitoneal tumor masses. After chemotherapy, [¹⁸F]FLT-PET scans were repeated to evaluate whether [¹⁸F]FLT can evaluate the response to chemotherapy.

Patients and methods

Patients

In this prospective study, patients with nonseminomatous germ cell tumors with retroperitoneal lymph node metastases on CT and elevated tumor markers (stage II NS-GCT) were asked to participate. The study protocol was approved by the Medical Ethics Committee of the University Medical Center Groningen. All patients gave written informed consent. Patients with abnormal liver or kidney functions and patients with hematological abnormalities and peripheral neuropathy were not eligible. Staging was performed according to the Royal Marsden Classification System and the International Germ Cell Cancer Collaborative Group (IGCCCG) using chest and abdominal CT scans and tumor markers (alpha feto-protein (AFP, normal value <5 ng/ml), human chorionic gonadotrophin (HCG, normal value, 10 ng/ml) and lactate dehydrogenase (LDH, normal value < 235 U/l)) (Table 1)^{10,11}.

All patients underwent chemotherapy consisting of 3 courses of bleomycin, etoposide and cisplatin and one course of etoposide and cisplatin. After the last course of chemotherapy, a CT scan of the thorax and abdomen was performed for response evaluation. Tumor markers were determined regularly before, during and after chemotherapy according to protocol.

Tracer synthesis

[¹⁸F]FLT was synthesized according to the method of Machulla et al.¹² The 4,4'-dimethoxytrityl-protected anhydrothymidine was [¹⁸F]-fluorinated, followed by a deprotection

Table 1
Tumor staging

| Stage | Criteria |
|-------|--|
| I | No metastases |
| IM | No evidence of metastases, elevated tumour markers |
| II | Lymph node metastases below the diaphragm |
| IIA | metastases <2 cm |
| IIB | metastases 2-5 cm |
| IIC | metastases >5 cm |
| III | Lymph node metastases above the diaphragm |
| IIIA | metastases <2 cm |
| IIIB | metastases 2-5 cm |
| IIIC | metastases >5 cm |

step. After purification by reversed-phase high-performance liquid chromatography, the product was made isotonic and passed through a 0.22 µm filter. The radiochemical purity was >95% and the specific activity was >10 TBq/mmol.

PET studies

All patients underwent two [¹⁸F]FLT-PET scans. The first scan was performed shortly before the start of chemotherapy; the second scan was performed 4-6 weeks after the last course of chemotherapy. Prior to a PET scan, patients were instructed to fast for at least 6 hours. 400 (±10%) MBq of [¹⁸F]FLT was injected intravenously and 60 minutes after injection, the patient was placed in the PET camera. All [¹⁸F]FLT-PET scans were performed on an ECAT EXACT HR+ PET camera (Siemens/CTI Inc., Knoxville, TN, USA). Scanning took place in 3D whole body mode, with 3 and 5 minutes per bed position for transmission and emission respectively. Data were iteratively reconstructed (ordered-subsets expectation maximization) into attenuation corrected whole body images.

PET images were scored visually for areas of increased [¹⁸F]FLT uptake and the visibility was graded as not visible, moderately visible and clearly visible. [¹⁸F]FLT uptake was measured using the standardized uptake value (SUV).

In some patients, software fusion of PET and CT images was performed using Leonardo workstation (Syngo Leonardo, Siemens AG, Berlin, Germany).

Results

Patients

Ten patients (mean age at diagnosis 26.5 years, range 18-37) with metastatic NSTGCT were included (Table 2). All ten patients had retroperitoneal enlarged tumor masses with a mean size of 2.8 cm (range 1.0 – 5.4). One patient (patient no. 1) had a small pulmonary nodule on CT scan (1.0 cm)

After chemotherapy, in nine out of ten patients, retroperitoneal tumor masses were smaller than before chemotherapy. In one patient, retroperitoneal mass had grown from 5.4 to 6 cm. In four patients (patients 2, 4, 5 and 7) no enlarged masses could be found on CT after chemotherapy. In these patients without a residual mass, no surgery was performed and patients entered a 'wait and see' protocol. The remaining six patients underwent surgical resection of residual retroperitoneal tumor mass. In four patients, the resected tissue consisted of only fibrosis and in two patients, fibrosis and mature teratoma was found. There were no patients with vital carcinoma after chemotherapy.

**6**

Table 2
Histology and tumor markers

| No. | Age | Histology* | Tumour stage (ref 10) | Prognosis (ref 11) | Pre-chemotherapy | | | Post-chemotherapy | | | Pathology |
|-----|-----|-----------------|-----------------------|--------------------|------------------|-------------|-----------|-------------------|-------------|-----------|-----------|
| | | | | | HCG (ng/mL) | AFP (ng/mL) | LDH (U/L) | HCG (ng/mL) | AFP (ng/mL) | LDH (U/L) | |
| 1 | 26 | EC, YST, CC, MT | IIA | Good | 2501 | 4 | 99 | <1 | 3 | 114 | F |
| 2 | 37 | EC, YST | IIB | Good | 1504 | 187 | 204 | <1 | 3 | 184 | n.p. |
| 3 | 27 | EC, YST, MT, IT | IIB | Intermediate | 19905 | 3326 | 89 | <1 | 3 | 130 | MT, F |
| 4 | 33 | EC | IIB | Good | 106 | 4 | 535 | <1 | 3 | 232 | n.p. |
| 5 | 19 | EC | IIB | Good | 349 | 20 | 242 | <1 | 7 | 210 | n.p. |
| 6 | 28 | EC, IGN | IIB | Intermediate | 2 | 15 | 270 | <1 | 4 | 186 | F |
| 7 | 23 | EC | IIA | Good | 7 | 102 | 172 | <1 | 5 | 196 | n.p. |
| 8 | 23 | EC, IT | IIB | Good | 42 | 55 | 222 | <1 | 9 | 226 | F |
| 9 | 33 | EC, YST, MT, IT | IIC | Good | 57 | 509 | 232 | <1 | 3 | 241 | MT, F |
| 10 | 18 | IT | IIB | Good | <1 | 481 | 158 | <1 | 2 | 241 | F |

*EC=embryonal cell carcinoma; YST=yolk sac tumor; CC=choriocarcinoma; MT=mature teratoma; IT=immature teratoma; IGN=intratubular germ cell neoplasia; F=fibrosis; n.p. = not performed

PET imaging

Before chemotherapy, the retroperitoneal metastases were clearly visible on [¹⁸F]FLT-PET in 4 patients (Table 3). [¹⁸F]FLT showed only moderate uptake in 5 patients and in one patient, no [¹⁸F]FLT uptake was demonstrated in a small (1.0 cm) lesion. Also, no [¹⁸F]FLT uptake was demonstrated in the small pulmonary nodule of patient no. 1.

Max SUV in all lesion was 2.3, ranging from 1.5 to 3.3. Due to technical problems, SUV could not be measured the retroperitoneal tumor mass of patient 2.

In general, [¹⁸F]FLT-PET images were sometimes difficult to interpret due to physiological [¹⁸F]FLT uptake in the pyelum and ureter. Physiological uptake in this region can easily be mistaken by uptake in a retroperitoneal tumor mass. Therefore, we performed software fusion with CT images, thereby increasing the anatomical information (Fig. 1).

Table 3
CT and PET results

| No. | Pre-chemotherapy | | | Post-chemotherapy | | |
|-----|------------------|-----------------------------|------------------------------|-------------------|-----------------------------|------------------------------|
| | CT size (cm) | PET visibility [§] | Uptake (SUV _{max}) | CT size (cm) | PET visibility [§] | Uptake (SUV _{max}) |
| 1 | 1.6* | + | 1.5 | 1.3 | - | n.a. |
| 2 | 2.7 | +/- | n.a. [#] | 1.0 | - | n.a. |
| 3 | 4.0 | + | 2.4 | 3.5 | - | n.a. |
| 4 | 2.0 | +/- | 1.6 | <1.0 | - | n.a. |
| 5 | 2.0 | + | 2.0 | <1.0 | - | n.a. |
| 6 | 3.1 | +/- | 2.6 | 1.2 | - | n.a. |
| 7 | 1.0 | - | n.a. | <1.0 | - | n.a. |
| 8 | 2.0 | +/- | 3.3 | 1.3 | - | n.a. |
| 9 | 5.4 | +/- | 2.0 | 6.1 | - | n.a. |
| 10 | 4.1 | + | 2.6 | 1.6 | - | n.a. |

n.a. = not applicable

* this patient also had a pulmonary node

[#] due to technical problems not possible

[§] - = not visible, +/- = moderately; + = clearly visible

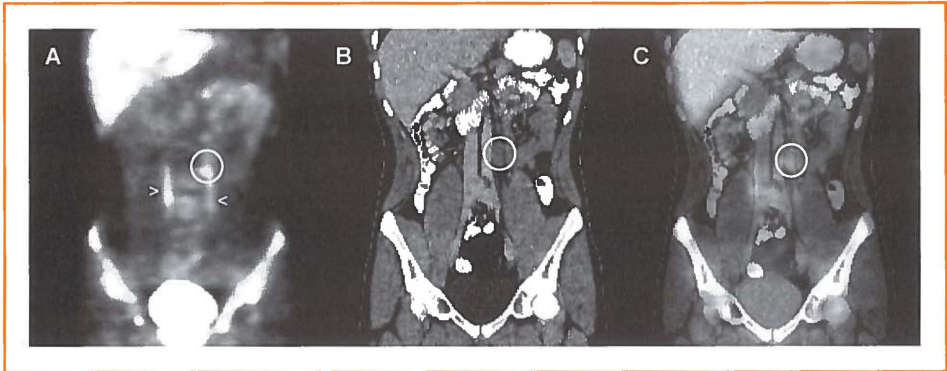


Figure 1a

Example of increased [¹⁸F]FLT uptake in the retroperitoneal space (circle). Note the physiological uptake in the ureters (arrows), which hampers the interpretation of these PET scans.

Figure 1b

CT coronal slice of the same patients, showing an enlarged lymph node metastasis

Figure 1c

Software fusion image showing that the area of increased [¹⁸F]FLT uptake corresponds with the enlarged lymph node.

After chemotherapy, no abnormal uptake was seen in any patient. Subsequently, no uptake was seen in the two patients with mature teratoma, although these lesions were 3.5 and 6.1 cm in largest diameter.

Discussion

This is the first study of [¹⁸F]FLT-PET in patients with metastatic NSTGCT. In this small feasibility study, [¹⁸F]FLT-PET was performed before and after chemotherapy.

To date, no PET tracer has been routinely used in patients with NSTGCT. The main problem of [¹⁸F]FDG in staging is the inability to detect small lesions (that can be seen by CT) ⁵. In evaluating the response to chemotherapy, [¹⁸F]FDG is not able to detect teratoma in residual tumor lesions ⁶.

[¹⁸F]FLT showed only moderate uptake in retroperitoneal metastases before chemotherapy. A possible explanation is the fact that most lesions are relatively small. However, a few larger lesions also showed only little [¹⁸F]FLT uptake. A second possible explanation is the relatively low proliferation activity in these retroperitoneal masses. Several studies have shown strong correlations between proliferation activity in tumors and [¹⁸F]FLT uptake ¹³⁻¹⁵.

Furthermore, [¹⁸F]FLT-PET images were sometimes difficult to interpret, due to physiological [¹⁸F]FLT uptake in this region (pyelum, ureter). Therefore, additional anatomical information by fusion with CT can be very helpful.

After chemotherapy, no increased [¹⁸F]FLT uptake was demonstrated in the retroperitoneal space of our patients, although two patients had large lesions containing mature teratoma. These lesions showed no [¹⁸F]FLT uptake, possibly because of the low proliferation activity in these lesions. There were no patients with vital carcinoma after chemotherapy. Therefore, we cannot give information about the sensitivity and specificity of [¹⁸F]FLT-PET in residual retroperitoneal masses after chemotherapy.


[¹⁸F]FLT is able to visualize metastatic retroperitoneal tumor lesions before chemotherapy. However, sensitivity is low and interpretation of images is hampered by physiological [¹⁸F]FLT uptake in this region. After chemotherapy, no [¹⁸F]FLT uptake was seen. It remains uncertain whether [¹⁸F]FLT will have advantages over [¹⁸F]FDG in patients with metastatic NSTGCT.

References

1. Hartmann JT, Schmoll HJ, Kuczyk MA, Candelaria M, and Bokemeyer C. Postchemotherapy resections of residual masses from metastatic non-seminomatous testicular germ cell tumors. *Ann Oncol* 1997;8:531-538.
2. Andre F, Fizazi K, Culine S, Droz J, Taupin P, Lhomme C et al. The growing teratoma syndrome: results of therapy and long-term follow-up of 33 patients. *Eur J Cancer* 2000;36:1389-1394.
3. Molenaar WM, Oosterhuis JW, Meiring A, Sleyfer DT, Schraffordt KH, and Cornelisse CJ. Histology and DNA contents of a secondary malignancy arising in a mature residual lesion six years after chemotherapy for a disseminated nonseminomatous testicular tumor. *Cancer* 1986;58:264-268.
4. Logothetis CJ, Samuels ML, Trindade A, and Johnson DE. The growing teratoma syndrome. *Cancer* 1982;50:1629-1635.
5. Albers P, Bender H, Yilmaz H, Schoeneich G, Biersack HJ, and Mueller SC. Positron emission tomography in the clinical staging of patients with Stage I and II testicular germ cell tumors. *Urology* 1999;53:808-811.
6. Spermon JR, Geus-Oei LF, Kiemeny LA, Witjes JA, and Oyen WJ. The role of (¹⁸)fluoro-2-deoxyglucose positron emission tomography in initial staging and re-staging after chemotherapy for testicular germ cell tumours. *BJU Int* 2002;89:549-556.
7. Nuutinen JM, Leskinen S, Elomaa I, Minn H, Varpula M, Solin O et al. Detection of residual tumours in postchemotherapy testicular cancer by FDG-PET. *Eur J Cancer* 1997;33:1234-1241.
8. Shields AF, Grierson JR, Dohmen BM, Machulla HJ, Stayanoff JC, Lawhorn-Crews JM et al. Imaging proliferation in vivo with [¹⁸F]FLT and positron emission tomography. *Nat Med* 1998;4:1334-1336.
9. Been LB, Suurmeijer AJ, Cobben DC, Jager PL, Hoekstra HJ, and Elsinga PH. [¹⁸F]FLT-PET in oncology: current status and opportunities. *Eur J Nucl Med Mol Imaging* 2004;31:1659-1672.
10. Peckham MJ, McElwain TJ, Barrett A, and Hendry WF. Combined management of malignant teratoma of the testis. *Lancet* 1979;2:267-270.



[¹⁸F]FLT-PET in patients with metastatic germ cell tumors

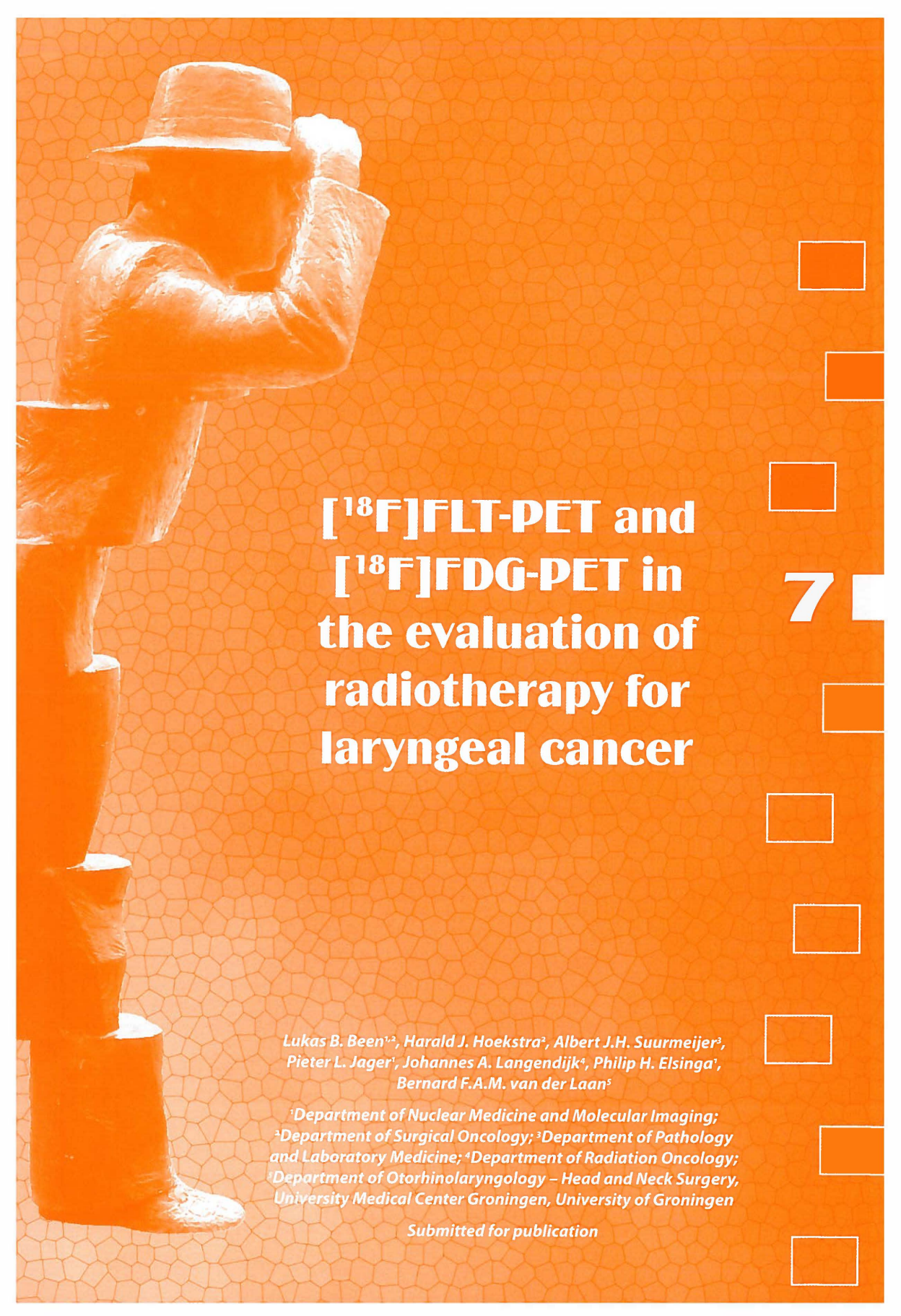
11. International Germ Cell Consensus Classification: a prognostic factor-based staging system for metastatic germ cell cancers. International Germ Cell Cancer Collaborative Group. *J Clin Oncol* 1997;15:594-603.
 12. Machulla HJ, Blochter A, Kuntzsch M, Piert M, Wei R, and Grierson JR. Simplified labeling approach for synthesizing 3'-deoxy-3'-[¹⁸F]fluorothymidine ([¹⁸F]FLT). *Journal of Radioanalytical and Nuclear Chemistry* 2000;243:843-846.
 13. Cobben DC, Elsinga PH, Suurmeijer AJ, Vaalburg W, Maas B, Jager PL et al. Detection and grading of soft tissue sarcomas of the extremities with (¹⁸F)-3'-fluoro-3'-deoxy-L-thymidine. *Clin Cancer Res* 2004;10:1685-1690.
 14. Buck AK, Halter G, Schirrmeister H, Kotzerke J, Wurziger I, Glatting G et al. Imaging proliferation in lung tumors with PET: ¹⁸F-FLT versus ¹⁸F-FDG. *J Nucl Med* 2003;44:1426-1431.
 15. Buck AK, Bommer M, Stilgenbauer S, Juweid M, Glatting G, Schirrmeister H et al. Molecular imaging of proliferation in malignant lymphoma. *Cancer Res* 2006;66:11055-11061.
- 



61







[¹⁸F]FLT-PET and [¹⁸F]FDG-PET in the evaluation of radiotherapy for laryngeal cancer

7

*Lukas B. Been^{1,2}, Harald J. Hoekstra², Albert J.H. Suurmeijer³,
Pieter L. Jager¹, Johannes A. Langendijk⁴, Philip H. Elsinga¹,
Bernard F.A.M. van der Laan⁵*

*¹Department of Nuclear Medicine and Molecular Imaging;
²Department of Surgical Oncology; ³Department of Pathology
and Laboratory Medicine; ⁴Department of Radiation Oncology;
⁵Department of Otorhinolaryngology – Head and Neck Surgery,
University Medical Center Groningen, University of Groningen*

Submitted for publication

Abstract

The evaluation of response to radiotherapy in patients with laryngeal cancer is a challenge because of the difficulty to differentiate between post-therapy changes and recurrent or residual tumor. Positron emission tomography is a non-invasive imaging tool that may be helpful in this differentiation. In this study, [¹⁸F]-fluoro-3'-deoxy-L-thymidine ([¹⁸F]FLT), a proliferation tracer is compared with 2-[¹⁸F]-fluoro-2-deoxy-D-glucose ([¹⁸F]FDG).

Methods

Patients with primary laryngeal cancer, scheduled to undergo radiotherapy were included in this study. Patients underwent both [¹⁸F]FLT-PET and [¹⁸F]FDG-PET shortly before radiotherapy. Ten patients underwent [¹⁸F]FLT-PET and [¹⁸F]FDG-PET 2-3 months after radiotherapy. Scans were analyzed visually for areas of increased tracer uptake. The standardized uptake value (SUV) was measured as a semi-quantitative value of tracer uptake.

Results

Fourteen patients, all male, were included in this study. Both [¹⁸F]FLT-PET and [¹⁸F]FDG-PET showed increased tracer uptake in 12 out of 14 patients (86%). [¹⁸F]FDG uptake was significantly higher than [¹⁸F]FLT uptake (SUV_{max}: 4.5 vs. 2.4 (P=0.002); SUV_{mean}: 3.4 vs. 1.9 (P=0.002)). After radiotherapy, 3 patients had histologically proven residual or recurrent laryngeal cancer. [¹⁸F]FDG was true positive in 2 out of 3 patients, whereas [¹⁸F]FLT showed increased tracer uptake in only one. Of the remaining 7 patients, [¹⁸F]FLT was true negative in all, whereas [¹⁸F]FDG showed increased uptake in one (false positive).

Conclusion

[¹⁸F]FLT-PET is feasible in visualizing laryngeal cancer and its evaluation of treatment. The overall uptake of this tracer is significantly lower as compared with [¹⁸F]FDG, but tumor to background ratios are comparable.

Introduction

Laryngeal cancer is the most frequently diagnosed malignant tumor in the head and neck region and it comprises approximately 2% of all malignancies. Treatment strategies for this type of malignancy are surgery, radiotherapy ± chemotherapy or a combination these modalities. In some cases, CO₂-laser evaporation or photodynamic therapy is an option, but this is limited to a small group of patients with superficial tumors.

Most small tumors (T₁ and T₂) can be curatively treated with radiotherapy alone, allowing for preservation of normal laryngeal function and voice, and subsequently good quality of life after treatment.

Evaluating the response to radiotherapy in patients with laryngeal cancer is a challenge because of the difficulty to differentiate between post-therapy changes and recurrent or residual tumor. Post-treatment surveillance consists of frequent physical examinations, laryngoscopy and, in case of clinical suspicion, conventional imaging (CT) and endoscopic examination with histological biopsies. Histological biopsies are the gold standard for diagnosing recurrent or residual disease, but false-negative biopsies are reported because of submucosal tumor growth ¹. Furthermore, repeated and deep biopsies are often needed, increasing the risk of radionecrosis or impaired voice ².

Positron emission tomography is a functional imaging modality that uses radioactive tracers to visualize different metabolic processes in vivo. 2-[¹⁸F]-fluoro-2-deoxy-D-glucose ([¹⁸F]FDG) is the most widely used PET tracer in oncology. In laryngeal cancer, however, there are only limited data available ^{1,3-6}. Drawbacks of [¹⁸F]FDG are the physiological uptake in muscles of the larynx, uptake in inflammatory tissues ⁷ and in reactive tissues (for example after radiotherapy) ⁸.

In case of suspicion of residual disease, it is essential to differentiate between inflammatory effects of radiotherapy and residual disease. Therefore, other tracers have been subject to investigations. Two amino acid tracers, [¹¹C]-methionine and [¹¹C]-tyrosine, were investigated in patients with laryngeal cancer ^{9,10}. Both tracers show promising results, however, commercial distribution of these [¹¹C] radiotracers to other PET sites without a cyclotron is limited owing to a relatively short half-life, thereby preventing the widespread use of these tracers.

In 1998, [¹⁸F]-fluoro-3'-deoxy-L-thymidine ([¹⁸F]FLT) was introduced as a proliferation tracer ¹¹. [¹⁸F]FLT uses the salvage pathway of DNA synthesis for PET visualization. After entering the cell, [¹⁸F]FLT is phosphorylated by thymidine kinase 1 into [¹⁸F]FLT-monophosphate, after which it is trapped in the cell. Thymidine kinase 1 is a principal enzyme in the salvage pathway of DNA synthesis. Its activity is increased in proliferating cells.

Previously, Cobben et al. showed the feasibility of [¹⁸F]FLT to visualize primary laryngeal cancer ¹². The sensitivity of [¹⁸F]FLT was comparable to the sensitivity of [¹⁸F]FDG. However, [¹⁸F]FLT uptake was significantly lower as compared with [¹⁸F]FDG. The aim of the current study was to investigate [¹⁸F]FLT as a proliferation tracer for the evaluation of the effect of radiotherapy in patients with laryngeal cancer. [¹⁸F]FLT-PET results were compared with [¹⁸F]FDG-PET results.

Patients and methods

Patients

In this prospective study, fourteen patients with primary laryngeal carcinomas suitable for radiotherapy were included. All patients underwent physical examination of the head and neck, laryngoscopy under general anesthesia with histological biopsies of suspicious areas and CT imaging of the neck.

Patients underwent definitive radiotherapy, using conventional fractionation to a total dose of 70 Gy, in fractions of 2 Gy (5 times per week).

After completion of therapy, patients visited the outpatient clinic regularly to undergo physical examinations and indirect laryngoscopy. In case of suspicion of residual or recurrent disease, additional CT and histological biopsy was performed.

This study protocol was approved by the Medical Ethics Committee of the University Medical Center Groningen and all patients gave written informed consent.

PET imaging

Synthesis of [¹⁸F]FLT was performed according to the method of Machulla et al. ¹³. [¹⁸F]FLT was produced by fluorination with [¹⁸F]fluoride of the 4,4'-dimethoxytrityl protected anhydrothymidine, followed by a deprotection step. After purification by reversed phase HPLC, the product was made isotonic and passed through a 0.22 μm filter. [¹⁸F]FLT was produced with a radiochemical purity of >95% and specific activity of >10 TBq/mmol. The radiochemical yield was 8.8% ± 3.7% (decay corrected).

[¹⁸F]FDG was produced according to the method of Hamacher et al. by an automated synthesis module ¹⁴. The radiochemical yield was 65.9% ± 7.1% (decay corrected).

Patients were scheduled for a separate [¹⁸F]FLT-PET and [¹⁸F]FDG-PET scan shortly before and 2-3 months after radiotherapy. For both scans, patients were instructed to fast for at least 6 h. Tracers were injected intravenously and after 60 min or 90 min (for [¹⁸F]FLT or [¹⁸F]FDG respectively) scanning was performed on an ECAT EXACT HR + PET camera (Siemens/CTI Inc.). PET images were iteratively reconstructed (ordered subset expectation maximization) ¹⁵.

Data analysis

Both [¹⁸F]FLT-PET and [¹⁸F]FDG-PET images were analyzed visually on a Leonardo workstation (Syngo Leonardo, Siemens AG, Berlin). Increased uptake of the tracer was considered as a 'positive scan'. The absence of increased tracer uptake was considered as a 'negative scan'.

Semi-quantitative analysis was performed using a volume of interest (VOI), consisting of a 70% isocontour of the maximum standardized uptake value (SUV). Within this VOI, the maximum and mean SUV were measured. In normal laryngeal tissue, the mean background SUV was measured to produce the tumor to non-tumor ratio (TNT).

SUV_{max}, SUV_{mean} and TNT of [¹⁸F]FLT and [¹⁸F]FDG were compared using Wilcoxon signed rank test.

Results

Patients

Fourteen patients, all male, were included in this study. Ten patients underwent all four PET scans. In four patients, only the pre-therapy scans were performed; two patients refused post-therapy scans, one patient died shortly after radiotherapy and in one patient there were technical problems. All patients had primary laryngeal cancer. T-classification was T1 in five patients, T2 in five, T3 in two and T4 in two patients. There were no patients with lymph node metastases (all patients No). Patient and tumor characteristics are given in Table 1.

Visualization of laryngeal cancer

Both [¹⁸F]FLT-PET and [¹⁸F]FDG-PET showed uptake in 12 out of 14 tumors (86%) (Table 2). Two T1 tumors showed no increased tracer uptake (both [¹⁸F]FLT and [¹⁸F]FDG false negative). Visual analysis of all scans revealed avid [¹⁸F]FDG uptake in most tumors, whereas [¹⁸F]FLT uptake was less avid. Mean SUV_{max} and mean SUV_{mean} for [¹⁸F]FDG were significantly higher than for [¹⁸F]FLT (SUV_{max}: 4.5 vs. 2.4 (P=0.002); SUV_{mean}: 3.4 vs. 1.9 (P=0.002)). Due to higher background activity of [¹⁸F]FDG, TNT did not differ significantly between [¹⁸F]FDG and [¹⁸F]FLT (5.1 vs. 3.9 (P=0.158)).

Additional findings

In one patient (patient 4), [¹⁸F]FDG-PET showed increased uptake in the right lobe of the thyroid gland (Fig. 1), whereas [¹⁸F]FLT-PET showed no increased tracer uptake in this region. Fine needle aspiration revealed medullary thyroid cancer, for which this patient was treated by thyroidectomy. In another patient (Patient 5), both [¹⁸F]FDG-PET and [¹⁸F]FLT-PET showed increased uptake in the thyroid region. Further analysis



71



Table 1
Patient characteristics and pretreatment PET results

| Pt/age | Localization | T-stage | Pretreatment | | | | | |
|--------|--------------|---------|--------------------|---------------------|------|--------------------|---------------------|------|
| | | | FDG | | | FLT | | |
| | | | SUV _{max} | SUV _{mean} | TNT | SUV _{max} | SUV _{mean} | TNT |
| 1/60 | Supraglottic | T1 | 8.6 | 4.1 | 5.9 | 2.7 | 2.3 | 5.4 |
| 2/70 | Subglottic | T4 | 3.4 | 2.6 | 4.4 | 1.6 | 1.3 | 3.0 |
| 3/67 | Glottic | T1 | 3.3 | 2.7 | 3.8 | 2.3 | 2.2 | 4.9 |
| 4/72 | Glottic | T1 | neg | neg | neg | neg | neg | neg |
| 5/74 | Glottic | T2 | 3.4 | 2.7 | 3.3 | 1.7 | 1.4 | 3.3 |
| 6/80 | Glottic | T1 | 3.4 | 2.8 | 3.6 | 2.3 | 1.9 | 3.0 |
| 7/54 | Glottic | T2 | 3.8 | 3.1 | 8.0 | 1.6 | 1.1 | 2.8 |
| 8/65 | Glottic | T2 | 2.1 | 1.6 | 2.3 | 1.4 | 1.3 | 3.0 |
| 9/65 | Transglottic | T4 | 6.4 | 5.2 | 7.6 | 2.3 | 1.9 | 3.7 |
| 10/57 | Transglottic | T2 | 2.5 | 2.0 | 3.4 | 2.3 | 1.9 | 3.4 |
| 11/71 | Transglottic | T3 | 5.8 | 4.8 | 5.9 | 5.7 | 3.5 | 6.5 |
| 12/66 | Transglottic | T1 | n.a. | n.a. | n.a. | n.a. | n.a. | n.a. |
| 13/66 | Supraglottic | T3 | 6.2 | 5.1 | 8.8 | 3.2 | 2.7 | 5.1 |
| 14/81 | Glottic | T2 | 4.6 | 3.7 | 4.9 | 1.6 | 1.3 | 2.3 |

showed that this patient was suffering from Hashimoto’s thyroiditis (Fig. 2). Therefore, both [¹⁸F]FLT-PET and [¹⁸F]FDG-PET were false positive.

Evaluation of radiotherapy

Ten out of 14 patients underwent post-treatment [¹⁸F]FDG-PET and [¹⁸F]FLT-PET. Three patients had histologically proven residual or recurrent disease at the time of the second PET scan. [¹⁸F]FDG was true positive in two patients and false negative in one. [¹⁸F]FLT was true positive in one patient and false negative in two.

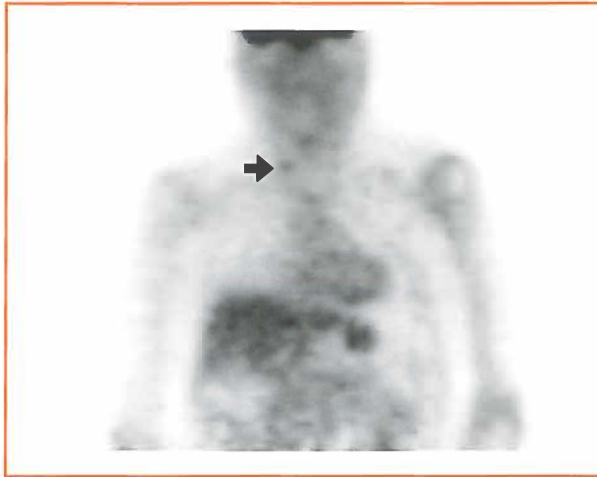


Figure 1

$[^{18}\text{F}]\text{FDG}$ -PET of patient 4 with T1 laryngeal cancer. Uptake is seen in the right thyroid gland. Further analysis showed a medullary carcinoma of the thyroid, for which this patient received treatment. Both scans did not show increased uptake in the laryngeal cancer

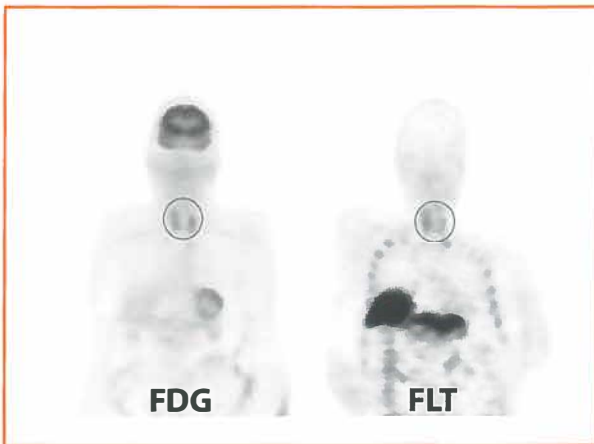


Figure 2

$[^{18}\text{F}]\text{FDG}$ -PET (left) and $[^{18}\text{F}]\text{FLT}$ -PET in patient 5 with a T2 laryngeal cancer. Both scans show diffuse increased tracer uptake in the thyroid region. Further analysis revealed Hashimoto's thyroiditis. Both scans also showed uptake in the laryngeal cancer (not shown in this figure)

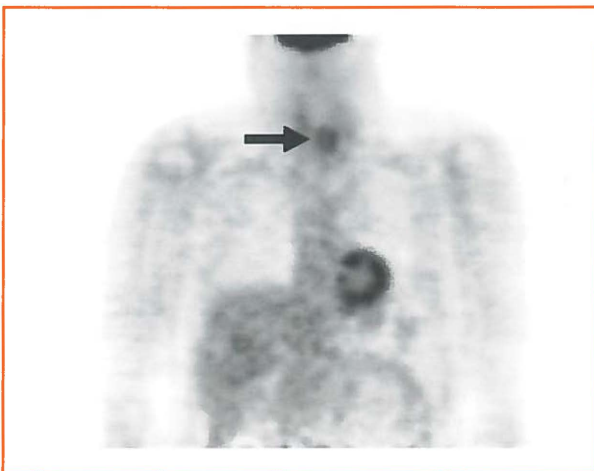


Figure 3

$[^{18}\text{F}]\text{FDG}$ -PET after radiotherapy with increased uptake in patient 8. This patient was at the time of scanning without disease. Three years later, this patient developed recurrent disease, for which he underwent laryngectomy



71



Table 2
Posttreatment PET results and follow up

| Pt | Posttreatment | | | | | | Follow up |
|----|--------------------|---------------------|------|--------------------|---------------------|------|---|
| | FDG | | | FLT | | | |
| | SUV _{max} | SUV _{mean} | TNT | SUV _{max} | SUV _{mean} | TNT | |
| 1 | 4.8 | 3.9 | 4.5 | 1.6 | 1.2 | 2.6 | Recurrent/residual disease within 1y; laryngectomy After 3y 2 nd primary; died 3y after diagnosis |
| 2 | neg | neg | neg | neg | neg. | neg | Recurrent/residual disease within 1y; laryngectomy; alive |
| 3 | 2.3 | 2.4 | 1.9 | neg | neg | neg | Recurrent/residual disease within 1y; laryngectomy; alive |
| 4 | neg | neg | neg | neg | neg | neg | N.E.D.; Alive |
| 5 | neg | neg | neg | neg | neg | neg | N.E.D.; Alive |
| 6 | neg | neg | neg | neg | neg | neg | Recurrent disease after 2y; laryngectomy. Died without disease |
| 7 | neg | neg | neg | neg | neg | neg | Died without disease |
| 8 | 3.4 | 2.5 | 1.6 | neg | neg | neg | Recurrent disease after 3y; laryngectomy. Died without disease |
| 9 | neg | neg | neg | neg | neg | neg | N.E.D.; Alive |
| 10 | n.p. | n.p. | n.p. | n.p. | n.p. | n.p. | Alive |
| 11 | n.p. | n.p. | n.p. | n.p. | n.p. | n.p. | Alive (refused posttreatment scans) |
| 12 | n.p. | n.p. | n.p. | n.p. | n.p. | n.p. | Alive |
| 13 | n.p. | n.p. | n.p. | n.p. | n.p. | n.p. | Recurrent/residual disease within 1y; laryngectomy; alive |
| 14 | n.p. | n.p. | n.p. | n.p. | n.p. | n.p. | Died shortly after radiotherapy |

neg = negative scan; n.a. not applicable; N.E.D. no evidence of disease

Of the remaining 7 patients, [¹⁸F]FLT was negative in all patients. However, [¹⁸F]FDG was positive in one patient (Fig. 3). Laryngoscopy under general anesthesia and histopathological biopsies showed no recurrent or residual disease. Therefore, this [¹⁸F]FDG-PET scan was considered false positive. In follow up, three years after diagnosis this patient developed recurrent laryngeal cancer and was treated with laryngectomy.

Discussion

The aim of the current study was to compare [¹⁸F]FLT-PET and [¹⁸F]FDG-PET with respect to the evaluation of radiotherapy for primary laryngeal cancer.

Before therapy, both [¹⁸F]FLT and [¹⁸F]FDG showed increased tracer uptake in 12 out of 14 tumors. This sensitivity of 86% is in accordance with the literature on [¹⁸F]FDG^{1,12,16,17}. Although in this study [¹⁸F]FLT had the same sensitivity, overall [¹⁸F]FLT uptake was significantly lower than [¹⁸F]FDG uptake. In the recent literature, [¹⁸F]FLT has demonstrated lower tracer uptake than [¹⁸F]FDG in most tumor types¹⁸. A possible explanation for this lower tracer uptake is the fact that tumors consist of malignant cells and inflammatory tissue. In fact, in laryngeal cancer, many tumors show ulceration with inflammation. [¹⁸F]FLT is probably taken up only by the malignant cells, whereas [¹⁸F]FDG is taken up by malignant cells and inflammatory tissues. Furthermore, [¹⁸F]FLT is in competition with native thymidine for the enzyme thymidine kinase 1. The affinity of [¹⁸F]FLT for this enzyme is 30% less, leading to preferable phosphorylation of native thymidine¹⁹. Finally, tumors vary in the relative contribution of the salvage pathway of DNA synthesis. Some tumors rely solely on the 'de novo' pathway, leading to decreased [¹⁸F]FLT uptake and phosphorylation^{20,21}.

[¹⁸F]FLT is expected to be a more cancer specific PET tracer, showing no uptake in inflammatory tissues. Van Waarde et al. demonstrated this in an acute inflammation model in rats²². However, in this study we found that both [¹⁸F]FLT and [¹⁸F]FDG showed uptake in the thyroid gland of a patient suffering from Hashimoto's thyroiditis, a chronic autoimmune inflammation of the thyroid gland. False positive [¹⁸F]FLT uptake has been demonstrated earlier in reactive lymph nodes^{23,24}.

In a patient with medullary thyroid cancer, [¹⁸F]FLT showed no increased tracer uptake and was therefore false negative. [¹⁸F]FDG did show increased uptake in this malignant lesion.

After radiotherapy, the sensitivity for [¹⁸F]FDG to detect residual tumor or recurrent tumor was higher as compared with [¹⁸F]FLT; [¹⁸F]FDG missed one out of three tumors, whereas [¹⁸F]FLT missed two out of three tumors. [¹⁸F]FDG images showed diffuse slightly increased tracer uptake, whereas [¹⁸F]FLT showed decreased background tracer uptake (for example in the irradiated vertebral bodies). In one patient, [¹⁸F]FDG showed focal increased uptake, suspect for residual tumor. [¹⁸F]FLT and histopatho-



logical biopsies were negative at that time. Three years later, this patient did develop recurrent disease. We do not believe that [¹⁸F]FDG detected this lesion three years before it became clinically and histologically apparent. Therefore, [¹⁸F]FDG produced one false positive scan after radiotherapy.

To determine the true value of both tracers in the detection, staging and therapy evaluation of laryngeal cancer, larger patient populations are needed. Low overall [¹⁸F]FLT uptake will probably result in lower sensitivity as compared with [¹⁸F]FDG. In our population, there were no patients with lymph node metastases. In other tumor types, the sensitivity of [¹⁸F]FLT to detect lymph node metastases has been poor^{25,26}. In primary head and neck cancer, Troost et al. reported high sensitivity for [¹⁸F]FLT-PET for lymph node metastases²³. However, [¹⁸F]FLT also showed uptake in many reactive lymph nodes, resulting in a specificity of only 17%.

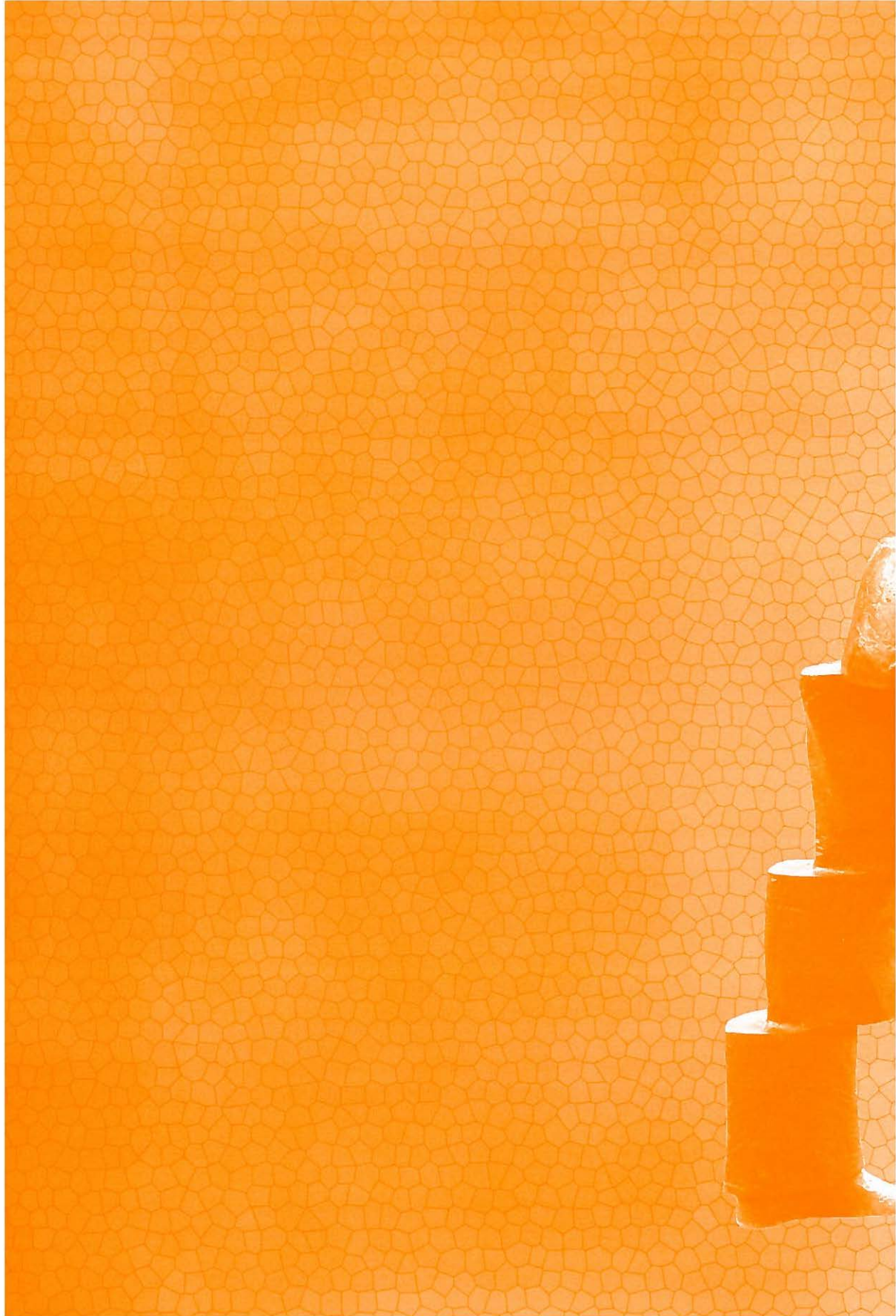
In evaluating the response to radiotherapy, our study population was small and only three patients had residual tumor directly after radiotherapy. Sensitivity for [¹⁸F]FLT seems to be lower than for [¹⁸F]FDG, but [¹⁸F]FDG-PET produced a false positive scan. In conclusion, as reported earlier, [¹⁸F]FLT-PET is feasible in visualizing primary laryngeal cancer, however, uptake of this proliferation tracer is significantly lower as compared with [¹⁸F]FDG. In evaluating the response to radiotherapy, our study population was small and only three patients had residual tumor directly after radiotherapy. Therefore, it is difficult to predict what the true value of [¹⁸F]FLT-PET will be. In the future, therapy evaluation using PET/CT might be very interesting.

References

1. McGuirt WF, Greven KM, Keyes JW, Jr, Williams DW, III, Watson NE, Jr, Geisinger KR et al. Positron emission tomography in the evaluation of laryngeal carcinoma. *Ann Otol Rhinol Laryngol* 1995;104:274-278.
2. Fu KK, Woodhouse RJ, Quivey JM, Phillips TL, and Dedo HH. The significance of laryngeal edema following radiotherapy of carcinoma of the vocal cord. *Cancer* 1982;49:655-658.
3. Terhaard CH, Bongers V, van Rijk PP, and Hordijk GJ. F-¹⁸-fluoro-deoxy-glucose positron-emission tomography scanning in detection of local recurrence after radiotherapy for laryngeal/pharyngeal cancer. *Head Neck* 2001;23:933-941.
4. Greven KM, Williams DW, III, Keyes JW, Jr, McGuirt WF, Watson NE, Jr, and Case LD. Can positron emission tomography distinguish tumor recurrence from irradiation sequelae in patients treated for larynx cancer? *Cancer J Sci Am* 1997;3:353-357.
5. Oe A, Kawabe J, Torii K, Kawamura E, Kotani J, Hayashi T et al. Detection of local residual tumor after laryngeal cancer treatment using FDG-PET. *Ann Nucl Med* 2007;21:9-13.
6. Schwartz DL, Rajendran J, Yueh B, Coltrera MD, Leblanc M, Eary J et al. FDG-PET prediction of head and neck squamous cell cancer outcomes. *Arch Otolaryngol Head Neck Surg* 2004;130:1361-1367.
7. Strauss LG. Fluorine-18 deoxyglucose and false-positive results: a major problem in the diagnostics of oncological patients. *Eur J Nucl Med* 1996;23:1409-1415.
8. Conessa C, Herve S, Foehrenbach H, and Poncet JL. FDG-PET scan in local follow-up of irradiated head and neck squamous cell carcinomas. *Ann Otol Rhinol Laryngol* 2004;113:628-635.

9. Jager PL, Vaalburg W, Pruim J, de Vries EG, Langen KJ, and Piers DA. Radiolabeled amino acids: basic aspects and clinical applications in oncology. *J Nucl Med* 2001;42:432-445.
10. de Boer JR, van der Laan BF, Pruim J, Que TH, Burlage F, Krikke A et al. Carbon-11 tyrosine PET for visualization and protein synthesis rate assessment of laryngeal and hypopharyngeal carcinomas. *Eur J Nucl Med Mol Imaging* 2002;29:1182-1187.
11. Shields AF, Grierson JR, Dohmen BM, Machulla HJ, Stayanoff JC, Lawhorn-Crews JM et al. Imaging proliferation in vivo with [F-18]FLT and positron emission tomography. *Nat Med* 1998;4:1334-1336.
12. Cobben DC, van der Laan BF, Maas B, Vaalburg W, Suurmeijer AJ, Hoekstra HJ et al. 18F-FLT PET for Visualization of Laryngeal Cancer: Comparison with (18)F-FDG PET. *J Nucl Med* 2004;45:226-231.
13. Machulla HJ, Blochler A, Kuntzsch M, Piert M, Wei R, and Grierson JR. Simplified labeling approach for synthesizing 3'-deoxy-3'-[18F]fluorothymidine ([18F]FLT). *Journal of Radioanalytical and Nuclear Chemistry* 2000;243:843-846.
14. Hamacher K, Coenen HH, and Stocklin G. Efficient stereospecific synthesis of no-carrier-added 2-[18F]-fluoro-2-deoxy-D-glucose using aminopolyether supported nucleophilic substitution. *J Nucl Med* 1986;27:235-238.
15. Lonneux M, Borbath I, Bol A, Coppens A, Sibomana M, Bausart R et al. Attenuation correction in whole-body FDG oncological studies: the role of statistical reconstruction. *Eur J Nucl Med* 1999;26:591-598.
16. Lowe VJ, Kim H, Boyd JH, Eisenbeis JF, Dunphy FR, and Fletcher JW. Primary and recurrent early stage laryngeal cancer: preliminary results of 2-[fluorine 18]fluoro-2-deoxy-D-glucose PET imaging. *Radiology* 1999;212:799-802.
17. Henze M, Mohammed A, Mier W, Rudat V, Dietz A, Nollert J et al. Pretreatment evaluation of carcinomas of the hypopharynx and larynx with 18F-fluorodeoxyglucose, 123I-alpha-methyl-L-tyrosine and 99mTc-hexakis-2-methoxyisobutylisocyanide. *Eur J Nucl Med Mol Imaging* 2002;29:324-330.
18. Been LB, Suurmeijer AJ, Cobben DC, Jager PL, Hoekstra HJ, and Elsinga PH. [18F]FLT-PET in oncology: current status and opportunities. *Eur J Nucl Med Mol Imaging* 2004;31:1659-1672.
19. Eriksson S, Kierdaszuk B, Munch-Petersen B, Oberg B, and Johansson NG. Comparison of the substrate specificities of human thymidine kinase 1 and 2 and deoxycytidine kinase toward antiviral and cytostatic nucleoside analogs. *Biochem Biophys Res Commun* 1991;176:586-592.
20. Bardot V, Dutrillaux AM, Delattre JY, Vega F, Poisson M, Dutrillaux B et al. Purine and pyrimidine metabolism in human gliomas: relation to chromosomal aberrations. *Br J Cancer* 1994;70:212-218.
21. Cole PD, Smith AK, and Kamen BA. Osteosarcoma cells, resistant to methotrexate due to nucleoside and nucleobase salvage, are sensitive to nucleoside analogs. *Cancer Chemother Pharmacol* 2002;50:111-116.
22. Van Waarde A, Cobben DCP, Suurmeijer AJH, Maas B, Vaalburg W, De Vries EFJ et al. Selectivity of 3'-deoxy-3'-[18F]fluorothymidine (FLT) and 2-[18F]fluoro-2-deoxy-D-glucose (FDG) for tumor versus inflammation in a rodent model. *J Nucl Med* 2004;45:695-700.
23. Troost EG, Vogel WV, Merx MA, Slootweg PJ, Marres HA, Peeters WJ et al. 18F-FLT PET does not discriminate between reactive and metastatic lymph nodes in primary head and neck cancer patients. *J Nucl Med* 2007;48:726-735.
24. Cobben DC, Elsinga PH, Suurmeijer AJ, Vaalburg W, Maas B, Jager PL et al. Detection and grading of soft tissue sarcomas of the extremities with (18)F-3'-fluoro-3'-deoxy-L-thymidine. *Clin Cancer Res* 2004;10:1685-1690.
25. Been LB, Elsinga PH, de VJ, Cobben DC, Jager PL, Hoekstra HJ et al. Positron emission tomography in patients with breast cancer using (18)F-3'-deoxy-3'-fluoro-L-thymidine ((18)F-FLT)-a pilot study. *Eur J Surg Oncol* 2006;32:39-43.
26. Yap CS, Czernin J, Fishbein MC, Cameron RB, Schiepers C, Phelps ME et al. Evaluation of thoracic tumors with 18F-fluorothymidine and 18F-fluorodeoxyglucose-positron emission tomography. *Chest* 2006;129:393-401.







8



**Summary
and future
perspectives**



Summary and future perspectives

Summary

[¹⁸F]-fluoro-3'-deoxy-3'-L-thymidine ([¹⁸F]FLT) is a relatively new tracer for positron emission tomography (PET). Its uptake reflects the activity of thymidine kinase 1 (TK₁), which is a principle enzyme in the salvage pathway of DNA synthesis. Therefore, [¹⁸F]FLT acts as a proliferation tracer, offering high potential for tumor grading and therapy evaluation.

In this thesis, several aspects of this tracer have been investigated in different tumor types, however, the emphasis in this thesis lies on the evaluation of therapy with [¹⁸F]FLT. In some studies, [¹⁸F]FLT was compared with other PET tracers.

In **Chapter 2** the currently available literature on [¹⁸F]FLT is reviewed. Firstly, the basis of [¹⁸F]FLT as a proliferation tracer is discussed. The toxicity data and different synthetic strategies of [¹⁸F]FLT are mentioned. Subsequently, all available preclinical and clinical studies are reviewed. Three different aspects of [¹⁸F]FLT have been described in the literature: firstly, the ability to visualize malignant tissues (detection and staging). When compared with [¹⁸F]FDG, [¹⁸F]FLT uptake is lower in almost all tumor types, leading to lower sensitivity for primary tumor lesions and metastases. Secondly, the value of [¹⁸F]FLT as a proliferation tracer (correlations with histopathological proliferation markers) has been investigated by different research groups. [¹⁸F]FLT shows strong correlations with different proliferation markers. Therefore, we can conclude that [¹⁸F]FLT is a good proliferation tracer. Thirdly, the evaluation of response to anti-cancer treatment with [¹⁸F]FLT. This property is probably the most interesting and important for the future of [¹⁸F]FLT as a PET tracer in oncology. The currently available literature shows that [¹⁸F]FLT can reflect the decrease in proliferative activity early after therapy.

The feasibility of [¹⁸F]FLT to visualize breast cancer is investigated in **Chapter 3**. Ten patients with primary breast cancer underwent [¹⁸F]FLT-PET. Uptake in the breast was described and measured (using standardized uptake values (SUVs)). Eight out of ten primary tumors (80%) were visualized with [¹⁸F]FLT-PET. Overall uptake was low (mean SUV 1.7 and T/NT 5.0). Seven out of ten patients had axillary lymph-node metastases ranging in size from isolated tumor cells to 2 cm. [¹⁸F]FLT showed only uptake in the two large (2 cm) and clinically apparent (palpable) lymph node metastases. We concluded that [¹⁸F]FLT-PET is not indicated in the detection of breast cancer. For staging the axilla, the sentinel lymph node biopsy is superior to any PET study, owing to the limited spatial resolution of PET.

Chapter 4 is an in vitro study in which different PET tracers are evaluated in C6 glioma cells with respect to their response to three forms of chemotherapy. [¹⁸F]FLT was com-



81



pared with [^{11}C]choline, [^{11}C]methionine, [^{18}F]FDG and two extracellular sigma receptor ligands ([^{18}F]FE-SA5845 and [^{11}C]SA4503). Cells were treated with doxorubicin, cisplatin and 5-fluorouracil and effects on cellular parameters were measured after 0, 1, 2, 3, 4 and 24 h.

The uptake of the two sigma ligands and [^{11}C]choline was strongly increased after chemotherapy, possibly reflecting active cellular membrane repair mechanisms. [^{18}F]FDG uptake showed little or no changes after chemotherapy, whereas [^{18}F]FLT and [^{11}C]methionine showed a rapid decrease in tracer accumulation. Uptake of these tracers was related to the percentage of cells in S-phase. However, cisplatin treatment caused inhibition of [^{11}C]methionine transport across the cell membrane. Doxorubicin treatment caused a more rapid decline in [^{18}F]FLT uptake than the percentage of cells in S-phase, probably because of the depletion of adenosine triphosphate, a necessary cofactor for phosphorylation by thymidine kinase 1.

We concluded that all six PET tracers showed different uptake kinetics after chemotherapy. [^{11}C]methionine and [^{18}F]FLT acted as proliferation tracers, whereas [^{18}F]FDG reflected the number of viable cells. The accumulation of the two sigma receptor ligands and [^{11}C]choline reflected active membrane repair mechanisms. Based on these data, we can conclude that [^{18}F]FLT, being a proliferation tracer, is useful for monitoring response to treatment at an early stage.

In **Chapter 5**, patients with locally advanced soft tissue sarcomas were treated with hyperthermic isolated limb perfusion with TNF α and melphalan (HILP). The effect of HILP was monitored by [^{18}F]FLT-PET. Ten patients underwent [^{18}F]FLT-PET before and after HILP. Before HILP, all tumors were clearly visible on [^{18}F]FLT-PET (mean SUV_{max} of 3.5). [^{18}F]FLT uptake correlated with mitotic index of the tumors ($r=0.82$, $P=0.004$). After HILP, [^{18}F]FLT uptake decreased significantly ($P=0.008$ and $P=0.002$ for SUV_{max} and SUV_{mean} respectively). Histopathological examination of the resected tumor specimens showed that all but one tumor showed necrosis after HILP (ranging from 10-99%). Tumors with high initial [^{18}F]FLT uptake showed better response to HILP ($r=0.64$, $P<0.05$). Software fusion of PET images with images from conventional imaging modalities revealed the heterogeneity of the tumors before and after HILP.

Although [^{18}F]FLT-PET did not directly influence the decision whether to perform a local resection or an amputation, [^{18}F]FLT-PET was able to show the heterogeneity of these tumors after therapy. This supports our opinion that [^{18}F]FLT is a tracer that monitors the response to anti-cancer treatment by visualizing the proliferation activity of tumor cells.

Another study in which [^{18}F]FLT is used to monitor therapy is described in **Chapter 6**. Patients with metastatic nonseminomatous testicular germ cell tumors are treated with cisplatin based chemotherapy. Some of these patients have residual retroperito-

neal tumor mass after chemotherapy. This tumor mass can consist of teratoma or vital carcinoma (which should be resected) or fibrosis or necrosis (which does not need further treatment). Until now, no PET tracer has been able to reliably differentiate between these components.

In our study, ten patients with metastatic nonseminomatous testicular germ cell cancer underwent [¹⁸F]FLT-PET before and after chemotherapy. Overall uptake in metastatic retroperitoneal lesions before chemotherapy was low with a mean SUV of 2.3. In four patients, lesions were clearly visible on [¹⁸F]FLT-PET, five lesions showed only moderate [¹⁸F]FLT uptake and one lesion was not visualized. Physiological uptake in the pyelum and ureter can be mistaken by uptake in retroperitoneal tumor mass, since these masses are frequently located nearby. Fusion of PET images with conventional imaging techniques (for example CT) increases anatomical information and thereby helps interpretation of these scans.

After chemotherapy, six patients underwent surgical resection of the residual retroperitoneal tumor mass. There were no patients with viable tumor in the retroperitoneal tumor mass. In four patients, only fibrosis and necrosis was found, whereas in two patients, retroperitoneal tumor mass consisted of fibrosis and mature teratoma. These lesions were 3.5 and 6.1 cm in largest diameter. No [¹⁸F]FLT uptake was demonstrated in these lesions.

We concluded that metastatic nonseminomatous testicular germ cell lesions can be visualized by [¹⁸F]FLT-PET, however, sensitivity is low and interpretation of scans is hampered by physiological [¹⁸F]FLT uptake in this region. After chemotherapy, [¹⁸F]FLT showed no uptake in two lesions containing mature teratoma. There were no patients with vital carcinoma after chemotherapy. Therefore, it remains uncertain whether [¹⁸F]FLT will have advantages over other tracers in detecting vital carcinoma in residual retroperitoneal tumor masses.

Chapter 7 describes a study in which [¹⁸F]FLT and [¹⁸F]FDG are compared in patients with laryngeal cancer undergoing curative radiotherapy. Fourteen patients with primary laryngeal cancer underwent [¹⁸F]FLT-PET and [¹⁸F]FDG-PET before and after radiotherapy. Before radiotherapy, both [¹⁸F]FLT and [¹⁸F]FDG detected 12 out of 14 tumors (sensitivity 86%). However, overall [¹⁸F]FDG uptake was significantly higher as compared with [¹⁸F]FLT (SUV_{max}: 4.5 vs. 2.4 (P=0.002); SUV_{mean}: 3.4 vs. 1.9 (P=0.002)). Surprisingly, both tracers showed increased uptake in the thyroid gland of a patient, suffering from Hashimoto's disease (an autoimmune inflammation of the thyroid gland). Furthermore, [¹⁸F]FDG detected a medullary thyroid carcinoma, whereas [¹⁸F]FLT did not show increased tracer uptake in this malignancy.

Post-treatment studies were performed in 10 out of 14 patients. Three patients had residual tumor at the time of post-treatment scanning. [¹⁸F]FDG detected 2 out of 3



tumors, [^{18}F]FLT was positive in only one tumor. [^{18}F]FLT did not produce false-positive post-treatment scans, whereas [^{18}F]FDG was false-positive in one.

We concluded that [^{18}F]FLT uptake was lower than [^{18}F]FDG uptake in laryngeal cancers, although sensitivity was 86% for both tracers. After treatment, [^{18}F]FLT seemed less sensitive in detecting residual cancer, whereas [^{18}F]FDG-PET produced a false-positive scan. Although this was a small patient study, based on these results, it is probably not safe to regard a patient having a negative [^{18}F]FDG or [^{18}F]FLT scan as having no residual tumor. Therefore, biopsies are still needed.

Overall conclusions

Detection and staging

Overall uptake of [^{18}F]FLT was low in most tumor types, and in direct comparison with [^{18}F]FDG, uptake of [^{18}F]FLT is lower in almost all cases. There are several possible explanations for the overall low uptake of [^{18}F]FLT in tumors.

Firstly, the affinity of [^{18}F]FLT for the pyrimidine transporter is lower as compared with thymidine, owing to the halogen substitution in the 3' position ¹. Therefore, in competition with endogenous thymidine, [^{18}F]FLT uptake will be less.

Secondly, there is also a 30% less affinity of [^{18}F]FLT for TK₁ as compared with thymidine ². For PET imaging, only low doses of [^{18}F]FLT are injected, resulting in a preferable uptake and phosphorylation of thymidine over [^{18}F]FLT.

A third explanation for the overall low uptake of [^{18}F]FLT is the fact that tumor cells vary in respect of the relative contributions of the salvage pathway and the de novo pathway of DNA synthesis ^{3,4}. [^{18}F]FLT shows uptake in those tumor cells that use the salvage pathway. Therefore, [^{18}F]FLT uptake is not reliable in tumor cells that use the de novo pathway.

Finally, it is well known that malignancies induce an infection reaction and that tumors consist not only of malignant cells, but also of infectious cell ⁵. These cells may contribute to the uptake pattern of a PET tracer. [^{18}F]FLT will probably show uptake only in the malignant cells of tumors, whereas [^{18}F]FDG will show uptake both in the malignant cells and in the infectious cells.

It is unclear what the value of [^{18}F]FLT is in the detection and staging of tumors. The low overall uptake as compared with [^{18}F]FDG will make it less attractive. Further research will have to focus on finding tumors that do exhibit high [^{18}F]FLT uptake or finding ways to improve [^{18}F]FLT uptake.

Monitoring response to therapy

The early evaluation of the effect of a certain treatment modality is very important. In order to avoid unnecessary toxicity and costs, clinicians will want to know at an early

stage whether it is wise to continue the current treatment approach, to change to second or third line regimes or to stop treatment.

Treatment evaluation using standard conventional imaging modalities relies on changes in tumor size. It may take weeks to months for the tumor to shrink (as a sign of response) or to grow (as a sign of progression). The increased or decreased uptake of PET tracers is a faster and biologically more logical method to determine the response to treatment.

Several preclinical and clinical studies have focussed on the value of [^{18}F]FLT to measure the response to therapy. Some chemotherapeutic agents interfere with DNA synthesis. For example, 5-fluorouracil treatment results in S phase accumulation and shuts down the de novo pathway, leading to a compensatory upregulation of the salvage pathway and therefore an increase in [^{18}F]FLT uptake ⁶. Our own data showed the same pattern for [^{18}F]FLT after 5-fluorouracil treatment. After doxorubicin treatment, a rapid decline was observed and after cisplatin treatment, no change was seen in the first 4 hours, after which a less rapid decline occurred. In comparison with other tracers, [^{18}F]FLT showed the most rapid reaction.

We believe that the [^{18}F]FLT shows promise in evaluating the effect of treatment at an early stage. Clinical studies will have to confirm these preclinical data. These studies will have to be performed in tumor types that show avid [^{18}F]FLT uptake.

Future perspectives

Ten years have passed since the first report of [^{18}F]FLT as a proliferation tracer for PET imaging. However, we are just at the beginning of determining the value of [^{18}F]FLT besides other PET tracers ⁷.

Looking back at the current literature, [^{18}F]FLT will probably not have additional value over [^{18}F]FDG in detecting and staging of tumors because of its lower tracer uptake and sensitivity. However, in those areas with increased physiological [^{18}F]FDG uptake, [^{18}F]FLT could have additional value. For example, in detecting brain tumors and determining the tumor grade [^{18}F]FLT-PET could be interesting.

The physiological uptake of [^{18}F]FLT in the bone marrow can be used in diagnosing bone marrow disorders and evaluating the treatment. Agool et al. recently published a small study in which they showed increased [^{18}F]FLT uptake in patients with myelodysplasia and myeloproliferative disorders, and decreased [^{18}F]FLT uptake in patients with myelofibrosis, aplastic anaemia and multiple myeloma ⁸.

The most interesting aspect for future [^{18}F]FLT-PET research will be the evaluation of response to treatment. Several studies have shown promising data for [^{18}F]FLT,⁹⁻¹² however, low tracer uptake after therapy sometimes hampers the visual interpretation. A possible solution for this problem could be PET/CT imaging. With this new and very



promising technique, a CT-based region of interest (ROI) or volume of interest (VOI) can be used for tumor delineation. In this ROI or VOI, [^{18}F]FLT uptake can be measured semi-quantitatively (SUV) or even quantitatively, using dynamic scanning protocols with arterial sampling.

Another possible indication for [^{18}F]FLT-PET could be the planning of radiotherapy. Until now, target volume definition relies on CT or MRI images, sometimes combined with ultrasound and clinical information. However, this is still subject to interobserver variability. Several studies have investigated the added value of PET in defining the target volume for radiotherapy ¹³. Until now, only one study reported the value of [^{18}F]FLT-PET in defining the target value in patients with rectal cancer ¹⁴. The introduction of PET in planning the target volume resulted in higher similarity index. In comparison with [^{18}F]FDG, [^{18}F]FLT showed the same results. Further research in other tumor types is to be expected in the near future.

Since the development of [^{18}F]FLT as a PET tracer, many other tracers have been introduced and investigated for PET imaging. For example, tumor hypoxia can be visualized and measured by [^{18}F]fluoromisonidazole ([^{18}F]FMISO) and [^{18}F]fluoroazomycin arabinoside ([^{18}F]FAZA) ¹⁵. Furthermore, the process of apoptosis, or programmed cell death, is of great clinical interest in oncology for determining prognosis or response to treatment. First in vivo results of [^{18}F]annexin show that this PET tracer is able to visualize cells that are in apoptosis. Therefore, this tracer could possibly be helpful in evaluating the early response to treatment ¹⁶.

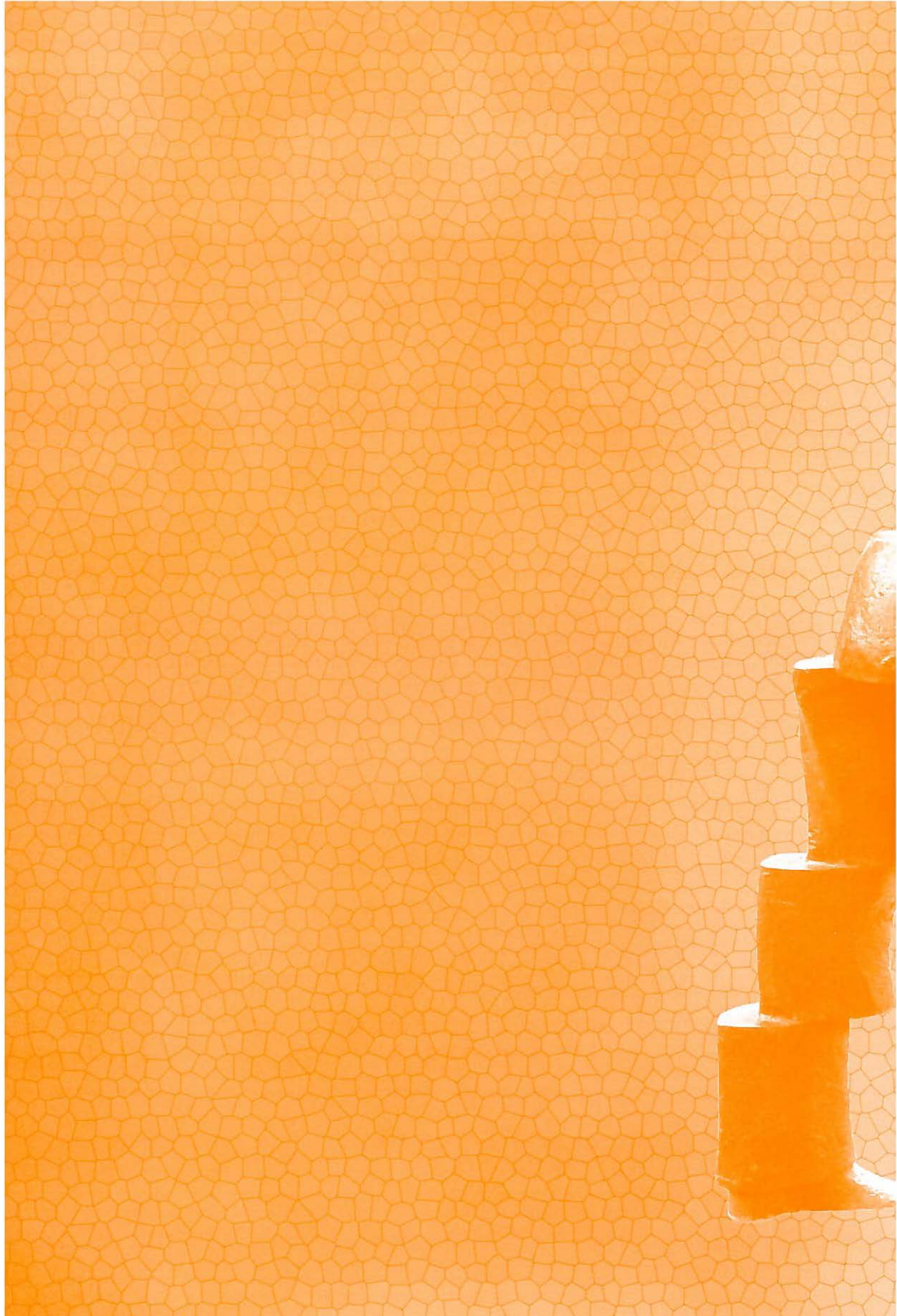
It is not likely that [^{18}F]FLT or any of the new tracers will replace [^{18}F]FDG as the most widely used PET tracer in oncology. More likely, in the future, based on the tumor type or clinical question from the oncologist, the nuclear medicine physician will choose from a number of different PET tracers for different diagnostic problems.

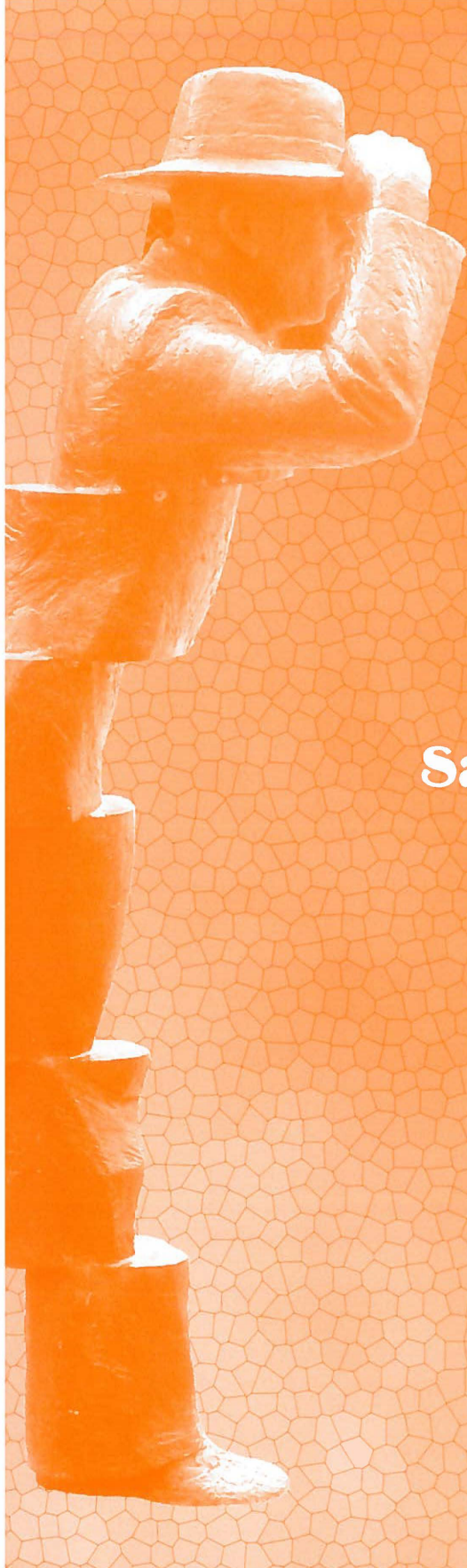
References

1. Gati WP, Misra HK, Knaus EE, and Wiebe LI. Structural modifications at the 2'- and 3'-positions of some pyrimidine nucleosides as determinants of their interaction with the mouse erythrocyte nucleoside transporter. *Biochem Pharmacol* 1984;33:3325-3331.
2. Eriksson S, Kierdaszuk B, Munch-Petersen B, Oberg B, and Johansson NG. Comparison of the substrate specificities of human thymidine kinase 1 and 2 and deoxycytidine kinase toward antiviral and cytostatic nucleoside analogs. *Biochem Biophys Res Commun* 1991;176:586-592.
3. Bardot V, Dutrillaux AM, Delattre JY, Vega F, Poisson M, Dutrillaux B et al. Purine and pyrimidine metabolism in human gliomas: relation to chromosomal aberrations. *Br J Cancer* 1994;70:212-218.
4. Cole PD, Smith AK, and Kamen BA. Osteosarcoma cells, resistant to methotrexate due to nucleoside and nucleobase salvage, are sensitive to nucleoside analogs. *Cancer Chemother Pharmacol* 2002;50:111-116.

5. Steele RJ, Brown M, and Eremin O. Characterisation of macrophages infiltrating human mammary carcinomas. *Br J Cancer* 1985;51:135-138.
6. Dittmann H, Dohmen BM, Kehlbach R, Bartusek G, Pritzkow M, Sarbia M et al. Early changes in [^{18}F]FLT uptake after chemotherapy: an experimental study. *Eur J Nucl Med Mol Imaging* 2002;29:1462-1469.
7. Shields AF, Grierson JR, Dohmen BM, Machulla HJ, Stayanoff JC, Lawhorn-Crews JM et al. Imaging proliferation in vivo with [$^{\text{F-18}}$]FLT and positron emission tomography. *Nat Med* 1998;4:1334-1336.
8. Agool A, Schot BW, Jager PL, and Vellenga E. ^{18}F -FLT PET in hematologic disorders: a novel technique to analyze the bone marrow compartment. *J Nucl Med* 2006;47:1592-1598.
9. Chen W, Delaloye S, Silverman DH, Geist C, Czernin J, Sayre J et al. Predicting treatment response of malignant gliomas to bevacizumab and irinotecan by imaging proliferation with [^{18}F] fluorothymidine positron emission tomography: a pilot study. *J Clin Oncol* 2007;25:4714-4721.
10. Solit DB, Santos E, Pratilas CA, Lobo J, Moroz M, Cai S et al. 3'-deoxy-3'-[^{18}F]fluorothymidine positron emission tomography is a sensitive method for imaging the response of BRAF-dependent tumors to MEK inhibition. *Cancer Res* 2007;67:11463-11469.
11. Molthoff CF, Klabbers BM, Berkhof J, Felten JT, van GM, Windhorst AD et al. Monitoring response to radiotherapy in human squamous cell cancer bearing nude mice: comparison of 2'-deoxy-2'-[^{18}F]fluoro-D-glucose (FDG) and 3'-[^{18}F]fluoro-3'-deoxythymidine (FLT). *Mol Imaging Biol* 2007;9:340-347.
12. Herrmann K, Wieder HA, Buck AK, Schoffel M, Krause BJ, Fend F et al. Early response assessment using 3'-deoxy-3'-[^{18}F]fluorothymidine-positron emission tomography in high-grade non-Hodgkin's lymphoma. *Clin Cancer Res* 2007;13:3552-3558.
13. Gregoire V, Haustermans K, Geets X, Roels S, and Lonneux M. PET-based treatment planning in radiotherapy: a new standard? *J Nucl Med* 2007;48 Suppl 1:68S-77S.
14. Patel DA, Chang ST, Goodman KA, Quon A, Thorndyke B, Gambhir SS et al. Impact of integrated PET/CT on variability of target volume delineation in rectal cancer. *Technol Cancer Res Treat* 2007;6:31-36.
15. Piert M, Machulla HJ, Picchio M, Reischl G, Ziegler S, Kumar P et al. Hypoxia-specific tumor imaging with ^{18}F -fluoroazomycin arabinoside. *J Nucl Med* 2005;46:106-113.
16. Yagle KJ, Eary JF, Tait JF, Grierson JR, Link JM, Lewellen B et al. Evaluation of ^{18}F -annexin V as a PET imaging agent in an animal model of apoptosis. *J Nucl Med* 2005;46:658-666.







8

Samenvatting





Samenvatting

Samenvatting

Positron emissie tomografie (PET) is één van de moleculaire beeldvormende technieken. In toenemende mate wordt in de oncologie gebruik gemaakt van PET voor detectie van tumoren, (re)stadiëring en voor het evalueren van het effect van behandelingen. 2- ^{18}F -fluoro-2-deoxy-D-glucose (^{18}F FDG) is de meest gebruikte tracer. ^{18}F FDG maakt gebruik van de verhoogde glucoseconsumptie van maligniteiten. In de afgelopen jaren zijn de eigenschappen vele andere PET tracers onderzocht. Enkele daarvan hebben hun weg gevonden naar klinische toepassingen.

Dit proefschrift beschrijft de klinische toepasbaarheid van een in 1998 ontwikkelde proliferatietracer, ^{18}F -fluoro-3'-deoxy-3'-L-thymidine (^{18}F FLT). ^{18}F FLT wordt in cellen opgenomen en vervolgens gefosforyleerd door thymidine kinase 1 (TK_1). TK_1 is een intracellulair enzym dat deel uitmaakt van de 'salvage pathway' van de DNA synthese. In delende cellen is de concentratie van TK_1 hoger dan in niet delende cellen. Na fosforylering kan ^{18}F FLT de cel niet meer verlaten, waarna de radioactiviteit gemeten kan worden met behulp van een PET camera.

Het potentiële voordeel van een proliferatietracer is het feit dat specifiekere gekeken wordt naar een eigenschap van maligne cellen (namelijk verhoogde DNA synthese). ^{18}F FLT wordt, in tegenstelling tot ^{18}F FDG, niet opgenomen in onstekingsweefsel. Dit betekent dat ^{18}F FLT mogelijk geschikter is om te differentiëren tussen maligne en benigne weefsels. Daarnaast zou de opname van ^{18}F FLT in tumoren wat kunnen zeggen over de agressiviteit (gradering) van tumoren. Tenslotte biedt een proliferatietracer de mogelijkheid de activiteit van tumoren te meten vóór, tijdens en na allerlei vormen van therapie.

In **Hoofdstuk 2** wordt de huidige beschikbare literatuur over ^{18}F FLT besproken. Allereerst wordt het principe van ^{18}F FLT als proliferatietracer besproken. Daarnaast worden de toxiciteitgegevens en de verschillende productiestrategieën van ^{18}F FLT weergegeven. Vervolgens wordt de beschikbare literatuur van preklinische en klinische studies besproken, waarbij 3 eigenschappen van ^{18}F FLT de revue passeren: ten eerste de detectie en stadiëring van tumoren; vergeleken met ^{18}F FDG is de opname van ^{18}F FLT in bijna alle gevallen lager. Dit leidt tot lagere sensitiviteit voor primaire tumoren en metastasen. Ten tweede de waarde van ^{18}F FLT als proliferatietracer; verschillende onderzoeksgroepen hebben de correlatie tussen ^{18}F FLT opname en verschillende proliferatiemarkers onderzocht. Hieruit blijkt dat ^{18}F FLT een goede proliferatietracer is. Tenslotte wordt de therapie-evaluatie met ^{18}F FLT onderzocht. Dit is zeer waarschijnlijk het meest interessante en belangrijkste eigenschap van ^{18}F FLT voor toekomstig onderzoek. Uit het tot nu toe aanwezige onderzoek blijkt dat ^{18}F FLT het verschil in proliferatie kort na aanvang van therapie goed kan meten.

De toepasbaarheid van [¹⁸F]FLT bij patiënten met mammacarcinoom wordt onderzocht in **Hoofdstuk 3**. Tien patiënten met primair mammacarcinoom ondergingen [¹⁸F]FLT-PET. De opname van de tracer in de borst werd gemeten (standardized uptake value (SUV)). Acht van de tien tumoren (80%) waren zichtbaar op de [¹⁸F]FLT-PET scan. Over het algemeen werd [¹⁸F]FLT slecht opgenomen in het mammacarcinoom (gemiddelde SUV 1.7 met een tumor/non-tumor ratio van 5.0). Zeven patiënten hadden lymfekliermetastasen ten tijde van de PET scan. [¹⁸F]FLT werd alleen opgenomen in 2 grote metastasen (van 2 cm doorsnede).

Wij concludeerden dat [¹⁸F]FLT-PET geen plaats heeft in de detectie en/of stadiëring van patiënten met mammacarcinoom. De sensitiviteit is te laag om kleine primaire tumoren op te sporen. Voor de stadiëring van de axilla is de schildwachtklierprocedure superieur, aangezien minimale afwijkingen (bijvoorbeeld micrometastasen en geïsoleerde tumorcellen) hiermee opgespoord kunnen worden.

Hoofdstuk 4 beschrijft een in vitro studie waarbij verschillende PET tracers vergeleken werden met betrekking tot de evaluatie van drie verschillende vormen van chemotherapie. [¹⁸F]FLT werd vergeleken met [¹¹C]methionine, [¹⁸F]FDG en twee extracellulaire sigma receptor liganden ([¹⁸F]FE-SA5845 and [¹¹C]SA4503). Voor deze studie werden C6 glioom cellen behandeld met doxorubicine, cisplatin en 5-fluorouracil, waarna het effect van deze chemotherapie werd gemeten 0, 1, 2, 3, 4 en 24 u na start van de therapie.

De opname van de sigma receptor liganden en [¹¹C]choline nam sterk toe na chemotherapie, waarschijnlijk als gevolg van herstelmechanismen van het celmembraan. [¹⁸F]FDG liet weinig verschil zien na chemotherapie, terwijl [¹⁸F]FLT en [¹¹C]methionine een snelle en sterke afname liet zien.

Concluderend werd aangetoond dat alle 6 PET tracers verschillende patronen van tracer opname lieten zien na behandeling met chemotherapie. Globaal kan gezegd worden dat [¹¹C]methionine en [¹⁸F]FLT zich gedroegen als proliferatietracer, terwijl de [¹⁸F]FDG opname sterk afhankelijk was van het aantal vitale cellen. De opname van de sigma receptor liganden en [¹¹C]choline was een maat voor herstelmechanismen van het celmembraan. Op basis van deze onderzoeksdata kan gesteld worden dat [¹⁸F]FLT als proliferatietracer geschikt is als tracer om het effect van therapie te meten.

In **Hoofdstuk 5** worden patiënten beschreven met lokaal uitgebreid weke delen sarcoom die behandeld worden met geïsoleerde regionale perfusie met TNF α en melphalan. Het effect van de perfusie werd beoordeeld met behulp van [¹⁸F]FLT-PET. In deze studie ondergingen 10 patiënten [¹⁸F]FLT-PET voor en na perfusie. Voor perfusie waren alle tumoren goed zichtbaar (gemiddelde SUV_{max} van 3.5). De opname van [¹⁸F]FLT correleerde met de mitose index van de tumoren ($r=0.82$, $P=0.004$). Na perfusie nam de opname van [¹⁸F]FLT significant af (respectievelijk $P=0.008$ en $P=0.002$).

voor SUV_{max} en SUV_{mean}). Pathologisch onderzoek van de tumoren toonde necrose in op één na alle tumoren, variërend van 10% tot 99%. Daarnaast bleek dat tumoren met hoge initiële opname van [^{18}F]FLT beter reageerden op perfusie ($r=0.64$, $P<0.05$). Software fusie van PET beelden met MRI beelden toonde dat [^{18}F]FLT opname de heterogeniteit van tumoren goed in beeld kan brengen.

Alhoewel de beslissing tot het uitvoeren van een locale resectie of amputatie niet direct beïnvloed werd door de [^{18}F]FLT-PET scan, bleek wel dat [^{18}F]FLT-PET de heterogeniteit van deze tumoren kon aantonen na therapie. Deze bevinding ondersteunt de gedachte dat [^{18}F]FLT een PET tracer is die het effect van behandeling op tumoren in vivo kan volgen.

Hoofdstuk 6 beschrijft nog een studie waarbij [^{18}F]FLT-PET wordt gebruikt voor de evaluatie van anti-kanker therapie. In deze studie ondergaan patiënten met uitgezaaid testiscarcinoom [^{18}F]FLT-PET voor en na chemotherapie. Soms hebben deze patiënten een residuale retroperitoneale tumormassa na afronden van de chemotherapie. Deze tumormassa kan bestaan ofwel uit teratoom of vitaal carcinoom (hetgeen extra behandeling behoeft), ofwel uit necrose of fibrose (hetgeen geen aanvullende behandeling behoeft). Tot nu toe is geen PET tracer geschikt gebleken om onderscheid te maken tussen deze verschillende weefseltypen.

Voor deze studie ondergingen tien patiënten met uitgezaaid testiscarcinoom [^{18}F]FLT-PET voor en na chemotherapie. Het bleek dat de opname van [^{18}F]FLT voorafgaande aan chemotherapie reeds zeer laag was (gemiddelde SUV 2.3). Bij 4 patiënten was de afwijking duidelijk zichtbaar op [^{18}F]FLT-PET, bij 5 patiënten was de afwijking redelijk zichtbaar en bij 1 patiënt vertoonde de afwijking geen verhoogde opname van [^{18}F]FLT. Fysiologische opname van [^{18}F]FLT in het nierbekken en in de ureter kan gemakkelijk verward worden met opname in de uitzaaiing, omdat uitzaaiingen zich frequent dichtbij bovengenoemde structuren bevinden. Fusie van PET beelden met conventionele beeldvormende technieken (zoals bijvoorbeeld CT-scans) vergemakkelijkt de interpretatie van deze scans.

Na afloop van de chemotherapiekuren ondergingen 6 patiënten chirurgische resectie van residuale retroperitoneale afwijkingen. Geen van de afwijkingen bleek te berusten op vitaal carcinoom. Bij 4 patiënten werd slechts fibrose en necrose gevonden, terwijl er bij 2 patiënten ook matuur teratoom werd gevonden. Deze afwijkingen waren 3.5 en 6.1 cm in doorsnede. In beide afwijkingen werd geen verhoogde opname van [^{18}F]FLT waargenomen.

Wij concludeerden dat uitzaaiingen van het testiscarcinoom met [^{18}F]FLT-PET gevisualiseerd kunnen worden, hoewel de sensitiviteit laag is en de beoordeling van de scans bemoeilijkt wordt door fysiologische tracer opname in dit gebied. Na chemotherapie hadden twee patiënten retroperitoneale afwijkingen die teratoom bevatten. [^{18}F]FLT toonde geen opname van tracer in deze afwijkingen. Er waren geen patiënten met



8 |



vitaal carcinoom na chemotherapie. Daarom blijft het onduidelijk of [¹⁸F]FLT voordelen biedt ten opzichte van [¹⁸F]FDG met betrekking tot het aantonen van vitaal tumorweefsel in residuale tumormassa's.

Hoofdstuk 7 beschrijft een studie waarin [¹⁸F]FLT en [¹⁸F]FDG vergeleken worden bij patiënten met primair larynxcarcinoom die behandeld worden met radiotherapie. 14 patiënten met primair larynxcarcinoom ondergingen [¹⁸F]FLT-PET en [¹⁸F]FDG-PET voor en na radiotherapie. De sensitiviteit voorafgaande aan radiotherapie was 86% (12 van de 14 tumoren) voor zowel [¹⁸F]FLT als [¹⁸F]FDG. De opname van [¹⁸F]FDG was veel hoger dan van [¹⁸F]FLT (SUV_{max} : 4.5 vs. 2.4 ($P=0.002$); SUV_{mean} : 3.4 vs. 1.9 ($P=0.002$)). Als toevalsbevinding vertoonden beide tracers opname in de schildklier van een patiënt met de ziekte van Hashimoto (auto-immuun thyreoiditis). Daarnaast detecteerde [¹⁸F]FDG een medullair schildkliercarcinoom in een andere patiënt, terwijl [¹⁸F]FLT geen verhoogde opname liet zien in deze schildklier.

Na radiotherapie werden bij 10 van de 14 patiënten opnieuw PET scans verricht. Drie patiënten hadden resttumor ten tijde van deze scans; [¹⁸F]FDG detecteerde 2 van de 3 tumoren, [¹⁸F]FLT slechts 1. [¹⁸F]FLT vertoonde geen fout-positieve tracer opname, terwijl [¹⁸F]FDG fout-positief was in 1 patiënt.

Wij concludeerden dat de opname van [¹⁸F]FLT in larynxcarcinoom lager was dan van [¹⁸F]FDG. Desondanks was de sensitiviteit van beide tracers 86%. Na radiotherapie lijkt [¹⁸F]FLT minder sensitief voor het opsporen van resttumor. [¹⁸F]FDG-PET was fout-positief in 1 patiënt. Ondanks dat het een kleine studiepopulatie betrof kunnen we concluderen dat het niet veilig is te zeggen dat een patiënt geen resttumor bevat bij een negatieve [¹⁸F]FLT of [¹⁸F]FDG-PET scan. Een biopsie zal nog nodig zijn om dat uit te sluiten.

Conclusies

Detectie en stagiering

De traceropname van [¹⁸F]FLT is relatief laag in de meeste tumorsoorten en, in vergelijking met [¹⁸F]FDG, bijna altijd lager. Hiervoor zijn verschillende mogelijke verklaringen. Ten eerste is de affiniteit van [¹⁸F]FLT voor de pyrimidine transporter lager dan van thymidine. Dit komt door de vervanging met een halogeen in de 3' positie ¹. Ten tweede heeft [¹⁸F]FLT 30% minder affiniteit voor TK₁ vergeleken met thymidine ². Er worden maar lage doses [¹⁸F]FLT geïnjecteerd. Dit leidt tot gemakkelijker fosforylering van thymidine dan van [¹⁸F]FLT. Een derde verklaring voor de lage opname van [¹⁸F]FLT is het feit dat tumoren deels gebruik maken van de salvage pathway en de de novo pathway van DNA synthese ³⁴ [¹⁸F]FLT vertoont alleen opname in die tumoren die de salvage pathway gebruiken voor DNA synthese. Het is tenslotte bekend dat tumoren

een onstekingsreactie veroorzaken en dat tumoren niet alleen bestaan uit kankercellen maar ook uit ontstekingscellen ⁵. [¹⁸F]FLT vertoont zeer waarschijnlijk geen opname in deze ontstekingscellen, terwijl [¹⁸F]FDG opname vertoont in zowel de kankercellen als de ontstekingscellen.

Het is nog onduidelijk wat de precieze waarde van [¹⁸F]FLT zal zijn met betrekking tot de detectie en stagiëring van tumoren zal zijn. De relatief lage opname in tumoren maken het minder geschikt voor deze doeleinden (lage sensitiviteit). Toekomstig onderzoek zal zich moeten richten op tumoren die wel [¹⁸F]FLT opname vertonen en op manieren om de opname van [¹⁸F]FLT te verhogen.

Evaluatie van therapie

Het vroegtijdig evalueren van therapie is erg belangrijk om onnodig kosten en toxiciteit te veroorzaken. Conventionele beeldvormende technieken gebruiken verandering in grootte als evaluatie van behandeling. Soms duurt het weken tot maanden voordat een tumor kleiner wordt (ten teken van respons) of groter wordt (ten teken van progressie). De verhoogde of verminderde opname van een PET tracer is een snellere en biologisch logischer methode om de respons op therapie te bepalen.

Meerdere preklinische en klinische studies hebben deze eigenschap van [¹⁸F]FLT onderzocht. Enkele chemotherapeutica interfereren met de DNA synthese. 5-fluorouracil bijvoorbeeld veroorzaakt een accumulatie van cellen in de S fase van de celcyclus. Hierbij stopt de de novo pathway en wordt de salvage pathway geactiveerd. Dit leidt tot een toegenomen [¹⁸F]FLT opname ⁶. Onze eigen data lieten een zelfde patroon zien na behandeling met 5-fluorouracil. Na behandeling met doxorubicine werd een snelle afname in [¹⁸F]FLT opname gezien en na behandeling met cisplatina werd geen verandering gezien in de eerste 4 uur, gevolgd door een snelle afname in tracer opname. Vergeleken met andere tracers vertoonde [¹⁸F]FLT de snelste reactie op chemotherapie.

Wij denken van [¹⁸F]FLT zeer waarschijnlijk zeer waardevol zal zijn voor de vroegtijdige evaluatie van therapie. Meer preklinische en klinische studies zullen dat moeten bevestigen.

Toekomst

Er zijn 10 jaar voorbij gegaan sinds het eerste bericht van [¹⁸F]FLT als proliferatie tracer voor PET. Desondanks staan we nog maar aan het begin van het bepalen van de waarde van deze tracers naast ander PET tracers ⁷.

Terugkijkend naar de beschikbare literatuur zal [¹⁸F]FLT zeer waarschijnlijk geen toegevoegde waarde hebben naast [¹⁸F]FDG in de detectie en stagiëring van tumoren. Dit komt door de lage opname van deze tracer en de daaruit voortvloeiende lagere



sensitiviteit. Echter, in die gebieden met verhoogde fysiologische [^{18}F]FDG opname zou [^{18}F]FLT toegevoegde waarde kunnen hebben. Bijvoorbeeld voor de detectie van hersentumoren en het bepalen van de tumorgraad.

Daarnaast kan de fysiologische opname van [^{18}F]FLT in het beenmerg mogelijk ook gebruikt worden voor het aantonen en determineren van beenmergaandoeningen en voor de evaluatie van de ingestelde behandeling. Agool en anderen hebben onlangs een studie gepubliceerd waarin verhoogde opname van [^{18}F]FLT werd gezien in patiënten met myelodysplasie en myeloproliferatieve aandoeningen. In patiënten met myelofibrose, aplastische anemie en multiple myeloom werd verminderde opname van [^{18}F]FLT gezien ⁸.

Het interessantste toekomstige [^{18}F]FLT onderzoek zal betrekking hebben op de evaluatie van therapie met deze tracer. Verschillende studies hebben veelbelovende resultaten laten zien ⁹⁻¹², echter, de lage tracer opname verhindert soms de visuele interpretatie van deze scans. Een mogelijke oplossing voor dit probleem zou de PET/CT techniek kunnen zijn. Met deze nieuwe een veelbelovende techniek kan een regio of volume van interesse (ROI en VOI) van de tumor bepaald kunnen worden met CT scans. In deze ROI of VOI kan de opname van [^{18}F]FLT gemeten worden op verschillende manieren (semi-kwantitatief (SUV) of kwantitatief met behulp van dynamische scanprotocollen en arteriële bloedafnames).

Een andere mogelijke indicatie voor [^{18}F]FLT-PET zou de planning van radiotherapie kunnen zijn. Tot nu toe wordt het doelvolumen van radiotherapie bepaald met CT en MRI, soms in combinatie met echografie en lichamelijk onderzoek. Deze methode is onderhevig aan persoonsgebonden verschillen. Verschillende studies hebben de toegevoegde waarde van PET onderzocht voor het bepalen van het doelvolumen voor radiotherapie ¹³. Tot nu toe heeft slechts 1 studie de waarde van [^{18}F]FLT-PET onderzocht in patiënten met rectumcarcinoom ¹⁴. De invoering van PET voor het plannen van de radiotherapie resulteerde in meer overeenstemming van het bestralingsvolumen. [^{18}F]FDG en [^{18}F]FLT vertoonden vergelijkbare resultaten. Toekomstig onderzoek in andere tumorsoorten zullen zeer waarschijnlijk binnenkort verschijnen.

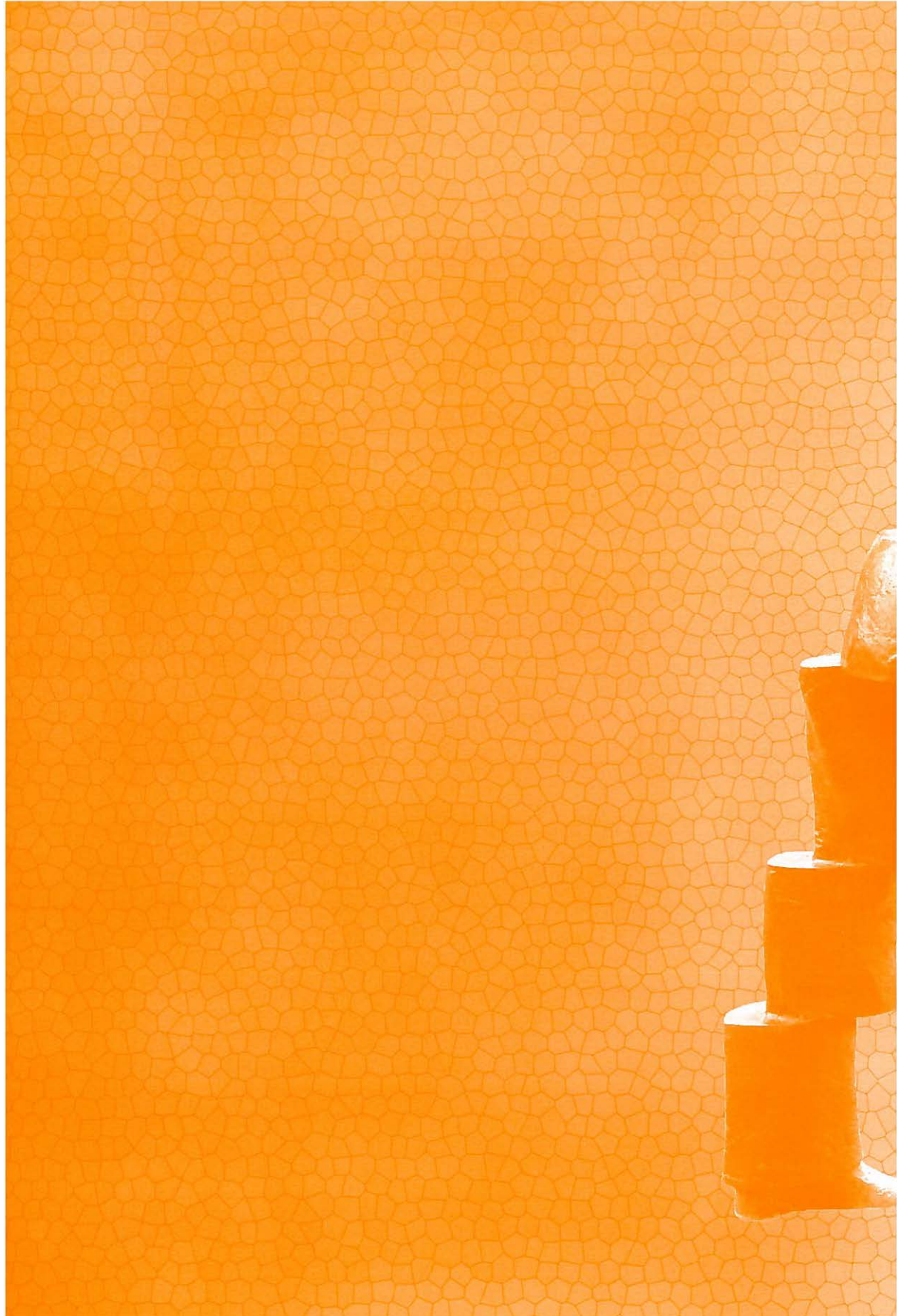
Sinds de invoering van [^{18}F]FLT als PET tracer zijn er vele andere tracers ontwikkeld en onderzocht. Hypoxie in tumoren kan gevisualiseerd en gemeten worden met [^{18}F]fluoromisonidazole ([^{18}F]FMISO) en [^{18}F]fluoroazomycin arabinoside ([^{18}F]FAZA) ¹⁵. Het proces van geprogrammeerde celdood (apoptosis) is van groot belang voor het bepalen van prognose of effect van behandeling in de oncologische praktijk. De eerste resultaten van in vivo onderzoek van [^{18}F]annexin tonen dat deze nieuwe tracer cellen kan visualiseren die in apoptose zijn. Deze tracer zou waarde kunnen hebben in de evaluatie van respons op therapie ¹⁶.

Het is niet waarschijnlijk dat [^{18}F]FLT of een van de andere nieuwe tracers [^{18}F]FDG als meest gebruikte tracer zal vervangen. Waarschijnlijker is dat in de toekomst, afhankelijk van de tumorsoort en de klinische vraag van de oncoloog, de nucleair ge-

neeskundige zal kunnen kiezen uit een arsenaal van PET tracers voor verschillende diagnostische problemen.

Referenties

1. Gati WP, Misra HK, Knaus EE, and Wiebe LI. Structural modifications at the 2'- and 3'-positions of some pyrimidine nucleosides as determinants of their interaction with the mouse erythrocyte nucleoside transporter. *Biochem Pharmacol* 1984;33:3325-3331.
2. Eriksson S, Kierdaszuk B, Munch-Petersen B, Oberg B, and Johansson NG. Comparison of the substrate specificities of human thymidine kinase 1 and 2 and deoxycytidine kinase toward antiviral and cytostatic nucleoside analogs. *Biochem Biophys Res Commun* 1991;176:586-592.
3. Bardot V, Dutrillaux AM, Delattre JY, Vega F, Poisson M, Dutrillaux B et al. Purine and pyrimidine metabolism in human gliomas: relation to chromosomal aberrations. *Br J Cancer* 1994;70:212-218.
4. Cole PD, Smith AK, and Kamen BA. Osteosarcoma cells, resistant to methotrexate due to nucleoside and nucleobase salvage, are sensitive to nucleoside analogs. *Cancer Chemother Pharmacol* 2002;50:111-116.
5. Steele RJ, Brown M, and Eremin O. Characterisation of macrophages infiltrating human mammary carcinomas. *Br J Cancer* 1985;51:135-138.
6. Dittmann H, Dohmen BM, Kehlbach R, Bartusek G, Pritzkow M, Sarbia M et al. Early changes in [¹⁸F]FLT uptake after chemotherapy: an experimental study. *Eur J Nucl Med Mol Imaging* 2002;29:1462-1469.
7. Shields AF, Grierson JR, Dohmen BM, Machulla HJ, Stayanoff JC, Lawhorn-Crews JM et al. Imaging proliferation in vivo with [¹⁸F]FLT and positron emission tomography. *Nat Med* 1998;4:1334-1336.
8. Agool A, Schot BW, Jager PL, and Vellenga E. ¹⁸F-FLT PET in hematologic disorders: a novel technique to analyze the bone marrow compartment. *J Nucl Med* 2006;47:1592-1598.
9. Chen W, Delaloye S, Silverman DH, Geist C, Czernin J, Sayre J et al. Predicting treatment response of malignant gliomas to bevacizumab and irinotecan by imaging proliferation with [¹⁸F] fluorothymidine positron emission tomography: a pilot study. *J Clin Oncol* 2007;25:4714-4721.
10. Solit DB, Santos E, Pratilas CA, Lobo J, Moroz M, Cai S et al. 3'-deoxy-3'-[¹⁸F]fluorothymidine positron emission tomography is a sensitive method for imaging the response of BRAF-dependent tumors to MEK inhibition. *Cancer Res* 2007;67:11463-11469.
11. Molthoff CF, Klabbers BM, Berkhof J, Felten JT, van GM, Windhorst AD et al. Monitoring response to radiotherapy in human squamous cell cancer bearing nude mice: comparison of 2'-deoxy-2'-[¹⁸F]fluoro-D-glucose (FDG) and 3'-[¹⁸F]fluoro-3'-deoxythymidine (FLT). *Mol Imaging Biol* 2007;9:340-347.
12. Herrmann K, Wieder HA, Buck AK, Schoffel M, Krause BJ, Fend F et al. Early response assessment using 3'-deoxy-3'-[¹⁸F]fluorothymidine-positron emission tomography in high-grade non-Hodgkin's lymphoma. *Clin Cancer Res* 2007;13:3552-3558.
13. Gregoire V, Haustermans K, Geets X, Roels S, and Lonneux M. PET-based treatment planning in radiotherapy: a new standard? *J Nucl Med* 2007;48 Suppl 1:68S-77S.
14. Patel DA, Chang ST, Goodman KA, Quon A, Thorndyke B, Gambhir SS et al. Impact of integrated PET/CT on variability of target volume delineation in rectal cancer. *Technol Cancer Res Treat* 2007;6:31-36.
15. Piert M, Machulla HJ, Picchio M, Reischl G, Ziegler S, Kumar P et al. Hypoxia-specific tumor imaging with ¹⁸F-fluoroazomycin arabinoside. *J Nucl Med* 2005;46:106-113.
16. Yagle KJ, Eary JF, Tait JF, Grierson JR, Link JM, Lewellen B et al. Evaluation of ¹⁸F-annexin V as a PET imaging agent in an animal model of apoptosis. *J Nucl Med* 2005;46:658-666.





Dankwoord

9



Het doen van onderzoek is bijna altijd een multidisciplinaire aangelegenheid. Ook aan dit onderzoek heeft (in meer of mindere mate) een groot aantal mensen vanuit verschillende disciplines bijgedragen. Naast alle patiënten, zonder wie dit onderzoek letterlijk onmogelijk zou zijn geweest, wil ik een aantal mensen met name bedanken voor hun samenwerking:

Allereerst mijn eerste promotor, **Prof. dr. H.J. Hoekstra**. Beste Harald, jij hebt mij het vertrouwen gegeven om onder jouw bezielende leiding promotieonderzoek te doen. Ik heb je leren kennen als een man met visie en enorme energie. Jij bent een inspirerende onderzoeker met meer dan eens originele onderzoeksvragen. Ik vind het een eer om als één van jouw (vele) promovendi de boeken in te gaan.

Vervolgens mijn tweede promotor, **Prof. dr. P.H. Elsinga**, beste Philip, in het begin hadden we dagelijks contact. Later werd het wekelijks en op het eind had ik me zo verstoppt in de chirurgische kliniek dat we elkaar bijna niet meer troffen. Ik heb jou leren kennen als een echte bètawetenschapper, een man met veel kennis van zaken, maar ook iemand met een goed gevoel voor humor. Ik wil je bedanken voor de samenwerking en hoop dat de (uiteindelijke) voltooiing van dit proefschrift een goedmaker is voor mijn steeds minder frequente bezoeken aan de afdeling Nucleaire Geneeskunde en Moleculaire Beeldvorming.

Dr. A.J.H. Suurmeijer, beste Albert, jouw heldere en gestructureerde kijk op ons onderzoek en jouw kritische en relativiserende opmerkingen hebben mij zeer geholpen. Je bent een patholoog met enorme vakkennis. Ik wil je danken voor het feit dat ik iets van deze kennis heb mogen overnemen.

Dr. P.L. Jager, beste Piet, jij bent de brug tussen de technische en klinische kanten van PET. Je hebt een frisse kijk op zaken en een gevoel van humor waar ik me goed in kan vinden. Misschien komt dat door de gezamenlijke oost-groningse afkomst? Je bent onlangs vertrokken naar Canada. Ik hoop dat je daar een mooie carrière en een goed leven zult hebben.

De leden van de beoordelingscommissie, **Prof. dr. J.Th.M. Plukker**, **Prof. dr. R.A. Dierckx** en **Prof. dr. O.S. Hoekstra** wil ik danken voor hun goedkeuring van het proefschrift.

Dr. D.C.P. Cobben, beste David, ik wil jou bedanken voor het voorwerk dat jij heb verricht, waardoor ik kon instappen in een spreekwoordelijke 'lopende trein'. Jouw onderzoeksprotocollen waren een basis voor een groot deel van dit proefschrift. Hartelijk dank daarvoor! Ik wens je veel geluk in je toekomstige carrière.

Dr. A. van Waarde, beste Aren, jij hebt een hele bijzondere manier van werken die mij zeer aanspreekt. Jouw ervaring en kennis hebben ervoor gezorgd dat onze studie in ratten geworden is wat het is. Hartelijk dankvoor de vruchtbare samenwerking.

Bram Maas, de [¹⁸F]FLT-analist. Het produceren van PET-tracers is met recht een vak apart. Dank je voor de stabiele productie van [¹⁸F]FLT.

Vervolgens wil ik alle mensen van de afdelingen Chirurgische Oncologie, Nucleaire Geneeskunde en Moleculaire Beelvorming, Pathologie, Medische Oncologie en KNO die hebben bijgedragen aan dit onderzoek danken voor hun medewerking.

Mijn kamergenoten, **Liesbet Ruytjens** en **Carolien Verhoogt** hebben mij gezelschap gehouden tijdens de beginperiode van mijn onderzoek. Het was een leuke tijd met voor ons allen 'ups' en 'downs'. Het begrip 'even de deur dicht' is exemplarisch voor de momenten dat we even stoom moesten afblazen.

De onderzoeksmaatjes van de afdeling chirurgie, plastische chirurgie en urologie: **Erik van Westreenen, Marten Kapma, Anne Brecht Francken, Kirsten Kuizenga, Martin Stenekes, Esther Bastiaanet, Carlijn Buis, Mark-Hugo Maathuis** en **Anton Breeuwsma**. We hebben veel gezellige momenten beleefd met voor velen als climax de sollicitatieronde voor de chirurgie. Die heeft ertoe geleid dat we nu door het land verspreid terecht zijn gekomen. Ik hoop dat we elkaar in de toekomst nog regelmatig zullen treffen.

Alle vrienden, familieleden en collega's die mij hebben gesteund wil ik danken daarvoor. **Adriaan Riemslag** wil ik danken dat hij het aandurft als paranimf aan te treden.

Ik ben geboren en opgegroeid in een liefdevol en harmonieus gezin. Daarvoor wil ik mijn ouders, **Simon** en **Jenneke**, maar ook mijn broer(tjes) **Matthijs, Thomas** (tevens paranimf) en **Andries** bedanken. Mede dankzij hen ben ik wie ik ben. Ik hoop dat ze daar trots op zijn.

'Last, but certainly not least', **Anne Crijns**. ik kan me geen leven zonder jou voorstellen. We hebben het geweldig samen. Dat we nu samen promoveren op dezelfde dag is een leuke afronding van een enorm drukke tijd. Nu kunnen we ons (nog meer) richten op onze klinische carrière, maar vooral ook op onze prachtige dochter **Hannah!**

Groningen, februari 2008

Lukas Been







10

Curriculum vitae





Curriculum vitae

Lukas Been werd geboren op 19 april 1976 in Vlagtwedde. Na de lagere school ging hij naar het Ubbo Emmius Lyceum in Stadskanaal, alwaar hij in 1994 zijn Gymnasium- β diploma behaalde.

Vanwege uitloten begon hij met de studie geneeskunde in Leuven (België). Het kandidaat-arts examen werd in 1998 behaald, waarna de studie voortgezet werd in Amsterdam (Vrije Universiteit). Tijdens de studie werd de wetenschappelijke stage verricht op de afdeling Longziekten van het VU Medisch Centrum (Dr. A. Boonstra) en in deze tijd werkte hij tevens gedurende 2 jaar bij de afdeling Anatomie en Embryologie als student-assistent, waarna hij in 2001 met de co-schappen begon. Het laatste jaar co-schappen werd in Groningen verricht met een afrondend klinisch keuze-co-schap op de afdeling Chirurgische Oncologie van het Universitair Medisch Centrum Groningen (begeleider: Prof. dr. H.J. Hoekstra).

Na het behalen van het artsexamen in 2003 werd een KWF-project overgenomen van Dr. D.C.P. Cobben (projectgroepbegeleiders Dr. P.H. Elsinga, Prof. dr. H.J. Hoekstra, Dr. A.J.H. Suurmeijer). Vanaf februari 2005 werd dit onderzoek gecombineerd met een ANIOS functie op de afdeling chirurgie van het Universitair Medisch Centrum Groningen (UMCG).

Op 1 januari 2006 is Lukas begonnen met de opleiding tot chirurg, waarvan de eerste vier jaar in het UMCG zullen plaatsvinden (opleider: Prof. dr. H.J. ten Duis). De laatste twee jaar zal de opleiding in het Martini Ziekenhuis (Groningen) plaatsvinden (opleider: Dr. P.C. Baas).

Lukas Been is getrouwd met Anne Crijns; zij hebben een prachtige dochter (Hannah).



10 |



